

Titre: Evaluation of the Effect of Polymer Structures on the Composting
Title: Degradability of Nitrogen-Rich Energetic Binders

Auteur: Mario Esteban Araya Marchena
Author:

Date: 2020

Type: Mémoire ou thèse / Dissertation or Thesis

Référence: Araya Marchena, M. E. (2020). Evaluation of the Effect of Polymer Structures on
Citation: the Composting Degradability of Nitrogen-Rich Energetic Binders [Thèse de
doctorat, Polytechnique Montréal]. PolyPublie.
<https://publications.polymtl.ca/5565/>

 **Document en libre accès dans PolyPublie**
Open Access document in PolyPublie

URL de PolyPublie: <https://publications.polymtl.ca/5565/>
PolyPublie URL:

**Directeurs de
recherche:** Charles Dubois
Advisors:

Programme: Génie chimique
Program:

POLYTECHNIQUE MONTRÉAL

affiliée à l'Université de Montréal

**Evaluation of the effect of polymer structures on the composting degradability
of nitrogen-rich energetic binders**

MARIO ESTEBAN ARAYA MARCHENA

Département de génie chimique

Thèse présentée en vue de l'obtention du diplôme de *Philosophiæ Doctor*

Génie chimique

Décembre 2020

POLYTECHNIQUE MONTRÉAL

affiliée à l'Université de Montréal

Cette thèse intitulée :

Evaluation of the effect of polymer structures on the composting degradability of nitrogen-rich energetic binders

présentée par **Mario Esteban ARAYA MARCHENA**

en vue de l'obtention du diplôme de *Philosophiæ Doctor*

a été dûment acceptée par le jury d'examen constitué de :

Marie-Claude HEUZEY, présidente

Charles DUBOIS, membre et directeur de recherche

Nick VIRGILIO, membre

John F. ZEVENBERGEN, membre externe

DEDICATION

To my Mother, for all the phone calls and the Laughter, the Love, the Strength, and the Generosity.

To my Sister, for her Support, her Love, her Selflessness, and her Determination.

To the memory of my Father, because we remember him, and we Love him from here to Heaven.

ACKNOWLEDGEMENTS

I want to thank all the people that helped me during my Ph.D.

To my supervisor, Ph.D. Charles Dubois, for his patience, his trust, and for his kindness. It was a big pleasure to make this project under his guidance.

To Ph.D. John F. Zevenbergen for accepting to examine this dissertation.

To Ph.D. Marie-Claude Heuzey, and Ph.D. Nick Virgilio for being part of my Jury, and for giving me the opportunity to be a TA in their classes.

To Jean-Christophe St-Charles and Jonathan Lavoie, for their support, their advices and expertise, and for all the coffee, and the brunches.

To professors Louis Deschênes and Basil Favis for their classes and their help.

To Anic Desforges, Matthieu Gauthier, Gino Robin and Martine Lamarche, for their invaluable help, their patience, their diligence, and because they always helped me very kindly and with the best attitude.

To my colleagues and friends at Poly: Luis Pereira, Adrian, Fatma, Ivan, Julien, Navid, Teodora.

To my friends of so many Tuesdays: Mauricio, Atyab, Zofia, Jonas, Lisette, Adrien, Sebastien, Genevieve, Martine, and the rest of the staff at McCarold's, because their support and their friendship made all of this possible.

To my friends in Costa Rica, who gave me their love and their support: Vanessa, Carlos, Alicia, Fabio, Luis Chaves, Ricardo C., David. I cannot thank you enough.

RÉSUMÉ

La recherche de nouveaux composés « énergétiques » pour des applications militaires, feux d'artifice, aérospatiales, coussins gonflables (automobiles), s'est concentrée ces dernières décennies sur des substances à forte teneur en azote, y compris les polymères à hétérocycles comme les 1,2,3-triazoles et les tétrazoles. Dans cette étude, quatre polymères (deux à base de tétrazoles: PVT et PVT-PAN ; et deux à base de polyazoture de glycidyle, GAP réticulé au triazole : GAP-BPM et GAP-DCHD) ont été synthétisés et leur biodégradabilité a été étudiée par compostage pendant 18 jours. Les échantillons ont été analysés avant et après le compostage par ^{13}C -RMN d'état solide, FTIR, microscopie IR, SEM-EDS, DSC, DMA et détermination de la fraction soluble dans le dichlorométhane. Les polymères à base de tétrazoles, le polyvinyl tétrazole (PVT) et le polyvinyl tétrazole-co-acrylonitrile (PVT-PAN), ont montré une biodégradabilité élevée et, dans certains cas, une disparition totale de l'échantillon au jour 18. Le groupement nitrile du PVT -PAN a montré une hydrolyse en sels carboxyliques.

Les polymères réticulés de GAP, soient GAP réticulé avec du bis propargyl malonate (GAP-BPM) et GAP réticulé avec du 4,4'-dicyanohepta-1,6-diyne (GAP-DCHD), n'ont pas montré de biodégradabilité significative lors des tests de caractérisation effectués, et le principal processus de dégradation est la libération de polymère d'azide de glycidyle dans le sol, ce qui pourrait empêcher le processus de biodégradation, car on soupçonne que les groupes azoture peuvent présenter une activité biocide. Enfin, un échantillon de PVT marqué avec des isotopes ^{15}N a été préparé (PVT 1- ^{15}N) pour évaluer la stabilité du cycle tétrazole au cours des premières étapes de la biodégradation par compostage pendant 6 jours au terme desquels l'analyse par RMN ^{15}N n'a pas démontré de dégradation dans le cycle tétrazole.

Les résultats obtenus dans cette étude suggèrent que la biodégradation du PVT et du PVT-PAN se fait via la rupture de la chaîne principale, avec une possible élimination des groupes tétrazole, et, pour le cas spécifique du PVT-PAN, l'hydrolyse de groupes nitrile en groupes carboxylate. Dans le cas du GAP-BPM et du GAP-DCHD, les échantillons n'ont pas montré de biodégradation significative, sauf peut-être la libération d'oligomères GAP dans le milieu de compost. Au meilleur de nos connaissances, ces résultats n'ont pas été rapportés auparavant dans la littérature, et ils

ouvrent la porte à davantage de recherche vers la compréhension de la biodégradation et des effets environnementaux des matériaux énergétiques avec les groupes triazole et tétrazole.

ABSTRACT

The research for new “energetic” compounds with various applications (military, fireworks, aerospace, airbags) has focused during the last decades on substances with high nitrogen content, including polymers with heterocyclic rings like 1,2,3- triazoles, and tetrazoles. In this study, four polymers (two based on tetrazoles and two based on triazole-crosslinked glycidyl azide polymer GAP) were synthesized and their biodegradability was studied by composting for 18 days. The samples were analyzed before and after the composting by SS ^{13}C -NMR, FTIR, IR Microscopy, SEM-EDS, DSC, DMA, and soluble fraction determination in dichloromethane. The polymers based on tetrazoles, Poly vinyl tetrazole (PVT) and Poly vinyl tetrazole-co- acrylonitrile (PVT-PAN), showed high biodegradability, and in some cases even total disappearance of the sample by day 18. The nitrile moiety of the PVT-PAN showed hydrolysis into carboxylic salts.

The GAP crosslinked polymers, GAP crosslinked with bis propargyl malonate (GAP-BPM) and GAP crosslinked with 4,4'-dicyanohepta-1,6-diyne (GAP-DCHD), did not show significant biodegradability in any of the characterisation tests performed, and it can be seen that the main degradation process is the release of glycidyl azide polymer into the soil, which might prevent the biodegradation process, as it is suspected that azide groups may present biocidal activity.

Lastly, a ^{15}N labeled PVT sample was prepared ($1\text{-}^{15}\text{N}$ PVT) to evaluate stability of the tetrazole ring during the early stages of the biodegradation by composting for 6 days. The ^{15}N -NMR analysis did not show any degradation in the tetrazole ring.

The results obtained in this study suggest that the biodegradation of PVT and PVT-PAN occurs via the breakdown of the backbone chain, with possible elimination of the tetrazole groups, and, for the specific case of the PVT-PAN, the hydrolysis of the nitrile groups into carboxylate groups. In the case of GAP-BPM and GAP-DCHD, the samples did not show significant biodegradation, except possibly the release of GAP oligomers into the compost medium. To the best of our knowledge, these findings have not been reported before in the literature, and they open the door for more research towards the understanding of the biodegradation and environmental effects of energetic materials with triazole and tetrazole groups.

TABLE OF CONTENTS

| | |
|---|------|
| DEDICATION | III |
| ACKNOWLEDGEMENTS | IV |
| RÉSUMÉ..... | V |
| ABSTRACT..... | VII |
| TABLE OF CONTENTS | VIII |
| LIST OF TABLES | XI |
| LIST OF FIGURES..... | XII |
| LIST OF SYMBOLS AND ABBREVIATIONS..... | XVII |
| LIST OF APPENDICES | XX |
| CHAPTER 1 INTRODUCTION..... | 1 |
| 1.1 Research Context..... | 1 |
| 1.2 Research Objectives | 2 |
| 1.2.1 Main Objective..... | 2 |
| 1.2.2 Specific Objectives..... | 2 |
| CHAPTER 2 LITERATURE REVIEW..... | 4 |
| 2.1 Explosives and Energetic Materials | 4 |
| 2.1.1 Research of New Energetic Materials..... | 13 |
| 2.2 Synthetic techniques for preparation of energetic polymers..... | 15 |
| 2.2.1 Polycondensation or Step-Growth Polymerization | 16 |
| 2.2.2 Ring Opening Polymerization..... | 17 |
| 2.2.3 Radical Polymerization or Addition Polymerization | 18 |
| 2.2.4 Nitration of materials | 19 |
| 2.2.5 Modification of energetic polymers | 20 |

| | | |
|-----------|---|----|
| 2.3 | Biodegradation and Biodegradable polymers | 23 |
| 2.3.1 | Environmental fate and effects of Energetic Materials | 24 |
| 2.3.2 | Solutions to the pollution with Energetic Materials | 30 |
| 2.3.3 | Biodegradability | 34 |
| 2.3.4 | Biodegradability of energetic materials | 35 |
| 2.3.5 | Isotope Analysis for Biodegradability studies | 41 |
| CHAPTER 3 | METHODOLOGY AND EXPERIMENTAL DESIGN | 45 |
| 3.1 | Experimental Constraints and Limitations | 45 |
| 3.1.1 | Low solubility of the polymers after solvent casting: | 45 |
| 3.1.2 | High molecular mass of PAN polymers: | 46 |
| 3.1.3 | Laboratory Safety | 46 |
| 3.1.4 | Economic factors | 46 |
| 3.2 | Experimental Design | 47 |
| 3.2.1 | Synthesis of the Polymers | 51 |
| 3.2.2 | Reagents for the synthesis | 52 |
| 3.2.3 | Synthesis and preparation of samples | 54 |
| 3.2.4 | Polymer Characterization | 61 |
| 3.2.5 | Biodegradability Experiments | 64 |
| CHAPTER 4 | RESULTS | 70 |
| 4.1 | Physical Properties of Synthesized Polymers | 70 |
| 4.1.1 | Experimental yields of Synthesis | 70 |
| 4.1.2 | NMR analysis: ¹ H-NMR and ¹³ C-NMR | 73 |
| 4.1.3 | FTIR | 81 |
| 4.2 | Thermal and Mechanical Properties of Synthesized Polymers | 83 |

| | | |
|------------|---|-----|
| 4.2.1 | DSC | 83 |
| 4.2.2 | DMA..... | 87 |
| 4.3 | Composting Results..... | 87 |
| 4.3.1 | Soluble Fraction | 87 |
| 4.3.2 | Infrared Spectroscopy | 92 |
| 4.3.3 | NMR Spectroscopy | 98 |
| 4.3.4 | DSC | 103 |
| 4.3.5 | Dynamic Mechanical Analysis, DMA | 107 |
| 4.3.6 | Scanning Electronic Microscopy and Energy-Dispersive X-Ray Spectroscopy (SEM-EDS) 110 | |
| 4.4 | Characterization of an Isotope-marked Polymer..... | 116 |
| 4.4.1 | DSC | 116 |
| 4.5 | Composting of Isotope-marked Polymers..... | 117 |
| 4.5.1 | ¹⁵ N-NMR..... | 117 |
| CHAPTER 5 | GENERAL DISCUSSION..... | 121 |
| CHAPTER 6 | CONCLUSION AND RECOMMENDATIONS..... | 128 |
| 6.1 | Scientific Contribution | 128 |
| 6.2 | Conclusions | 128 |
| 6.3 | Recommendations | 129 |
| REFERENCES | | 130 |
| APPENDICES | | 139 |

LIST OF TABLES

| | |
|--|-----|
| Table 2.1 Physical properties of TNT, RDX and HMX [8, 9] | 7 |
| Table 2.2 Toxicity risk of energetic materials in various ecological receptors..... | 28 |
| Table 2.3 Examples of biodegradation studies using isotopes as molecular markers..... | 42 |
| Table 3.1 Experimental conditions and variables for the composting experiments..... | 49 |
| Table 3.2 Techniques used for the characterization of the samples | 50 |
| Table 3.3 Chemical structure of the synthesized polymers..... | 51 |
| Table 3.4 Reagents to be used for synthesis and polymerization..... | 52 |
| Table 3.5 Compost composition as reported by the manufacturer..... | 65 |
| Table 4.1 Experimental yields of the polymers prepared..... | 71 |
| Table 4.2 Characterization tests run in the prepared samples | 72 |
| Table 4.3 Expected ^1H -NMR chemical shifts in liquid state | 73 |
| Table 4.4 Expected ^{13}C -NMR chemical shifts | 73 |
| Table 4.5 Expected FTIR bands | 81 |
| Table 4.6 Comparison of the behavior of different energetic materials in composting experiments | 90 |
| Table 4.7 DSC and DMA thermal analysis results for the composted samples..... | 107 |
| Table 4.8 Abundance and relative sensitivity of isotopes of H, C and N | 118 |
| Table 4.9 General ^{15}N -NMR chemical shifts in liquid state (using $\text{NH}_3(\text{l}) = 0$ ppm) | 119 |
| Table 5.1 Summary of the observed biodegradation reactions | 126 |

LIST OF FIGURES

| | |
|--|----|
| Figure 2.1 Energetic Materials used as explosives: a) TNT b) RDX c) HMX d) CL-20 | 5 |
| Figure 2.2 Secondary products on the synthesis of TNT | 6 |
| Figure 2.3 Structure of a) Poly (BAMO) b) Poly(AMMO) c) Poly(NIMMO) d) GAP | 8 |
| Figure 2.4 Synthesis of GAP-Triol and GAP-Diol from epichlorhydrin | 9 |
| Figure 2.5 Structure of a) 1,2,3 triazole b) 1,2,4 triazole c) tetrazole d) Poly vinyl tetrazole PVT | 11 |
| Figure 2.6 Scheme of formation of Poly Vinyl Tetrazole from Poly Acrylonitrile. | 11 |
| Figure 2.7 Structure of a) Poly Vinyl Azide PVAz b) Poly Vinyl Nitrate PVN c) Poly Glycidyl Nitrate, “Poly Glyn” | 13 |
| Figure 2.8 Structure of a) Dinitro anisole (DNAN) b) Nitroguanidine (NQ) c) 3-Nitro-1,2,4-triazol- 5-one (NTO) | 14 |
| Figure 2.9 Structures of a) FOX-7, b) FOX-12 and c) TKX-50 | 15 |
| Figure 2.10 Scheme of a Fischer’s Condensation between a) an alcohol and either a carboxylic acid (X=OH) or an acyl halide (X=Cl, Br, I) b) an anhydride and an alcohol | 16 |
| Figure 2.11 Scheme of the reaction of an isocyanate and a) an alcohol to form a urethane b) water, to form an amine | 17 |
| Figure 2.12 Synthesis of PECH by Ring-Opening Polymer followed by azidation to produce GAP | 17 |
| Figure 2.13 Scheme for the synthesis of Poly BAMO: a) Azidation and then ring opening polymerization b) Polymerization preceding the azidation..... | 18 |
| Figure 2.14 Scheme of the free-radical polymerization of acrylonitrile in the presence of AIBN to form PAN | 19 |
| Figure 2.15 Structure of a) Nitrocellulose (NC) b) Nitroglycerin (NG) | 20 |
| Figure 2.16 Structures of a) Hexamethylene diisocyanate b) Lysine Diisocyanate c) Lysine Triisocyanate d) chain extension reaction between a diol and isocyanates | 21 |

| | |
|--|----|
| Figure 2.17 Cycloaddition of azide to triple bonds to form (a) tetrazole rings or (b) 1,2,3-triazole rings..... | 22 |
| Figure 2.18 Reaction scheme of the crosslinking of GAP with bisalkynes | 23 |
| Figure 2.19 Classical bioisosteric replacements: a) hydrogen to fluorine, b) phenyl to thiophene, c) amide to triazole, d) carboxylic acid to tetrazole. | 29 |
| Figure 2.20 Structure of a) valsatan b) methyl benzotriazole | 30 |
| Figure 2.21 Synthesis of a thermoset polyurethane from poly epichlorohydrin (Se=sebacoyl groups; R= OH for sebacic acid, and R = Cl for sebacoyl chloride..... | 33 |
| Figure 2.22 Structures of: a) Hydrazinium nitroformate HNF and b) Ammonium dinitramide.... | 34 |
| Figure 2.23 Biotransformation of TNT in compost [116]..... | 36 |
| Figure 2.24 Proposed biotic degradation pathways for RDX (based on [67][118]) | 37 |
| Figure 2.25 Proposed biotic degradation pathways for HMX (based on [67][118]) | 38 |
| Figure 2.26 Proposed biotic degradation pathways for CL-20 (based on [67][118]) | 39 |
| Figure 3.1 Scheme of the experimental methodology..... | 48 |
| Figure 3.2 Reaction scheme for the synthesis of PVT | 54 |
| Figure 3.3 Reaction scheme for the synthesis of PVT-PAN..... | 55 |
| Figure 3.4 Reaction scheme for the synthesis of PVT-PMA | 55 |
| Figure 3.5 Reaction scheme for the synthesis of tBu-PVT | 56 |
| Figure 3.6 Reaction scheme for the synthesis of PVT-Allyl..... | 56 |
| Figure 3.7 Reaction scheme for the synthesis of PVAz..... | 57 |
| Figure 3.8 Reaction scheme for the synthesis of Poly Acrylonitrile-co-Allyl Chloride PAN-PAC | 57 |
| Figure 3.9 Reaction scheme for the synthesis of Poly Vinyl Tetrazole-co-Allyl Azide PVT-PAAz | 58 |
| Figure 3.10 Reaction scheme for the synthesis of BPM | 58 |

| | |
|---|----|
| Figure 3.11 Reaction scheme for the synthesis of DCHD | 59 |
| Figure 3.12 Reaction of the crosslinking of GAP with BPM..... | 60 |
| Figure 3.13 Reaction of the crosslinking of GAP with DCHD..... | 60 |
| Figure 3.14 Reaction scheme for the synthesis of isotope-marked PVT (1- ¹⁵ N PVT)..... | 61 |
| Figure 3.15 Preparation of the samples for FTIR Microscopy and EDS a) Scheme of the sample cut for resin encasing b) final samples after sanding and polishing (PVT samples shown) .. | 63 |
| Figure 4.1 Spectra of PVT a) ¹ H-NMR b) ¹³ C-NMR..... | 74 |
| Figure 4.2 Spectra of PVT-PAN a) ¹ H-NMR b) ¹³ C-NMR | 75 |
| Figure 4.3 Spectra of GAP a) ¹ H-NMR b) ¹³ C-NMR | 77 |
| Figure 4.4 Spectrum HSQC of GAP (X-axis: ¹ H-NMR, Y-axis: ¹³ C-NMR) | 78 |
| Figure 4.5 Spectra of BPM a) ¹ H-NMR b) ¹³ C-NMR..... | 79 |
| Figure 4.6 Spectra of DCHD a) ¹ H-NMR b) ¹³ C-NMR..... | 80 |
| Figure 4.7 FTIR Spectrum for PVAz | 82 |
| Figure 4.8 FTIR Spectrum for PVT-PMA | 82 |
| Figure 4.9 FTIR Spectra for PAN, PVT, and PVT-PAN..... | 83 |
| Figure 4.10 DSC decomposition curve for PVAz..... | 84 |
| Figure 4.11 DSC decomposition curve for PVT..... | 84 |
| Figure 4.12 DSC decomposition curve for PVT-PAN..... | 85 |
| Figure 4.13 DSC decomposition curve for PVT-PMA..... | 85 |
| Figure 4.14 DSC curves for GAP-700 a) T _g b) Decomposition..... | 86 |
| Figure 4.15 Polymeric samples after the composting experiment: a) PVT b) PVT-PAN c) GAP-BPM d) GAP-DCHD | 88 |
| Figure 4.16 Mass change for the composted samples..... | 89 |
| Figure 4.17 Soluble fraction results for the composted samples..... | 92 |
| Figure 4.18 FTIR Spectra of PVT at depths: a) Surface b) 150 μm c) 300 μm d) 450 μm..... | 93 |

| | |
|--|-----|
| Figure 4.19 FTIR Spectra of PVT-PAN at depths: a) Surface b) 150 μm c) 300 μm d) 450 μm . | 94 |
| Figure 4.20 General equation of the hydrolysis of nitriles to carboxylates | 95 |
| Figure 4.21 FTIR Spectra of GAP-BPM at depths: a) Surface b) 150 μm c) 300 μm d) 450 μm | 96 |
| Figure 4.22 FTIR Spectra of GAP-DCHD at depths: a) Surface b) 150 μm c) 300 μm d) 450 μm | 97 |
| Figure 4.23 FTIR Spectra of GAP-BPM extracts | 98 |
| Figure 4.24 FTIR Spectra of GAP-DCHD extracts | 98 |
| Figure 4.25 Solid State ^{13}C NMR spectra for PVT composted samples at 0, 9 and 18 days..... | 99 |
| Figure 4.26 General equation of the elimination of tetrazole groups in PVT | 99 |
| Figure 4.27 Solid State ^{13}C NMR spectra for PVT-PAN composted samples at 0, 9 and 18 days | 100 |
| Figure 4.28 Solid State ^{13}C NMR spectra for GAP-BPM composted samples at 0, 9 and 18 days | 101 |
| Figure 4.29 Comparison of the ^{13}C -NMR spectra of a) BPM b) extract from sample GAP-BPM 18 days c) GAP | 102 |
| Figure 4.30 Solid State ^{13}C NMR spectra for GAP-DCHD composted samples at 0, 9 and 18 days | 102 |
| Figure 4.31 DSC curve for PVT..... | 103 |
| Figure 4.32 DSC curves for PVT-PAN..... | 104 |
| Figure 4.33 DSC curves for GAP-BPM showing: a) T_g b) Decomposition | 105 |
| Figure 4.34 DSC Decomposition curves for GAP-DCHD showing a) T_g b) Decomposition | 106 |
| Figure 4.35 DMA curves for GAP-BPM: a) 0 days b) 9 days c) 18 days E'' (green) and $\text{Tan } \delta$ (red) | 109 |
| Figure 4.36 DMA curves for GAP-DCHD: a) 0 days b) 9 days c) 18 days E'' (green) and $\text{Tan } \delta$ (red) | 109 |
| Figure 4.37 SEM images of PVT during composting, at different magnifications | 110 |

| | |
|---|-----|
| Figure 4.38 Progression of the elemental composition of PVT during composting a) middle of the sample b) surface of the sample | 111 |
| Figure 4.39 SEM images of PVT-PAN during composting, at different magnifications | 112 |
| Figure 4.40 Progression of the elemental composition of PVT-PAN during composting a) middle of the sample b) surface of the sample | 113 |
| Figure 4.41 SEM images of GAP-BPM during composting, at different magnifications | 114 |
| Figure 4.42 Progression of the elemental composition of GAP-BPM during composting a) middle of the sample b) surface of the sample | 114 |
| Figure 4.43 SEM images of GAP-DCHD during composting, at different amplifications | 115 |
| Figure 4.44 Progression of the elemental composition of GAP-DCHD during composting a) middle of the sample b) surface of the sample | 116 |
| Figure 4.45 DSC of ^{15}N PVT in powder and after solvent casting preparation | 116 |
| Figure 4.46 Possible positions of the ^{15}N isotope in the azidation products of PAN..... | 118 |
| Figure 4.47 Solid State ^{15}N -NMR spectra for PVT composted samples at 0, 3 and 6 days | 120 |
| Figure 5.1 Observed biodegradation reactions for PVT. | 124 |
| Figure 5.2 Observed biodegradation reactions for PVT-PAN. | 124 |
| Figure 5.3 Observed biodegradation reactions for GAP-BPM. | 125 |
| Figure 5.4 Observed biodegradation reactions for GAP-DCHD. | 125 |
| Figure 5.5 Graphic summary of the observed biodegradation reactions..... | 126 |

LIST OF SYMBOLS AND ABBREVIATIONS

| | |
|-----------------|--|
| 2A-DNT | 2-Amino-4,6-dinitrotoluene |
| 4A-DNT | 4-Amino-2,6-dinitrotoluene |
| 24-DANT | 2,4- Diamino 6-nitrotoluene |
| 26-DANT | 2,6- Diamino 4-nitrotoluene |
| 2NOH-DNT | 2-Hydroxylamino- 4,6-dinitrotoluene |
| 4NOH-DNT | 4-Hydroxylamino- 2,6-dinitrotoluene |
| ADN | Ammonium Dinitramide |
| AIBN | Azobisisobutyronitrile |
| AMMO | Azidomethyl-3'-methyl oxetane |
| ATR | Attenuated Total Reflectance |
| BABE | Bisfenol A bispropargyl ether |
| BAMO | 3,3'-Bis-azidomethyl oxetane |
| BPHQ | Bis Propargyl Hydroquinone |
| BPM | Bis Propargyl Malonate |
| BPS | Bis Propargyl Succinate |
| CL-20 | "China Lake"-20, hexanitrohexaazaisowurtzitane |
| CPMAS | Cross-Polarized Magic Angle Spinning |
| CSIA | Compound Stable Isotope Analysis |
| CuAAC | Copper(I)-catalyzed Alkyne-Azide Cycloaddition |
| DCHD | 4,4'-Dicyanohepta-1,6-diyne |
| DMA | Dynamic Mechanical Analysis |
| DMF | Dimethyl formamide |
| DNAN | Dinitro Anisole |
| DNT | Dinitro Toluene |
| DSC | Differential Scanning Calorimetry |
| EDS | Energy-Dispersive X-Ray Spectroscopy (also called EDX in some sources) |
| EM | Energetic Materials |
| ETPE | Energetic Thermoplastic Elastomer |

| | |
|--------------|--|
| FTIR | Fourier's Transformed Infrared spectroscopy. |
| GAP | Glycidyl Azide Polymer |
| GEM | Green Energetic Materials |
| GIM | Green Insensitive Munitions |
| GPC | Gel Permeation Chromatography |
| HMX | "High Melting Explosive", Octahydro-1,3,5,7-tetranitro-1,3,5,7-tetrazocine |
| HNF | Hydrazinium Nitroformate |
| HNIW | Hexanitrohexaazaisowurtzitane, also known as CL-20 |
| HSQC | Heteronuclear Single Quantum Correlation |
| IUPAC | International Union for Pure and Applied Chemistry |
| KIE | Kinetic Isotope Effect |
| MAS | Magic Angle Spinning |
| MeCN | Acetonitrile |
| MENA | Methoxynitroaniline |
| MNT | Mononitrotoluene |
| MS | Mass Spectrometry. |
| MW | Molecular Weight. |
| NC | Nitrocellulose |
| NG | Nitroglycerin |
| NIMMO | 3,3-(Nitratomethyl) methyl oxetane |
| NQ | Nitroguanidine |
| NTO | 3-Nitro-1,2,4-triazol-5-one |
| PAAz | Poly Allyl Azide |
| PAC | Poly Allyl Chloride |
| PAN | Poly Acrylonitrile |
| PCL | Poly Caprolactone |
| PECH | Poly Epichlorohydrin |
| PEG | Polyethylene Glycol |
| PLA | Poly Lactic Acid |
| PMA | Poly Methyl Acrylate |

| | |
|---|--|
| PVA | Poly Vinyl Alcohol |
| PVAz | Poly Vinyl Azide |
| PVC | Poly Vinyl Chloride |
| PVN | Poly Vinyl Nitrate |
| PVT | Poly Vinyl Tetrazole |
| RDX | “Research Department Explosive”, Hexahydro-1,3,5-trinitro-1,3,5-triazine |
| ROP | Ring Opening Polymerization |
| SEM | Scanning Electronic Microscopy |
| SPME | Solid phase microextraction technique |
| T_g | Glass Transition temperature. |
| TGA | Thermo Gravimetric Analysis |
| T_m | Melting Point. |
| TNT | 2,4,6-trinitro toluene. |
| UXO | Unexploded Ordnances |
| ΔH_{cryst} | Crystallization Enthalpy Change |

LIST OF APPENDICES

| | |
|--|-----|
| Appendix A SEM images of composted samples | 139 |
|--|-----|

CHAPTER 1 INTRODUCTION

1.1 Research Context

The need for energetic compounds with better performance and stability has pushed the development of better materials in the last decades, for uses in military applications, aeronautics, demolition, etc. The use of chemical methods such as “click chemistry” for the synthesis of triazole and tetrazole groups has facilitated the production of new materials, amongst them the glycidyl azide polymer, or GAP, which can be tuned by crosslinking with dialkynes through triazole ring formation; and compounds derived from polyvinyl tetrazole, or PVT, which are a family of polymers with high nitrogen content. These substances and their formulations are going to be present on the training grounds, either by their deployment, but also by the accumulation and storage of materials no longer apt to be used. The use of these facilities during long periods, implies a build up on the concentration of these substances in the environment.

Various environmental problems have been linked to TNT, RDX and other energetic compounds in the past, like ecotoxicity, biocide effects, and spread of materials with carcinogenic potential in water bodies and soil. These problems must serve as a warning for a more integral development of new energetic materials that would include a “Cradle-to-Grave” perspective in which the optimal performance is researched, but there is also an early assessment of the possible effects on the soil, the ground, and the human health from the conception phases.

Part of the work of our research group has focused on a better understanding of the degradation processes of these macromolecules. The azide group (key to the production of materials through “click chemistry” reactions) has been identified as a toxic moiety and even has been expected to have antimicrobial properties, but it is not clear if some heterocycles like triazoles or tetrazoles could degrade under composting conditions to produce azide compounds. It is also not clear if the heterocycles remain attached to the polymeric backbone during their biodegradation, or if the triazole/tetrazole cycles suffer ring-opening reactions.

During the biodegradation of polymers with pendant groups like tetrazole, triazole or azide, it is unclear if the polymer degrades via either a) a scission of the polymer backbone, b) a loss of the

pendant group or c) an opening reaction of the heterocyclic ring (for the cases of triazoles and tetrazoles). It is difficult to precise if the tetrazole ring is reacting or is just leaving the polymer backbone, as this functional group has a carbon atom with a very small signal in ^{13}C -NMR, and a labile proton with a broad, small signal in ^1H -NMR. One way to surpass these obstacles is the use of a molecular marker in the tetrazole ring. To this purpose, in this study, the sodium azide was substituted with an azide salt in which one of the nitrogen atoms is replaced with a ^{15}N isotope, which was later detected by ^{15}N -NMR.

1.2 Research Objectives

1.2.1 Main Objective

“Evaluation of the effects of the polymer structure on the biodegradability of novel energetic polymers by composting of samples with and without ^{15}N as a molecular label”.

The synthesis and characterization of polymer samples, some of them marked with ^{15}N isotopes is used for assessing the biodegradability in composting conditions of a variety of novel energetic polymers with different functional groups and backbone chains.

1.2.2 Specific Objectives

1- Synthesis and characterization of energetic polymeric molecules through Click Chemistry reactions.

A variety of energetic polymers with different functional groups, and backbones were prepared mostly through “click chemistry”, or through modifications of energetic polymers prepared by this method. The samples were characterized through various techniques, and four of the polymers prepared were selected for the next stage of the project.

2- Characterization of the degradation process of energetic materials during composting experiments.

The degradation of the samples was performed by composting in an environmental chamber for 18 days. Before and after their composting at different times, the samples were characterized by various methods, including FTIR (Fourier's Transform Infrared), DSC (Differential Scanning Calorimetry), and NMR (Nuclear Magnetic Resonance) of proton and carbon.

3- Analysis of the changes on the polymeric samples during composting degradation through isotopic detection with ^{15}N NMR.

The ^{15}N -labeled samples were composted in controlled laboratory conditions, to evaluate the changes in physical and chemical properties, like soluble polymeric fraction due to the degradation, FTIR spectroscopy, and DSC. Also, other changes were assessed by analysis through ^1H -NMR, ^{13}C -NMR, and ^{15}N -NMR. The changes detected in the samples helped determine the earlier stages of the decomposition of the studied polymers.

CHAPTER 2 LITERATURE REVIEW

The large-scale use of any chemical entails environmental concerns at each stage, from the extraction or production, storage, and distribution, to its applications and finally, its disposal. In the past decades, in the light of the different environmental problems caused by humanity, it has become more important to correctly assess the different effects that some chemicals can have in the wellbeing of the natural niches where they are being used, or where they are being disposed of.

In the case of explosives and energetic materials, it is expected that they disintegrate completely during its use; but it is possible for remnants of these materials to remain in the soil or in the water, and accumulate in sites where they are frequently used, as it happened in Camp Edwards in USA, or Cold Lake in Alberta.

2.1 Explosives and Energetic Materials

The combustion of materials is a chemical reaction between said material (a fuel) and an oxidizer (usually oxygen, or oxygen-rich substances), occurring at high-temperature with the release of heat and oxidized, often gaseous products, that may produce a flame. If the combustion occurs as a subsonic process, it is called “deflagration”, and there is propagation through heat transfer, for example flames and most of everyday fires. Meanwhile, a “detonation” is a supersonic combustion with an exothermic front that drives a shock in front of it as it propagates. [1]

Explosive materials (or explosives) are materials that store high quantities of potential energy (either by means of chemical energy, pressurized gas, or and nuclear energy) and are capable of detonation, releasing this energy very quickly, when a stimulus is applied, producing heat, gas expansion, sound, etc. at rates higher than the speed of sound. [2]. Explosives are typically divided in “primary” and “secondary”, according to their susceptibility to initiation. The term primary explosives, or “initiators” is used for substances that detonate when a stimulus is applied, like heat, friction, electricity, or mechanical shock, and are used in small quantities to prime the combustion or detonation of the main explosive [3].

Meanwhile, the Secondary Explosives are the main explosives, and they are relatively insensitive to shock, friction, or heat, and are detonated by the primary explosive. These substances can be subdivided in two categories: (1) “melt-cast explosives”, based primarily on TNT, which is melted and used to suspend the other components of the explosive formulation; and (2) “plastic-bonded explosives” (PBX), which consist of a polymer matrix filled with a crystalline explosive such as RDX. Another possible classification of secondary explosives is by structure: TNT and trinitrobenzene are classified as nitroaromatic, while RDX and HMX are nitramines. [4]

The term “Energetic materials” includes explosives, pyrotechnics, and propellants. Energetic materials are the chemical compounds or compositions containing functional groups like nitro NO_2^- , perchlorate ClO_4^- and azido N_3^- that by virtue of containing both fuel and oxidizer, can release significant amounts of energy in a short period of time when certain stimulus (thermal, mechanical or electrostatic) is applied, usually with the formation of various moles of gas per mole of the substance [5]. These materials can be “nitrogen-rich”, having molecular structures with high nitrogen-to-carbon proportion. The majority of the energetic materials have high concentration of nitrogen atoms, mostly in functional groups like nitro NO_2^- , nitrate NO_3^- and azido N_3^- , being the nitro group the most used, either in nitroaromatic compounds like TNT; nitroamines like RDX, HMX and CL-20; or nitrate esters like PETN, NG and NC [6]. Some examples of nitrated energetic materials are presented in Figure 2.1.

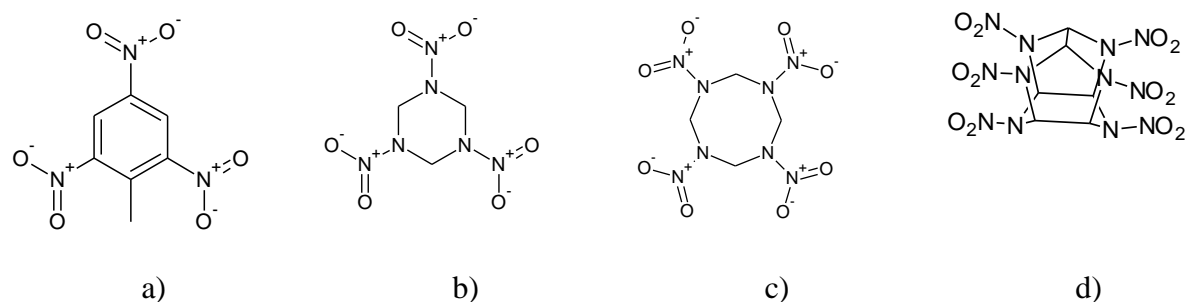


Figure 2.1 Energetic Materials used as explosives: a) TNT b) RDX c) HMX d) CL-20.

Other kinds of energetic materials are propellants and pyrotechnics. Propellants include gun propellants and rocket propellants, which consist of a rubbery substance, known as “binder”, in which are encapsulated the oxidizer and the fuel. Propellants can also be based on nitrate esters

like nitroglycerin and nitrocellulose, or nitramines like RDX and HMX. On the other hand, pyrotechnics include flares (for signaling or illumination), smoke generator, tracers, fuses, etc. The composition of these substances depends on their use: for example, illuminating flares contain NaNO_3 , magnesium and a binder, while signaling flares contain nitrates of other metals like barium or strontium; and smoke generators are usually composed of red and white phosphorous and organic colorants in the case of colored smoke [4].

Probably the most famous of the energetic materials is trinitrotoluene, TNT, which was prepared by Julius Wilbrand for the first time in 1863 and it became highly appreciated by its insensitivity to shock and friction, which reduced in great measure the risks of accidental detonation [2]. It has been criticized as a strong pollutant right from its synthesis and purification to its disposal and degradation products. During its synthesis, toluene is nitrated with nitric acid in the presence of sulphuric acid, which sometimes produces undesirable nitration in the position “meta” (3-nitro toluene in Figure 2.2), giving rise to other asymmetrical isomers of TNT: 2,4,5-, 2,3,4-, 2,3,6- 2,3,5- and 3,4,5-. The desired 2,4,6-isomer is usually purified by reaction of the mixture with sodium bisulfite, which produces water streams with up to 30 aromatic pollutants, that has been called “red waters” [7]. The production of this compound was discontinued in the mid-1980’s, but as it was used during the First and Second World Wars, there is still a high amount of it in unexploded and stored ammunitions, as well as a pollutant in warzones. A comparison of physical properties of various energetic materials is shown in Table 2.1.

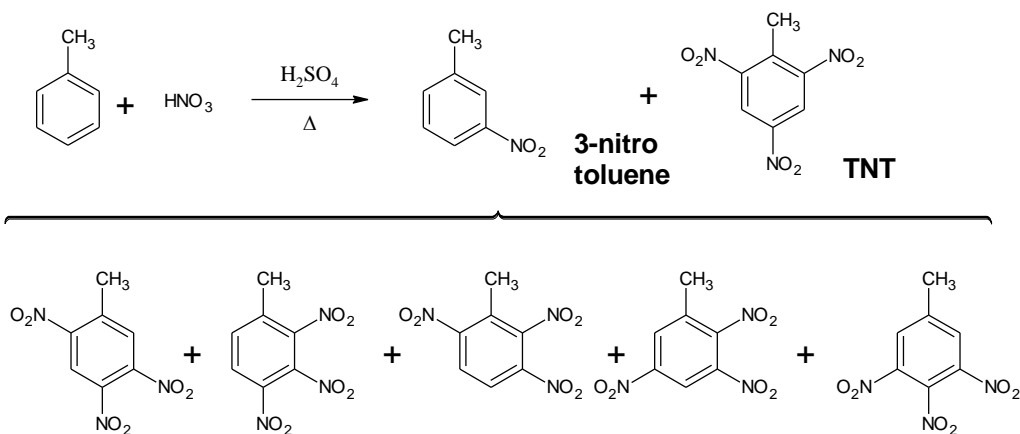


Figure 2.2 Secondary products on the synthesis of TNT

The energetic compound RDX (“Research Department Explosive”, Hexahydro-1,3,5-trinitro-1,3,5-triazine) was first developed in the 1930’s in UK as a better alternative to TNT against German boats [2], being now one of the most used explosives because of its high output. Closely related to RDX, HMX (“High Melting Explosive”, Octahydro-1,3,5,7-tetranitro-1,3,5,7-tetrazocine) is prepared by nitrolysis of the former, but as an energetic material, it is only used for military purposes and it has a higher melting temperature than RDX and a higher detonation velocity than RDX, being that the velocity at which the shock wave front travels through the explosive at detonation [8].

Table 2.1 Physical properties of TNT, RDX and HMX [8, 9]

| Compound | Density (g/cm³) | Melting point (°C) | Detonation Velocity (mm/μs) at density (g/cm³) |
|-----------------|---------------------------------------|-------------------------------|--|
| TNT | 1.65 | 80.8 | 6.9 at 1.60 |
| RDX | 1.82 | 204 | 8.75 at 1.76 |
| HMX | 1.96 | 275 | 9.10 at 1.9 |
| CL-20 | 2.04 | 273 | 9.5 at 2.04 |

More recently, CL-20 (“China Lake”, HNIW or hexanitro hexaaza isowurtzitane) was developed at the end of the 1970’s decade, and it was found that it produces 20% more energy than RDX and HMX, while producing less smoke, so it has been proposed as a substitute for those nitramines [2, 10].

Energetic materials can also be polymers, in which case, the possibility of controlling the number of monomers in the polymeric chain allows the design of polymeric materials with tunable physical and chemical characteristics. It is of interest that the structures of energetic polymers maximize the nitrogen content, either by having monomers with short alkylic chains, or by having a high amount of side groups that give the polymer explosive properties (“explosophoric” groups) consisting of functionalized nitrogen atoms, like nitro, nitroso, azo and azide groups [11].

Some of the most known energetic polymers (Figure 2.3), are the azide polymers BAMO (3,3-bis(azidomethyl) oxetane), AMMO ((3-azidomethyl 3-methyl) oxetane) and GAP (glycidyl azide polymer); and the organic nitrate NIMMO (3-nitratomethyl methyl oxetane). These energetic

polymers are used in binder formulations, increasing the compatibility between the different explosive components, without “diluting” its explosive energy[6].

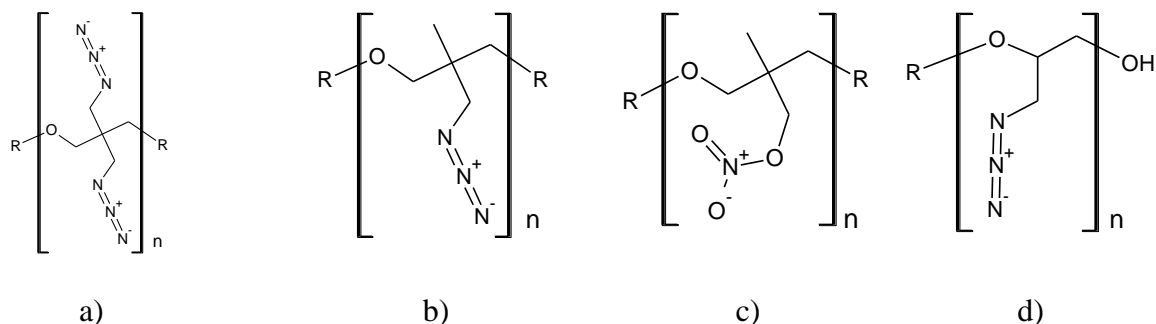


Figure 2.3 Structure of a) Poly (BAMO) b) Poly(AMMO) c) Poly(NIMMO) d) GAP

In the case of Poly-(BAMO), Poly-(AMMO) and GAP, they are prepared by the use of sodium azide, which presents some risks for their use and preparation in laboratories and industries, both in terms of safety and toxicity. The use of NaN_3 in acid conditions produces hydrazoic acid HN_3 which is highly toxic and explosive.

While NaN_3 has been used as a mutagenic agent to promote higher species variety in agriculture [12, 13], it is also highly toxic with a fatal dose for humans in exposures over 10 mg/kg, being deadly for individuals with hypotension under exposure conditions of more than an hour [14]. Other health effects include mild nausea, vomiting, diarrhea, temporary loss of vision, temporary loss of consciousness or mental status decrease.

Glycidyl azide polymer, GAP

Glycidyl azide polymer, GAP, is economic to produce and has excellent binder properties, which makes it an available energetic polymer [15], only surpassed by nitrocellulose. This azide polymer was first synthesized in 1972 by Vanderburg and its potential as an energetic material was discovered in the early 80's [16]. It consists typically of low molecular weight chains of around 5 to 50 monomers each [17], being this one of the reasons why it has to be cured to be used in energetic applications. In this polymer, with positive heat of formation of +117.2 kJ/mol [18], each one of the azido groups contributes with a heat release of about 350 kJ per unit of azide [19], while GAP itself is an insensitive and thermally stable polymer. The synthesis of GAP is performed by

the azidation of poly epichlorohydrin PECH with NaN_3 , with typical number average molecular weights (M_n) between 500 and 5000 g/mol [20] for the cationic ring opening polymerization. These advantages make this polymer a promising option as a binder in explosive formulations, as it could replace inert hydroxyl-terminated polymers like hydroxyl-terminated polyether (HTPE) and hydroxyl-terminated polybutadiene (HTPB), and it has been proved that by crosslinking of GAP with the latter through reaction with diisocyanates, the stability of the mixtures can be improved [21]. Still, the performance of GAP has to be improved, as it has a limited combustion capability at low pressures, which limits its application for example as a solid fuel [17].

Commercially, GAP is available in two product families depending on its ring-opening polymerization: “GAP-triol” if glycerol was used, and “GAP-diol” if ethylene glycol was used [22]. In both cases, the epichlorohydrin ECH is polymerized into polyepichlorohydrin (PECH), which is then made react with sodium azide to form the GAP polymers, as seen in Figure 2.4

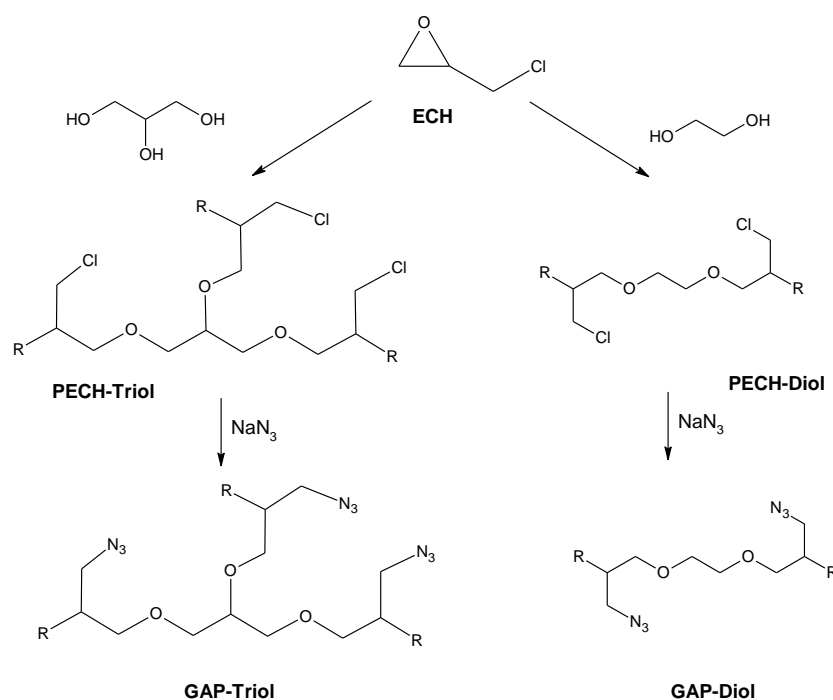


Figure 2.4 Synthesis of GAP-Triol and GAP-Diol from epichlorohydrin

GAP has also the advantage of being compatible with other energetic compounds like CL-20, RDX and HMX, as well as having different possibilities for the improvement of its performance: either

by being grafted into HTPB, or grafted with PEG and crosslinked with PCL or with isocyanates in the OH end-groups [18, 23]; or crosslinked with dialkynes like bis propargyl succinate (BPS), bis propargyl malonate (BPM), bis propargyl hydroquinone (BPHQ), bisphenol A bispropargyl ether (BABE), amongst others. These advantages are important for example in the propellant industry, because as new compounds are being produced to substitute former propellants like ammonium perchlorate, it is desirable to use energetic binders to replace the inert ones, like HTPB [24]. Nevertheless, the crosslinking of GAP is an exothermic reaction, so the conditions have to be controlled to ensure safety during the preparation, especially in case of scaling-up [17], to prevent the formation of hotspots that would difficult the heat load dissipation and might result in ignition of the mixture even in small batches.

Recently, the group of Athar reported the curing of GAP with acrylates for binder applications [25], by means of a reaction between GAP-diol and hexanediol diacrylate, which showed better properties than the sample cured with isocyanates. The resulting polymer has triazoline units instead of the triazole units typical of the crosslinking with bisalkynes. It was found that the stability of the acrylate-cured polymer was lower than that of the bisalkyne-cured polymers, as the formed triazoline rings evolved nitrogen gas over time, which lead to the formation of voids in the finished product.

The other polymers (AMMO, BAMO, and NIMMO) are prepared by more complicated synthetic routes that sometimes require the opening of the oxetane cycle (1,3-propylene oxide) after either the nitration or azidation of the monomer. These polymers, as with GAP, have been studied for binder applications in energetic formulations, as they have low viscosities and good mechanical properties after cross-linking. Nowadays, these polymers are usually used as copolymers, providing improved binding properties for solid formulations, while considering some characteristics like the high crystallinity of Poly BAMO, which limits its use as a homopolymer, requiring the co-polymerization of BAMO with the relatively less energetic AMMO or NIMMO to decrease the melting temperature and the glass transition temperature [6].

In the search for new options for energetic materials, the desired compounds must possess a high amount of explosives groups and be stable. One of the options studied has been the

azaheterocycle family, especially the triazoles and tetrazoles rings (Figure 2.5). The interest for polymers with these functional groups has pushed forward the research towards better synthesis procedures and different configurations that exploit the high nitrogen content of these compounds [26]. For example, the group of Kizhnyayev [27] prepared compounds with linear or branched geometries with a nitrogen content of up to 68%, by grafting poly vinyl polymers with either 5-chloromethyl tetrazole or 5-(β -chloroethyl) tetrazole.



Figure 2.5 Structure of a) 1,2,3 triazole b) 1,2,4 triazole c) tetrazole d) Poly vinyl tetrazole PVT

Poly Vinyl Tetrazole, PVT

Poly vinyl tetrazole (PVT) is a polymer synthesized in the 1960's, at first from the polymerization of vinyl tetrazole, but more recently by reacting polyacrylonitrile with sodium azide in the presence of ammonia chloride in a single step (Figure 2.6) [28], resulting in an almost quantitative transformation of the polymer. It has been reported that a conversion of 18% of the nitrile groups on the original polymer provides rubber-like properties, while at conversion rates 43%, the polymer becomes stiff and brittle [16].

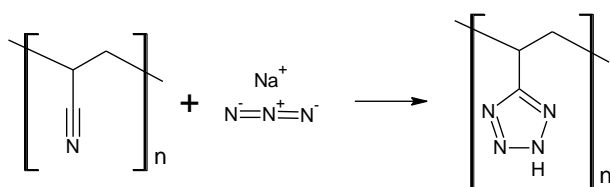


Figure 2.6 Scheme of formation of Poly Vinyl Tetrazole from Poly Acrylonitrile.

The tetrazole ring presents aromaticity, and it has a behaviour similar to pyridine, with a relatively high acidity (pKa around 4) [29], and it presents various possibilities for the modification of the polymer, including metal-containing species and alkylation in position 1 (with electron-donating substituents) or position 2 (with electron-accepting substituents) among other reactions [30]. The

fact that this molecule contains 58.3% nitrogen in weight, paired with its high stability and easy preparation, makes it a high-nitrogen molecule, and a very good candidate for energetic material preparations [26].

This polymer and its copolymer with polyacrylonitrile (known as PVT-PAN) with different percentages of the nitrile groups turned into tetrazoles, can be used in other applications besides as an energetic material, for example the absorption of CO₂ in hydrophobic membranes [31], or in the preparation of ultrafiltration membranes for heavy-metal ions absorption in water purification [32, 33]. For example the group of Chen [34] found that a poly-vinyltetrazole-grafted resin had high capacity for adsorption of heavy-metal ions like Pb²⁺, Cu²⁺ and Cr³⁺ from aqueous solutions to a maximum absorption of 1.52 mmol/g for lead, 2.65 mmol/g for copper and 3.36 mmol/g for chrome at pH 5.0. These results are similar to the ones found by the group of Yan with PVT-PAN membranes obtaining maximum adsorption capacities of 323 mg/g Cu²⁺, 278 mg/g Cd²⁺, 200 mg/g Ni²⁺, and 175 mg/g Zn²⁺ [35].

PVAzide, PVAz

Poly vinyl azide (Figure 2.7a) is synthesized by nucleophilic substitution on polymers like polyvinyl nitrate PVN [36], tosylated PVA, or polyvinyl chloride PVC [37] in an inert organic solvent like dimethylformamide at 20 - 80°C. The monomer, vinyl azide, is a sensitive liquid with a boiling point of 30 °C. This methodology was used also by the group of Ouerghui [38] to synthesize a copolymer of PVC and PVAz by partial substitution of chlorine atoms on PVC by sodium azide, as a precursor for a triazole-based co-polymer. It has been shown that in this kind of synthesis, the chlorine atoms in secondary positions were susceptible to elimination products, decreasing the yield and causing crosslinking [39]. This undesired crosslinking instead of the addition of an azide group, would decrease the nitrogen-to-carbon ratio, that is important for the performance of energetic materials.

Poly vinyl nitrate, PVN

Polyvinyl nitrate (PVN, Figure 2.7b) is a polymer, whose monomer (CH₂=CHONO₂) is practically unknown [36], and is usually prepared by nitration of PVA with a mixture of acids, mainly

sulphuric. Pure PVN has been found to be more stable than NC and has been added to improve mechanical properties in composite propellants [11]. Nevertheless, because of PVN having lower tensile strength and increased elongation, it is not acceptable as a replacement for NC [40].

Poly glycidyl nitrate, “Poly Glyn”

This liquid polymer has been used as a binder and can be seen as a nitrated version of the GAP polymer (see Figure 2.7c), and the glycidyl nitrate monomer is prepared by different synthetic routes. For example the nitration of the glycidol using N_2O_5 with high yields [40]. The monomer is then polymerized with a Lewis acid, generally BF_3 in ethyl ether or tetrahydrofuran, and the polymer, a pale yellow liquid, is later on cured with diisocyanates to produce a rubbery material [11]. This polymer imparts high density, high energy, and low vulnerability to both explosive and propellant formulations [16].

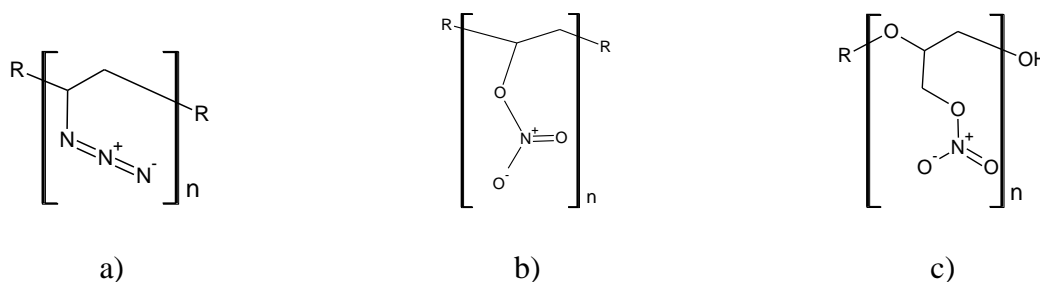


Figure 2.7 Structure of a) Poly Vinyl Azide PVAz b) Poly Vinyl Nitrate PVN c) Poly Glycidyl Nitrate, “Poly Glyn”

2.1.1 Research of New Energetic Materials

Several formulations of energetic materials have been developed with the goal of improving the performance of materials like TNT or RDX. One example is the GIM (Green Insensitive Material) formulation investigated by the Canadian Department of National Defense, as reported by Monteil-Rivera and her group [41], consisting of 51.5% HMX, 40.7% TNT and 7.8% of ETPE (“Energetic Thermoplastic Elastomer”) as a binder. The performance of this formulation is similar to that of the Octol formulation (70% HMX and 30% TNT). The study of dissolution rates in batches and

long-term dripping showed that GIM presents the advantage of dissolve more slowly in water than Octol, which would decrease the risk of explosives leakage from particles and would make the collection of unexploded particles easier. The slower solubilization of the GIM formulation might be due to the ETPE binder, which has a very low water solubility, preventing the particles of the formulation from collapsing, and retarding the dissolution of HMX and TNT by limiting their exposure to water.

In the last decades, it has been confirmed that the use of classic explosive materials like TNT or RDX has negative effects on the environment and in the human health, which has prompted the development of new energetic materials with physical properties and performance comparable to the ones of the compounds to be substituted. For example, it would be desirable for the new explosives to have melting points around 85 °C like TNT, which would facilitate the preparation of explosives by melt casting.

The development of insensitive explosives in the last years has focused in two families: the first one is polymer-bonded cast-cured explosives, and the second is the use of insensitive melt cast explosives, mostly based on 2,4-dinitro anisole (DNAN), nitroguanidine (NQ) and 3-nitro-1,2,4-triazol-5-one (NTO) [42, 43], shown in Figure 2.15.

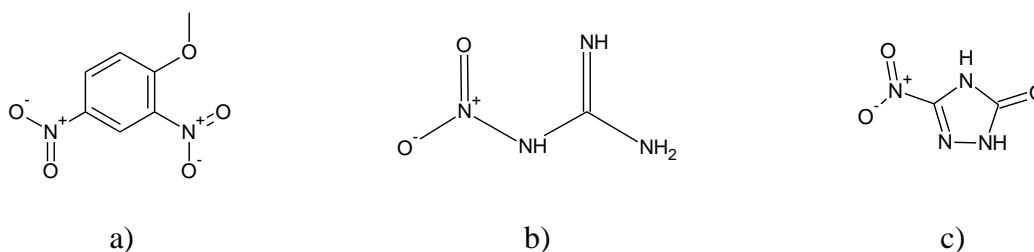


Figure 2.8 Structure of a) Dinitro anisole (DNAN) b) Nitroguanidine (NQ) c) 3-Nitro-1,2,4-triazol-5-one (NTO)

Some research has been done for the synthesis of derivatives of 5-nitrotetrazoles as energetic materials [16, 44], aiming towards the preparation of bridged bistetrazole compounds with melting points between those of TNT and RDX, and a thermal stability similar to that of RDX. These bridged bistetrazoles were soluble in water and some of them are promising insensitive energetic materials with good performances, especially 5-(5-nitrotetrazol-2-yl methyl) tetrazole. Besides CL-

20 discussed before, other compounds of interest because of their promising properties, are FOX-7 (1,1-diamino-2,2-dinitroethene) [45], FOX-12 (N-guanylurea-dinitramide) [46], and TKX-50 (dihydroxylammonium 5,5'-bistetrazole-1,1'-diolate) [47], shown in Figure 2.9, being salts the last two.

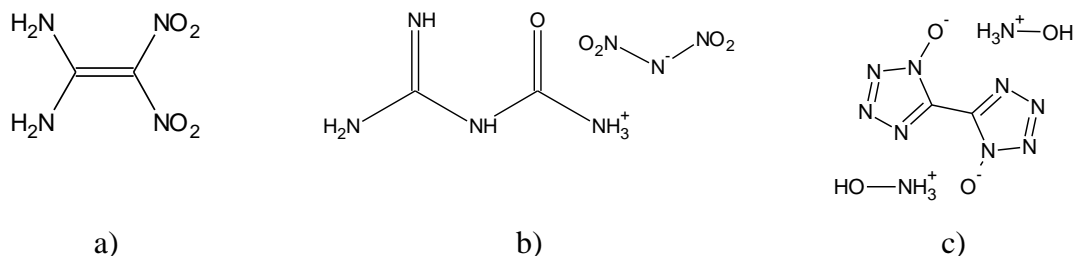


Figure 2.9 Structures of a) FOX-7, b) FOX-12 and c) TKX-50

2.2 Synthetic techniques for preparation of energetic polymers

The different synthetic techniques used for common polymeric materials can also be used for the preparation for energetic polymers. The usual strategy is the polymerization of a monomer which already has good energetic properties, while another is the modification of the polymeric chains to increase their energetic properties, by the addition of explosives groups, or modification of functional groups by oxidation, among others.

In the following sections, are shown different techniques and reactions for the preparation of energetic materials:

- Polymerization techniques: Step-Growth, Ring-Opening, and Addition
- Nitration
- Modification of polymers: Isocyanate Curing, Alkyne Curing

2.2.1 Polycondensation or Step-Growth Polymerization

The polycondensation or step-growth polymerization synthesis is the process in which the polymeric chain grows slowly by the combination of monomers into dimers, and then the combination of dimers, trimers or oligomers [48]. The most common condensation reaction for the synthesis of polymers is the “Fischer’s condensation” (Figure 2.10): an esterification reaction between a carboxylic acid and an alcohol. One disadvantage of this process is that the reaction is an equilibrium, which decreases the reaction yield unless an excess of reagents is used. Another problem is that for each ester group formed, one molecule of water will be produced, which can cause secondary reactions (like eliminations or additions), or form a second layer during the reaction, resulting in the separations of the reagents. As an alternative, the carboxylic acid can be substituted by halides of acyl or by anhydrides, forming volatile hydric acids or carboxylic acids, depending on the substance. In the case of the acyl halides, these substances are sensitive to humidity and will produce a molecule of hydric acid for every ester group formed, which requires neutralization during the work-up process. On the other hand, the use of an anhydride would form a second carboxylic group with lower reactivity as a sub product.

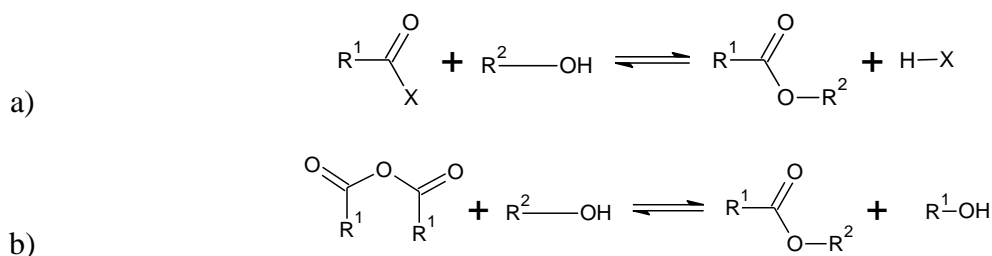


Figure 2.10 Scheme of a Fischer’s Condensation between a) an alcohol and either a carboxylic acid (X=OH) or an acyl halide (X=Cl, Br, I) b) an anhydride and an alcohol

Another common condensation reaction used in the final casting of a composite propellant is the reaction of hydroxyl groups with isocyanate groups to form urethane groups in a polymer consisting of monomers linked by a carbamate functional group (Figure 2.11a). Because of the high reactivity of the isocyanate group towards hydroxyl moieties, the reaction conditions must be anhydrous. In the production of polyurethane foams, a carefully measured amount of water in the

mixture generates the carbamic acid, that decomposes to carbon dioxide and heat (Figure 2.11b), acting as a foaming agent. The formed urethane groups can be used as linking groups between monomers or as crosslinking bonds in curing reactions for polymers that have poor mechanical and physical properties. The curing of polymers is discussed in detail in another section.

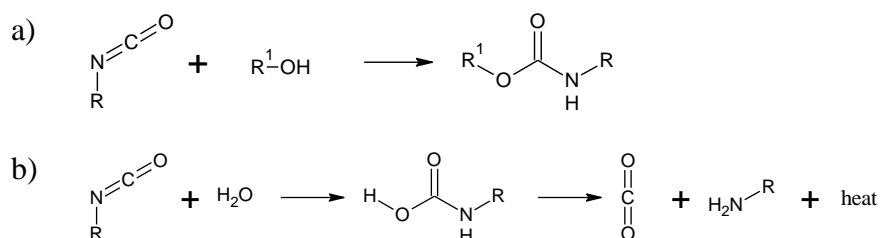


Figure 2.11 Scheme of the reaction of an isocyanate and a) an alcohol to form a urethane b) water, to form an amine

2.2.2 Ring Opening Polymerization

The Ring-Opening Polymerization (ROP) takes advantage of the usual high reactivity of compounds with highly strained cycles, especially those with three or four-member rings. For example, in the case of the synthesis of polymers derived from PECH using epichlorohydrin, whose three-member ring, an oxirane group, produces an active nucleophile when the ring is opened as can be seen in Figure 2.12, usually in the presence of a catalyst.

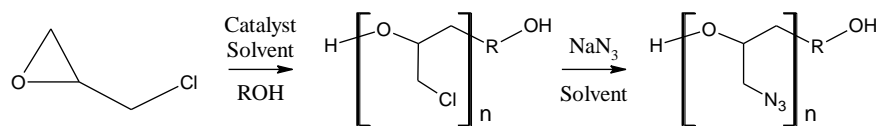


Figure 2.12 Synthesis of PECH by Ring-Opening Polymer followed by azidation to produce GAP

Other energetic polymers that can be prepared by ROP are those based on oxetane rings, like AMMO, BAMMO, and NIMMO (Figure 2.3). These oxetane-based polymers can be synthesized

by two main routes that will be illustrated using the poly (BAMO) molecule as an example: the first route is the azidation of a halo-oxetane (usually chloro-) with sodium azide, followed by the polymerization in the presence of a Lewis acid and an alcohol as initiator as seen in Figure 2.13a. The second synthetic route is to perform first the ROP followed by the nucleophilic substitution (Figure 2.13b) [49].

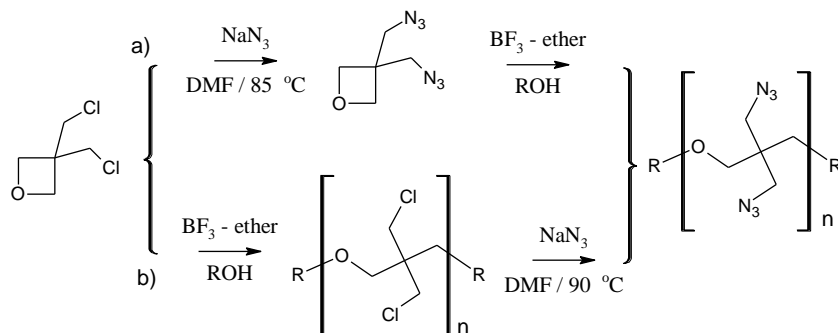


Figure 2.13 Scheme for the synthesis of Poly BAMO: a) Azidation and then ring opening polymerization b) Polymerization preceding the azidation.

2.2.3 Radical Polymerization or Addition Polymerization

One of the most common methods to form polymers is using substances that decompose homolytically, producing radicals that attack monomers in the propagation stage of the reaction. This methodology is especially used to polymerize monomers with double bonds, being the most used the vinyl derivatives [48]. This process, known as radical polymerization, implies first the formation of the free radicals, by light or by heating, and can be done with compounds like azobisisobutyronitrile (AIBN), peroxides, etc. After this, during the initiation step the free radical attacks the monomer, forming a new radical which in the following step known as propagation, will in turn attack another molecule of monomer, forming a larger radical. Some other side reactions can produce chain transfer in certain conditions, and the reaction will be completed when two radicals react to form a bond, in the termination step.

One example of free-radical polymer production is polyacrylonitrile, PAN shown in Figure 2.14, produced from acrylonitrile by use of a radical initiator, for example AIBN

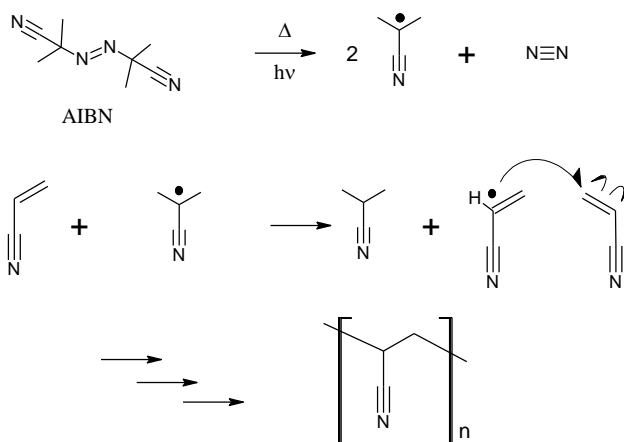


Figure 2.14 Scheme of the free-radical polymerization of acrylonitrile in the presence of AIBN to form PAN

2.2.4 Nitration of materials

The nitration process of different molecules with sulphuric and nitric acids has been used for a long time but is ineffective in deactivated molecules. Perhaps the most famous nitrated energetic material is TNT (Figure 2.1a), first used as a dye, and prepared by reaction of toluene with nitric and sulphuric acids, producing a very stable solid that can be melted and molded. Also, the wastewaters of this process, which in the case of TNT production are known as “rose-waters” represent a serious pollution threat [19].

Some of the first materials to be used for energetic applications proceed from biological materials, as is the case of nitrocellulose (NC) and nitroglycerin (NG) (Figure 2.15), which are produced by the reaction of concentrated nitric acid and cellulose and glycerin, respectively. For example, NC was selected as the obvious option to be used as a binder. Nevertheless, NC has a very low elongation at sub-ambient temperatures. Also, in the case of NG, it presents the disadvantage of being highly sensitive to external stimuli and to detonate easily by friction and impact [15, 50].

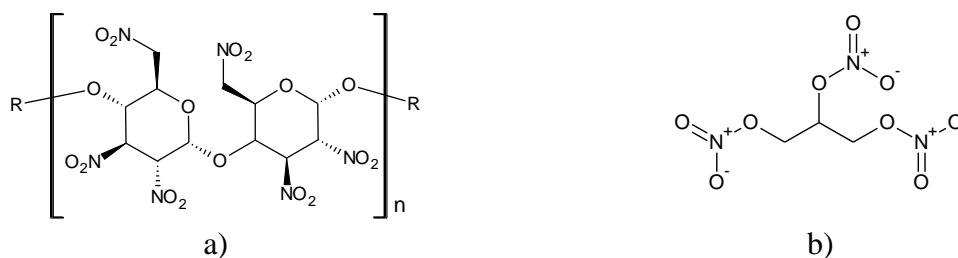


Figure 2.15 Structure of a) Nitrocellulose (NC) b) Nitroglycerin (NG)

The nitration of substrates is still a reaction of interest in the field of energetic materials but presents several disadvantages: the harsh conditions of the typical nitration with sulphuric and nitric acid, the low selectivity of the reaction, and the toxicity of the wastes generated. In the last decade, an example of new nitrating procedure is the use of dinitrogen pentoxide, N₂O₅, by itself or diluted in supercritical carbon dioxide, which can be used at different pressures, giving very high yields [51].

Nitroglycerin continues to be a widely used compound, due to the lower production cost, compared with newer energetic materials. This entails some environmental effects, including pollution emissions into the atmosphere, production of waste and sewage [52], and nitroglycerin's water solubility (1.5 g/L) is expected to make it mobile in soil [53].

2.2.5 Modification of energetic polymers

2.2.5.1 Curing by Isocyanate

In the case of polymers for energetic formulations, the binder components in the formulation must be mixed with solid components like metallic fuels, explosives, and oxidizers. The curing process is shown in Figure 2.16 and it is done typically by forming a functional group known as carbamate or urethane by reacting a hydroxyl-terminated polymer with a molecule with two or more isocyanate groups. These molecules will link two or more molecules of the hydroxyl-terminated polymer, producing a longer, rubbery molecule, with higher viscosity and higher melting point

[54]. In the case of the lysine diisocyanate, it has been shown that the polyurethanes produced are biodegradable and decompose into nontoxic products.

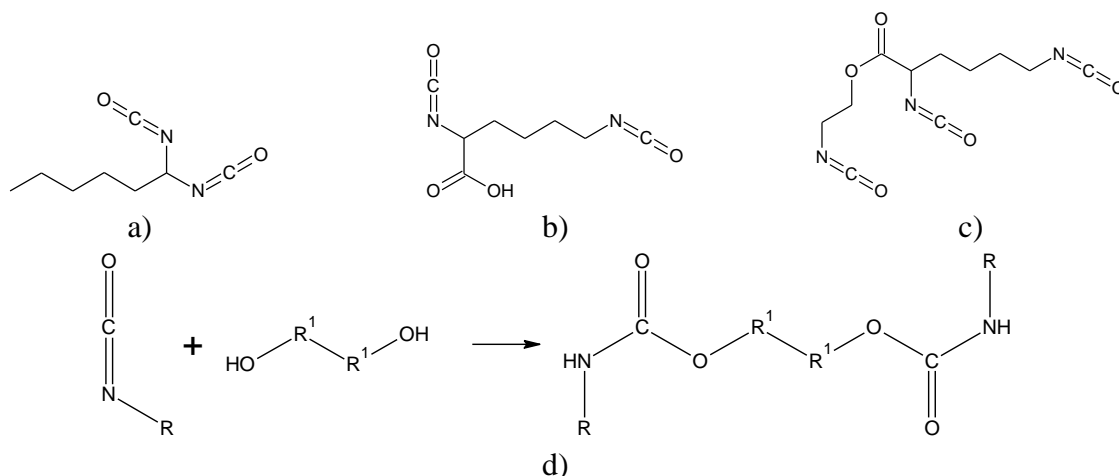


Figure 2.16 Structures of a) Hexamethylene diisocyanate b) Lysine Diisocyanate c) Lysine Triisocyanate d) chain extension reaction between a diol and isocyanates

One of the main problems with isocyanates as curing agents is their reactivity with water, to produce urea derivatives and CO_2 , which can create bubbles on the polymeric matrix, decreasing the mechanical performance of the material [54]. New formulations are using ammonium dinitramide (ADN) and hydrazinium nitroformate (HNF) as oxidizers, which has compatibility problems with isocyanates, generating gaseous products during the curing process; and these gaseous molecules will produce bubbles and voids in the propellant. Therefore, the trend is to look for isocyanate-free curing process that would not present this compatibility problem [55, 56].

2.2.5.2 Curing by Click Chemistry reactions

The term "Click Chemistry" refers to stereospecific reactions with high yields and with by-products that don't need chromatography for their separation, and it was first coined by Barry Sharpless in 1998 and fully described by him and Hartmuth Kolb in 2001[57]. These reactions are simple to perform, without solvent, or with a solvent that is easily removable during the work up. A wide variety of reactions fulfill these criteria, being mostly thermodynamically-favored reactions that lead specifically to one product, like the nucleophilic ring opening reactions of epoxides, or the

non-aldol type carbonyl reactions (such as formation of hydrazones and heterocycles), and the additions to carbon-carbon multiple bonds, for example, the cycloaddition reactions that can be used to synthesize heterocycles.

By this methodology, the azide group can be used to form heterocyclic rings, as seen in Figure 2.17: a) the reaction of NaN_3 with nitrile groups gives out a tetrazole ring, and b) the reaction of organic azides with an alkyne moiety will produce a 1,2,3-triazole ring. This synthetic method, also known as the Copper(I)-catalyzed Alkyne-Azide Cycloaddition (“CuAAC”) is easier than the polymerization of the vinyl tetrazole monomer, which is not available commercially. The cycloaddition reaction can be performed without a catalyst, by means of heating, but in this case, the heterocycle is not regiospecific: for example, the formation of a triazole by this reaction would give a mixture of isomers, while the use of a Copper (I) catalyst forms a triazole disubstituted in positions 1 and 4 [24].

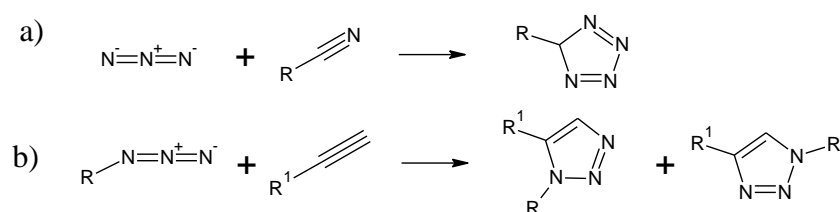


Figure 2.17 Cycloaddition of azide to triple bonds to form (a) tetrazole rings or (b) 1,2,3-triazole rings

One application of these reactions is in the development of hydrogels for the controlled delivery of drugs inside the body of patients: the materials must be biocompatible, degradable inside the body system, but also prepared easily and with a good yield, allowing a range of water content [58]. Another uses of this reaction are the preparation of highly crosslinked PEG-hydrogels [59], or the synthesis of polyvinyl alcohols functionalized with pendant acetylene and azide groups [60, 61], or polymerization between bis-azides and bis-alkynes producing triazoles as the polymeric bond between monomers, and not as crosslinking bonds [62].

Nowadays, the click reaction for the formation of the tetrazole group can be performed under very mild conditions, as can be seen in the study by DeFrancesco and her colleagues, where they synthesize benzyl tetrazoles from aromatic compounds with different substituents by use of a microwave, as an undergraduate experiment in the organic chemistry laboratory [63].

The modification of azide polymers with alkynes through cycloaddition has been explored widely. Recently, the partial substitution of chlorine atoms of PVC with azide groups was performed; and this PVC-PVAz co-polymer was made react with propargylamine to produce a type of PVC-PVT co-polymer, useful for the extraction of metallic ions, with good extraction yields for heavy metals (specifically Cd, Cu, Pb and Ni) [38].

The reaction of GAP with bisalkynes shown in Figure 2.18 results in a crosslinked polymer in which the bridging groups between the chains are triazoles. The reaction between GAP and bis-propargyl succinate (BPS) has been widely studied, as can be seen in the study by Keicher and his groups [55] where BPS was made react with GAP at 65 °C to produce a cured, triazole-crosslinked polymer without the use of isocyanates as curing agents. The amount needed for the curing was less than those needed for curing with isocyanates, with a higher glass transition temperature.

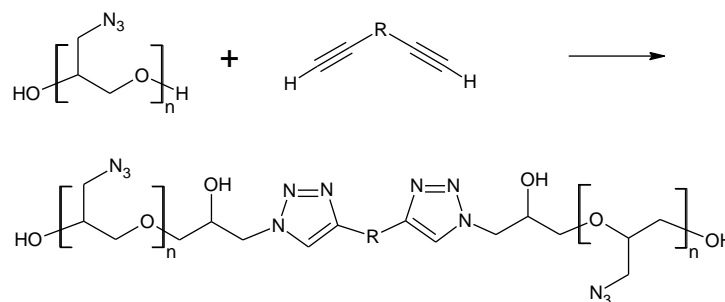


Figure 2.18 Reaction scheme of the crosslinking of GAP with bisalkynes

2.3 Biodegradation and Biodegradable polymers

A review of the literature on energetic materials can prove that the vast majority of the publications focus on the development or performance improvement of them, while a small portion of the total publications concentrates on the environmental assessment of these substances. It has to be noted that these studies are mostly done after the energetic materials have started to be widely used, and

usually concentrate on the possible effects of an accumulation or release of energetic materials into the environment.

2.3.1 Environmental fate and effects of Energetic Materials

According to the United States General Accounting Office, in 2003 it was reported that over 60 000 km² of territory in the United States are suspected or known of being contaminated with military munitions, and at 2009 the estimated costs of assessments and remediation of the contaminated sites was ranging from \$8 billion to \$141 billion. [64, 65]. This situation is an example of the environmental problem that might have all the countries with armed forces. The presence of these materials in the ground comes from training exercises in military facilities, but it is possible that the total amount of pollutant would be higher than that cited before, as it does not consider the pollution in water bodies from underwater detonations, demilitarization processes, or the sinking of military ships.

The environmental fate of a given substance depends on several factors, for example, a high solubility in water may indicate a tendency for the compound to be more bioavailable and contaminate groundwaters; biomagnification may cause concerns about the exposure to predators in high trophic levels, or in human fish consumption. For example, nitroglycerin has a moderate solubility (1.5 g/L) and it is considered persistent at contaminated sites, like the Massachusetts Military Reservation in the USA; and in Canada in Canadian Forces Base sites like Valcartier in Quebec and Gagetown in New Brunswick [53].

In the last decades, the concept of “Green Chemistry” has been proposed to guide the design of the manufacture and use of chemicals, to reduce or eliminate the use and generation of hazardous substances [66], and it is described in the following principles:

1. Prevention: It is better to prevent waste than to treat or clean up waste after it has been created.

2. Atom Economy: Maximize the incorporation of all materials used in the process into the final product.
3. Less Hazardous Chemical Syntheses: Synthetic methods should be designed to use and generate substances that possess little or no toxicity to human health and the environment.
4. Designing Safer Chemicals: Chemical products should be designed to affect their desired function while minimizing their toxicity.
5. Safer Solvents and Auxiliaries: The use of solvents, separation agents, etc. should be made unnecessary wherever possible and innocuous when used.
6. Energy Efficiency: If possible, synthetic methods should be conducted at ambient temperature and pressure.
7. Use of Renewable Feedstocks: A raw material or feedstock should be renewable rather than depleting whenever technically and economically practicable.
8. Reduce Derivatives: Unnecessary derivatization (blocking groups, protection/deprotection, etc.) should be minimized or avoided, to avoid additional reagents and waste.
9. Catalysis: Catalytic reagents (as selective as possible) are superior to stoichiometric reagents.
10. Design for Degradation: Chemical products should be designed so that at the end of their function they break down into innocuous degradation products and do not persist in the environment.
11. Real-time analysis for Pollution Prevention: Development and use of methodologies for real-time, in-process monitoring and control prior to the formation of hazardous substances.
12. Safer Chemistry: Substances and the form of a substance used in a chemical process should be chosen to minimize the potential for chemical accidents, including releases, explosions, and fires.

In the case of energetic materials, their intended use restricts the recycling and proper waste disposal, as they are designed to be disintegrated, and their combustion products are released into the environment, which makes it more important to incorporate the principles of green chemistry

in the design and manufacture of the energetic materials [67]. The synthesis of energetic materials might ensue environmental problems, as was mentioned in the case of the nitration of toluene to form TNT, or the use of N_2O_5 in the synthesis of Poly Glyn. The different characteristics of the energetic materials turn their presence in the environmental problem of great complexity, as the possible effects of them are varied, depending on their properties: for example, the probability of respiratory toxicity might be more pronounced in compounds more easily found in the air, because of their high vapor pressure [5], while the spread of pollution plumes in underground water bodies, would be related to a high solubility in water. It is also noteworthy the fact that as large volumes of water might be needed to produce energetic materials, it is common for the factories to be located near water bodies like rivers. Given the sandy nature of the soils typical of these locations, it is very possible for nitroaromatic compounds to be continually washed out from the soil and end up on the groundwaters. Also, as these soils are usually poor in humic substances, the capacity of TNT or its derivatives for binding will decrease [68].

Some energetic materials and explosives have been identified as contaminants, being the most famous examples RDX (hexahydro-1,3,5-trinitro-1,3,5-triazine), HMX (octahydro-1,3,5,7-tetranitro-1,3,5,7-tetrazocine) [69, 70], and TNT (2,4,6-trinitrotoluene)[71]. These molecules are usually produced by processes that contaminate the soil or water, and they continue to pollute during their storage, or as residues in shooting ranges and training fields, as it has been estimated that around 5% of the ammunition fired during trainings does not explode [72]. Given that at room temperature TNT has a higher water solubility compared to RDX and HMX (130 mg/L for TNT, 42 mg/L for RDX and 5 mg/L for HMX, TNT will penetrate the soil to a greater extent, and might reach underground water bodies forming “pollution plumes”, while RDX and HMX would stay in the upper layers of the soil, with more localized toxic effects [68].

The presence of secondary explosives like TNT, RDX and HMX in soils over 12% by weight might also represent a risk as they are capable of propagate a detonation initiated by flame, and if the content is over 15%, there is a chance of initiation by shock. These compounds can pollute underground water bodies once they are released on the soil or surface water due to their persistence and the fact that in spite of their low water solubility, they possess high mobility caused by the low sorption affinity to the minerals present in the soil in aerobic aquatic environments [68].

For example, in Camp Edwards, in Massachusetts, USA, which has been used for training activities since 1911 with a wide variety of explosive materials, ranging from perchlorates, TNT and RDX/HMX; a plume of RDX-polluted groundwater 3350 meters long by 1500 meters wide, affecting more than 3300 million liters in an area of 2.5 km² [70, 73]. The depth and extension of this pollution case with energetic materials has been thoroughly characterized in terms of the different degradation products for traditional energetic compound, and it can serve as a benchmark case to study other military ranges all over the world. In Canada, the Canadian Forces Base Valcartier was found to be a source of contamination for groundwater because of the use of RDX and the Octol formulation (70% HMX / 30% TNT). It is also noteworthy that in this country, the residues of energetic materials are usually found in antitank ranges, followed in second place by military demolition sites, with RDX concentrations of 90-100 mg/kg. [74]

For its part, HMX has shown to have a slower solubilization rate and a water solubility significantly lower than that of TNT, which means that HMX is not expected to reach underground waters to the same extent as TNT does [41]. Nevertheless, this also makes possible for HMX to be transported on the ground as fine particles or dust, which might pollute a bigger soil surface, as was described by Martel and his team in their study of the presence and distribution of TNT, RDX and HMX at Arnhem Anti-Tank Range in Valcartier Garrison in Québec [75]. It has been found that in conditions of soil contaminated with HMX (for example in anti-tank firing range soil), it can be absorbed by several species of indigenous and agricultural plants and get accumulated in the leaf's tissues, which on one hand suggests the potential of phytoremediation as way to concentrate this pollutant from the soil and avoid its spread [76]. On the other hand, though, it should be considered as a warning sign of its bioaccumulation in trophic chains.

The presence of energetic materials in the environment implies the possibility of being present also in various levels of trophic chains, which will turn into negative effects for human health. For example, the exposure to TNT and its degradation products has been linked to spleen and liver damage, and it has also been identified as a potent mutagen and a Group C carcinogen (possibly carcinogenic to humans, but there is limited animal evidence and little or no human data, according to USEPA) [77], and evidence of toxicity in rodents and higher animals has been found. It has also been shown that TNT and its degradation products get assimilated mostly in root tissues of plants,

and have negative effects on aquatic life, either bacteria, algae, or fish [2]. A similar case has been found for terrestrial plants, producing problems in growth and germination. The lifetime exposure drinking water health advisory limits for TNT are 2.0 µg/L. In the case of RDX, factory workers exposed to it in U.S.A and Europe have suffered from vertigo, convulsions, unconsciousness, and vomiting, but it is not known definitively if this is also the case for HMX. The lifetime exposure drinking water health advisory limits for RDX and HMX are 2.0 µg/L and 400 µg/L, respectively. In the Table 2.2 are summarized the toxicity risks that various energetic materials pose to different ecological populations, based on the published work of Sunahara [65]. The terms High, Medium and Low, are related to how consistent is the risk: for example, TNT shows a consistent ecotoxicity for soil microorganisms, while in the case of soil invertebrates, it depends on the species and the study conditions. In the case of RDX and HMX, it has been shown that these compounds have a low ecotoxicity to plants, but they can get assimilated in the leaf tissues [2], which might cause problems in higher trophic levels.

Table 2.2 Toxicity risk of energetic materials in various ecological receptors

| Compound | TNT | RDX | HMX | CL-20 |
|-------------------------|-------------------|------------|------------|--------------|
| Soil microorganisms | High | Low | Low | Low |
| Soil invertebrates | Medium | High | High | High |
| Water microorganisms | Medium | Medium | Medium | Medium |
| Plants | High ^a | Low | Low | Low |
| Amphibians and reptiles | High | High | High | High |
| Birds | Medium | Medium | Low | --- |
| Mammals | Medium | Medium | Medium | --- |

a Toxicity related to metabolites trinitrobenzene TNB and dinitrotoluene DNT.

In the case of the crosslinking of polymers with isocyanates, it is important to mention also that there might be environmental impacts linked to the isocyanate group itself, given the toxicity presented by various members of this family [78], but also it is necessary to consider the formed polyurethane, as the urethane functional group is present in some insecticides and it is suspected to have activity as an acetylcholinesterase inhibitor in various living beings [79].

2.3.1.1 Triazoles and tetrazoles

The case for triazoles and tetrazoles is interesting, as these functional groups have some appeal from the energetic perspective, being groups with high quantity of nitrogen atoms. But these functional groups have been already used in other applications, for example, the tetrazole ring is of interest as a fragment in a number of modern drugs, like anti-bacterial, anti-allergic, anti-inflammatory, etc. [80], because the tetrazole moiety is a good bioisosteric replacement for carboxylic acids. A bioisosteric replacement is a group that imparts similar biological properties to a chemical compound (usually of pharmaceutical interest), generally not changing the efficacy of an active substance, but changing the pharmacokinetic or pharmacodynamic of said compound [81]. Some bioisosteric replacements are shown in Figure 2.19, showing that triazoles and tetrazoles have been investigated as bioisosteric replacements for amide groups, and carboxylates, respectively [82]. The tetrazole group is uncommon in Nature and does not exhibit any remarkable biological activity, being more metabolically stable than the carboxylic group, and resistant to biological degradation. The interest of tetrazole as a bioisostere of carboxylic acids lies in the more lipophilic behavior of tetrazolate anions, which facilitates the passage of drug molecules through cell membranes [76].

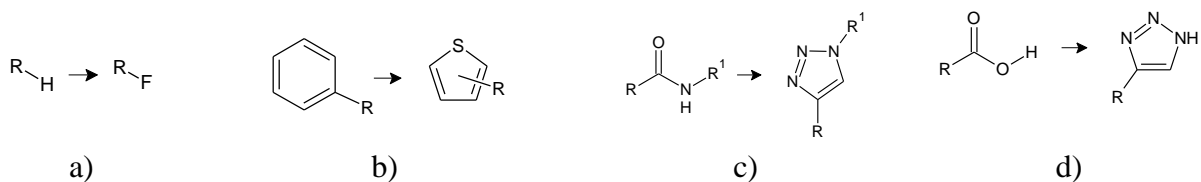


Figure 2.19 Classical bioisosteric replacements: a) hydrogen to fluorine, b) phenyl to thiophene, c) amide to triazole, d) carboxylic acid to tetrazole.

Triazole groups, especially 1,2,4 triazoles, have been used for the preparation of pharmaceutical products that have excellent antifungal activity in the case of invasive fungal infections. However, the triazole drugs can lead to drug-drug interactions, with adverse effects, as it has been seen in ICU critical patients who had received mould-active triazole drugs [83]. Both the triazole and tetrazole groups are present in different compounds used as herbicides and fungicides for agricultural applications, or as pharmaceutical agents, for example, valsartan (Figure 2.20a). The use of all these substances can carry the pollution of soils and water bodies, and their toxicity and biodegradation processes are not fully understood yet [84].

Another important family of compounds with triazole groups is the benzotriazoles, specifically the methyl benzotriazoles (Figure 2.20 b), used in anti-rusting formulations for aircrafts. Both isomers of methyl benzotriazole show poor biodegradability, insensitivity to visible light and poor removal in water treatment plants, implying the possibility of widespread in the soil and water supplies near the affected areas. This situation presents a health risk, as it has been suggested that methyl benzotriazole can cause acute effects on organisms at concentrations of 100 mg/L. [85, 86] . Other studies have analyzed the environmental fate and the effects of triazoles, benzotriazoles and benzotriazole derivatives, and found that these substances are rarely mineralized after 60 days in the soil or activated sludge biomass [87], and have toxic effects in various aquatic organisms [88].

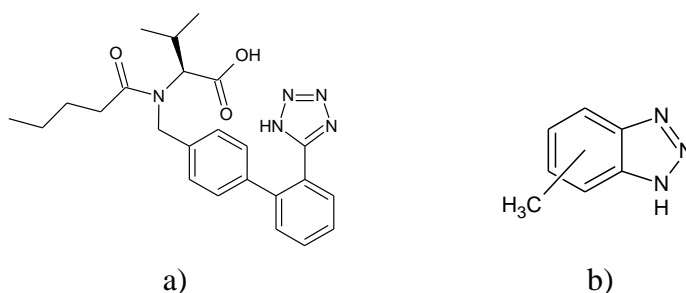


Figure 2.20 Structure of a) valsatan b) methyl benzotriazole

2.3.2 Solutions to the pollution with Energetic Materials

The challenges for the resolution of this pollution problem are varied and they include: a) adequate detection methods and instrumentation, b) treatment of the area to eliminate the contaminant, c) replacement of highly polluting EM and the development of EM that would have lesser impact in the environment.

In terms of the detection techniques, the most used are chromatographic ones, like HPLC (High Performance Liquid Chromatography), CE (Capillary Electrophoresis) or GC (Gas Chromatography), which are applied in studies related to soil or water contamination [89]. In the case of lower concentrations, which is usual in water bodies, solid-phase microextraction technique

(SPME) has proved to be useful to detect high explosives and ignitable liquids with concentration ranges of parts per trillion [90, 91].

After the detection of these contaminants in the ground or in water bodies, the alternatives to alleviating this problem include biodegradation, phytoremediation, composting, and extraction of the contaminants and their degradation products using techniques like supercritical CO₂ or SPME [89]. The biodegradation of energetic materials depends on many factors, including their structure and functional groups. In the case of RDX, for example, the use of “*in situ*” SPME techniques to show that the different biotic and abiotic reactions that the molecule can suffer are determined by the way the nitro-amino moiety is attacked [92], causing two main degradation routes: the first one is the sequential reduction of the molecule; and the second one is the denitration and then opening of the ring.

It has to be considered that up until now, the physical and chemical treatments for remediation, like incineration, adsorption and chemical reduction, have big disadvantages: first, they are really expensive, and second, they end up transferring the pollutants from one phase to another, causing new environmental problems to be solved [68]. In their study of Cold Lake Air Weapons Range in Alberta, Bordeleau and her group report that the behavior of compounds used in army munitions and air weapons, specifically TNT and RDX depends on the proportion of these compounds and in the size of the samples, being more notorious in the case of air force ranges, where the unexploded ordnances (also known as “UXO”) might penetrate the ground and reach underground water reservoirs to depths of ten meters or even deeper [93].

Other solutions to mitigate the pollution by energetic materials are the phytoremediation and the composting. Phytoremediation is the “application of plant-controlled interactions with groundwater, organic and inorganic molecules at contaminated sites to achieve site-specific remedial goals” [94]. As it uses solar energy, it has been said to be very cost-effective as a clean up technique, that can be used in soils, water bodies, groundwater, sediments, etc. Phytoremediation practices can be adapted for decontamination of larger surfaces contaminated with explosives or heavy metals [2], for example the use of conifer plants [95] or aquatic plants

[96] to remove TNT, or the use of transgenic plants for the degradation of RDX and HMX [97, 98].

Composting (also called “humification”) is understood as the accelerated biodegradation of organic materials by means of a controlled environment under a microbial population in a moist and warm soil or soil-like substrate [99]. The composting is usually an aerobic process in the surface of the compost, but in the case of deep or tall columns of material, the process becomes anaerobic, by lack of good aeration. As explained by Spain [100], the pH in the compost should be between 5.5 and 8.0, and it usually reaches a stable value without adding any regulating agents. The optimum moisture content for bacteria in compost is 50-60%, as a moisture content over 60% would cause anaerobic conditions.

There are different methods of composting, ranging from laboratory scale with incubation chambers, to large industrial setups where the temperature increment cause by the self-heating proliferation of microorganisms is controlled by the addition of water and the mixing of the compost. It is also possible to include amendments like agricultural waste product, manure, sawdust, etc., to either include some inoculum of bacteria, or to provide the microbial population a nutrient-rich environment [2]. Several studies have found that different setups of composting experiments, with or without amendments, are capable of degradation of TNT, RDX and HMX [101-104].

Another solution to the ecological problem that the use of EM represent, has been the substitution of compounds for less environmentally harmful substances, for example 2,4-dinitroanisole (“DNAN”) as a substitute for TNT and, which has proved in studies [105, 106] to have a similar or less damaging effect on various algae and bacteria species than TNT.

In the search of energetic polymers that are also biodegradable, various factors must be considered. Some polymers with ester groups, like poly lactides and poly ϵ -caprolactones, are usually considered as biodegradable polymers, but because of their physical and mechanical properties, are not good candidates as energetic binders. One example of a solution is the preparation of a copolymer based on PECH [107], in which the biodegradability was improved by the inclusion of ester groups with either sebacic acid or sebacoyl chloride by firstly substituting the chlorine atom

of the epichlorohydrin with an azide group and then, by crosslinking with poly ϵ -caprolactone triol (PCL triol) and lysine diisocyanate (LDI) to form a thermoset polyurethane (Figure 2.21). The resulting co-poly-(ester/ether) had energetic moieties in the form of azide groups, but the azide group decreased the biodegradability of the polymer.

A similar approach was taken in the development of an insensitive energetic binder by preparing a formulation called GIM (“green insensitive munitions”) [108] using melted TNT, RDX and a co-polyurethane thermoplastic elastomer from the reaction of GAP with 4,4'-methylenebis-phenyl isocyanate. The study of the biodegradability and decomposition of this formulation showed that the potential environmental problems of this formulation, would be due to the TNT content.

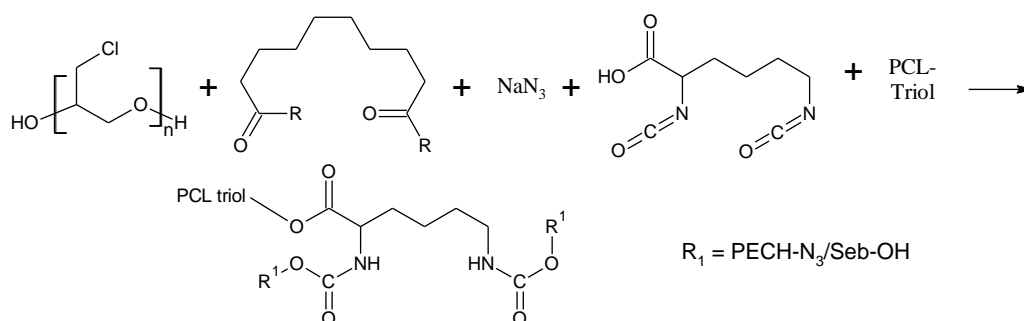


Figure 2.21 Synthesis of a thermoset polyurethane from poly epichlorohydrin (Se=sebacoyl groups; R= OH for sebacic acid, and R = Cl for sebacoyl chloride)

The interest in developing “Green Energetic Materials” (GEM) has been mostly focused on the development of compounds with higher stability, easier to produce, and that generate non-toxic products when they are burned or exploded. Nevertheless, the development of truly GEM has yet to consider the environmental “footprint” not only during the synthesis steps but also during the disposal and decomposition of these materials and their by-products [19], and their compliance to the principles of Green Chemistry. For example, some compounds have been proposed as substitutes for ammonium perchlorate, used as an oxidizer in solid propellants, and has the disadvantage of releasing HCl as a by-product during its combustion. In Figure 2.22 are shown hydrazinium nitroformate (HNF) which has shown compatibility problems with some binders, but

not with GAP and ammonium dinitramide (ADN), which has a smokeless combustion. Contrary to ammonium perchlorate, neither HNF nor ADN produce HCl as a by-product [67].



Figure 2.22 Structures of: a) Hydrazinium nitroformate HNF and b) Ammonium dinitramide

2.3.3 Biodegradability

The environmental problems related to the waste of plastic materials (water bodies contamination, formation of microplastics, etc.) have sparked the search for plastic materials not derived from oil. As a solution, the study of the so-called “bioplastics” has increased in the last years. This term was first used as a descriptor for a material that was at the same time biodegradable and produced from a natural source like crops, agricultural wastes, or by means of bioprocesses. However, the term “bioplastics” is not accurate, as some of these plastics can be bio-sourced, but this does not imply that they are biodegradable. On the other hand, some biodegradable materials can be obtained from synthetic materials and reagents instead of natural or bio-sourced reagents [109].

The term “biodegradable” can be used for different processes of breaking down, as it does not limit the conditions at which the material is treated (composting, fermentation, among others). It is described by the IUPAC as the decomposition of a substance by the confirmed action of microorganisms, leading to the recycling of the carbon atoms, and the release of water, carbon dioxide, salts, etc. [110, 111]. In this interpretation, it is important to remark that for a substance to be recognized as biodegraded, it is not enough a decrease on the molecular weight, but a deterioration to such an extent as to remove undesirable properties of the compound, and even beyond that, a complete breakdown to either fully oxidized (or reduced) molecules, depending on the environment and the conditions for the biodegradation, as the rate of biodegradation depends on the concentration of enzymes, microorganisms, temperature, humidity, pH value, oxygen supply and light [112, 113].

Nevertheless, the complexity of these biodegradation processes sometimes leads to confusion of terms and the use of inadequate techniques. Lucas et al [112] underlined the importance of dividing the biodegradation process into the following stages for a better understanding:

- 1- Biodeterioration: The sum of the actions of microbial communities and abiotic factors to reduce the original material to small fragments (fragmentation).
- 2- Depolymerization: Process in which the microorganisms secrete enzymes and free radicals to destroy the bonds of the polymeric material, generating oligomers, dimers, and monomers.
- 3- Assimilation: It occurs after some molecules enter the cell after being recognized by external enzymes. In the cytoplasm, these molecules are integrated into the metabolism, to produce new biomass, energy, and metabolites.
- 4- Mineralization: Some of the metabolites, simple or complex, are excreted from the cell and reach the extracellular surroundings. Simple molecules like water, methane, carbon dioxide and ammonia, and some salts that are completely oxidized are released into the environment.

It is important to mention that simple physical disintegration or fragmentation of a polymeric material cannot be considered as biodegradation and it could produce microplastics that could remain in the ecosystems for long time and be accumulated in the trophic chain. Still, it is extremely difficult to detect primary degradation products in matrices like soil or compost, due to their complexity; and full mineralization cannot be monitored as the analysis could be altered by the ongoing metabolism of different organisms in the environment [113].

2.3.4 Biodegradability of energetic materials

Even though TNT is slightly soluble in water, it starts its degradation in the soil by action of enzymes of the “Old Yellow” enzyme family; a group of oxidoreductase biocatalysts with a broad capacity to reduce commercially useful substrates, and are used in various applications, for example, the reduction of α,β -unsaturated ketones, and the nitrate ester reduction of nitroglycerin and cyclic triazines [114]. The resulting products tend to react with humic acid and other soil

components, becoming fixated in the soil, not migrating into the underground waters [7, 115]. The degradation path of TNT depends on the bacteria, but it usually implies the reduction of the nitro groups to produce hydroxylamino and/or amino groups, as well as the reduction of the aromatic ring with nitrite release. It has been found also that some of the degradation products of TNT, like dinitro toluenes (DNT) are as toxic or even more toxic than TNT [2]. As can be seen in Figure 2.23, the compost biodegradation of TNT as described by Pennington [116] and Kaplan [117], is mostly the reduction of the nitro groups to produce hydroxyamino dinitrotoluenes (2NOH-DNT and 4NOH-DNT). These compounds can dimerize to produce azoxytetranitro toluenes (marked with an asterisk), or can be reduced to amino dinitrotoluenes (2A-DNT and 4A-DNT) and eventually diamino nitrotoluenes (26-DANT and 24-DANT)

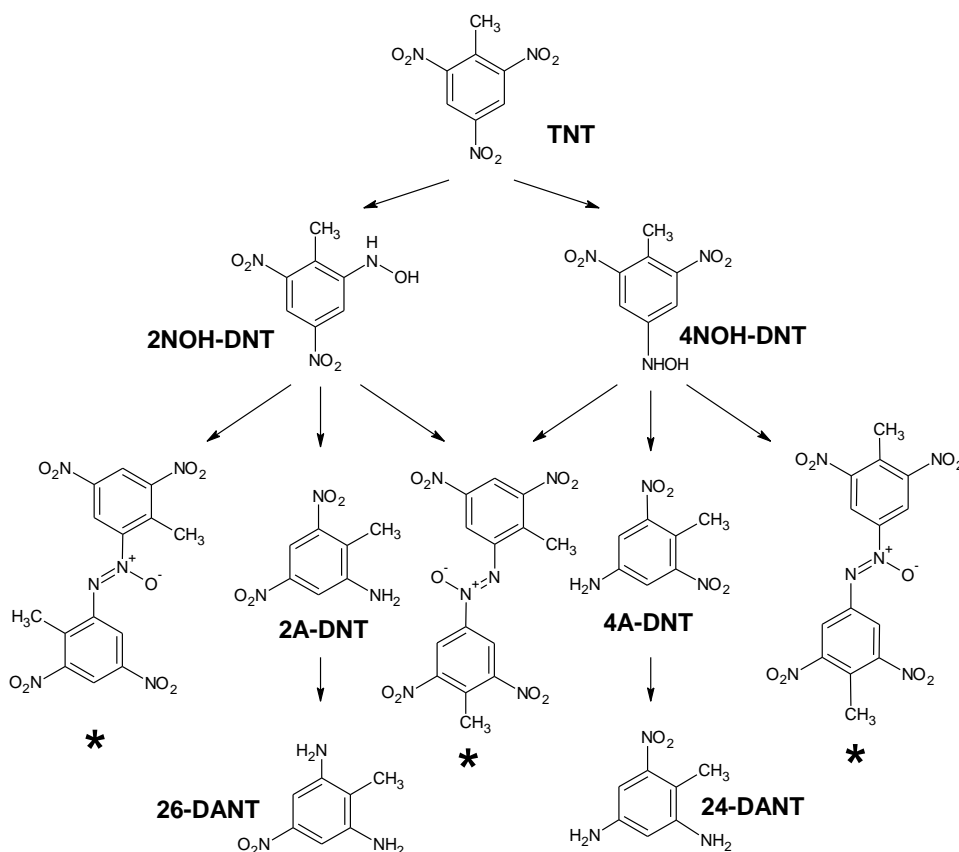


Figure 2.23 Biotransformation of TNT in compost [116]

RDX has a low volatility (vapor pressure of 133.3 Pa at 20°C), meaning that it will only migrate to the atmosphere when in fine dust. It has also been found to have a high mobility in the

contaminated areas, either by migration of its solid particles toward water bodies, or by its water solubility, that although slight, would allow it to infiltrate the soil profile and migrate towards underground water reservoirs [74]. The presence of this compound in the sites might be by incomplete detonation of ammunition, or corrosion and perforation of stored unexploded ordnances; and the expected degradation pathways are by alkaline abiotic hydrolysis, photolysis, and reduction by iron or clay mineral [74].

In the case of RDX and HMX, their biodegradation is usually faster than that of TNT and it is not susceptible to the absence of oxygen, comprising several stages [118]: a) loss of nitro groups and formation of a nitramine free radical; b) reduction of the nitro groups; c) ring cleavage through enzymatic activity; d) either alpha-hydroxylation or hydride ion transfer. The final products are usually nitrite, nitrous oxide, formaldehyde, and formic acid [2]; and all these substances can represent an environmental risk due to their toxicity.

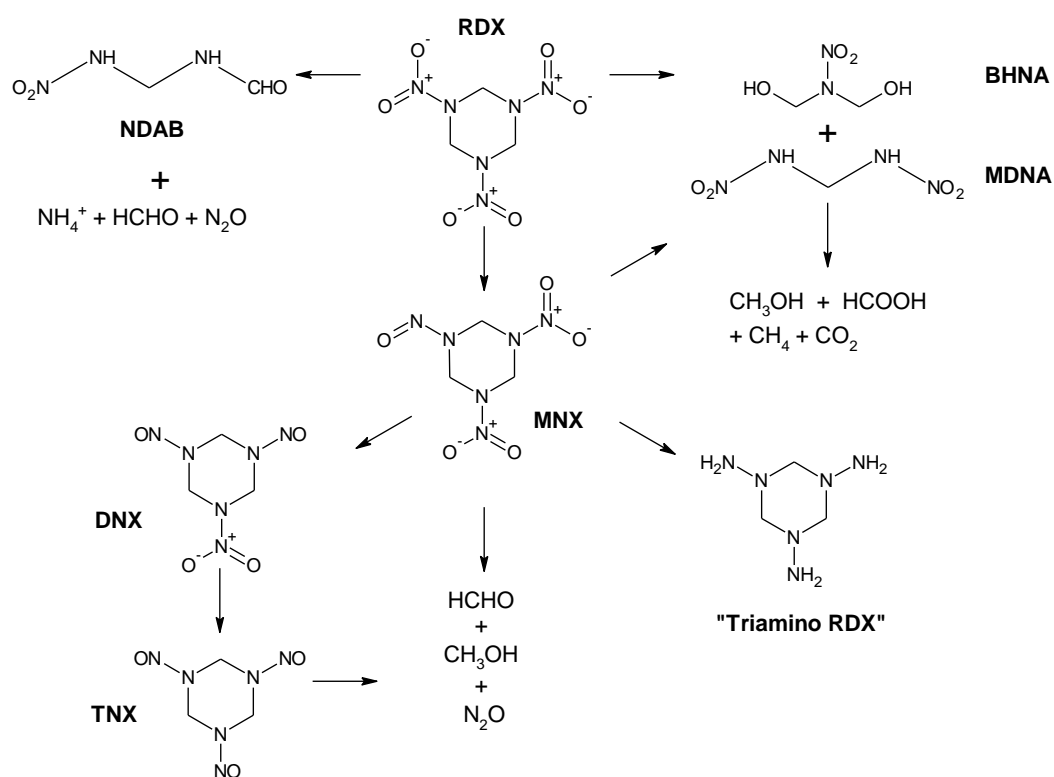


Figure 2.24 Proposed biotic degradation pathways for RDX (based on [67][118])

As it can be seen from Figure 2.24, Monteil-Rivera and Crocker both propose that the degradation of RDX can take several pathways, either by the breakdown of the ring to produce MDNA, BHNA or NDAB; or by the reduction of the nitro groups into nitroso as in MNX, DNX and TNX, or by the reduction of the nitro groups into amino groups. In all the cases, also, the formed products can continue to degrade to become smaller molecules, like methanol, formaldehyde, formic acid, ammonium salts, and gases like methane, carbon dioxide and nitrogen oxides. The specific pathway of degradation will depend on the conditions and the microorganisms present in the medium: the conversion into the nitroso or amino compounds will occur if the microbiota is predominantly reductive, while the ring opening might require conditions with different microorganisms and an environment with more capacity for oxidation reactions. These biodegradation pathways are very similar for HMX, which is present in formulations, or sometimes as an impurity in RDX formulations, as it is a by-product of the synthesis of the latter.

As it can be seen in Figure 2.25, the main degradation processes are the ring opening caused by the oxidation of one of the carbon atoms, and the reduction of the nitro groups. The final products of the mineralization are nitrous oxide or ammonia, and oxidized carbon species like carbon dioxide, formaldehyde, or formic acid.

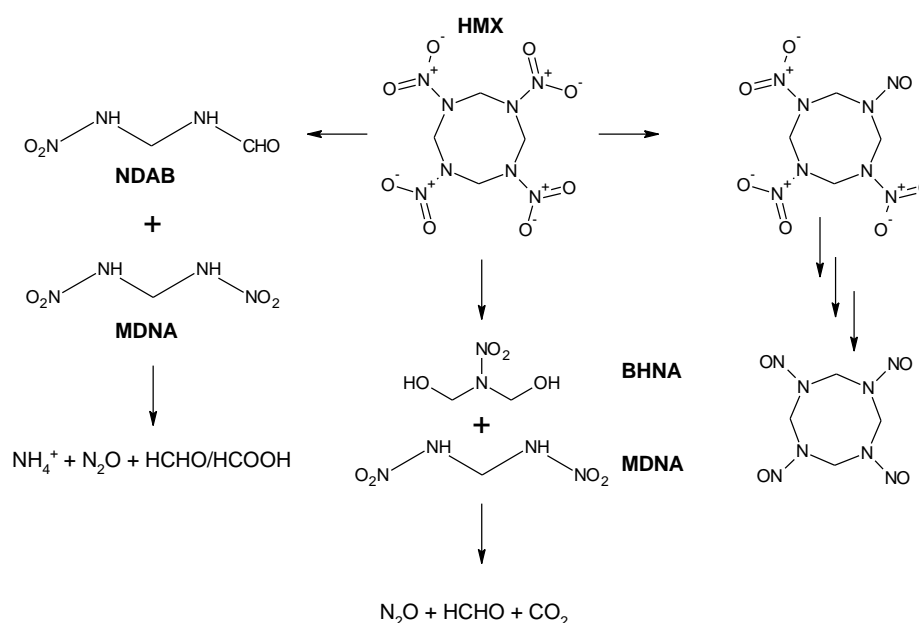


Figure 2.25 Proposed biotic degradation pathways for HMX (based on [67][118])

Several research groups have studied the hexanitro hexaaza isowurtzitane, also known as “China Lake 20” or CL-20, as a replacement for the currently used explosives RDX and HMX [119]. The rates of biodegradation for this explosive in the soil are low, and even though the concentrations found in contaminated sites do not imply toxic effects for plants and microorganisms, it can be toxic for some soil invertebrates. The biodegradation of CL-20 can be performed by some fungi and bacteria, by means of denitration and ring cleavage, as shown in Figure 2.26. Even though there are different theories about the mechanisms of mineralization, the consensus is that the degradation of CL-20 produces nitrite, nitrous oxide, ammonia, formate and glyoxal [120], which could be used as markers for future studies on the natural decomposition of this explosive [10, 121].

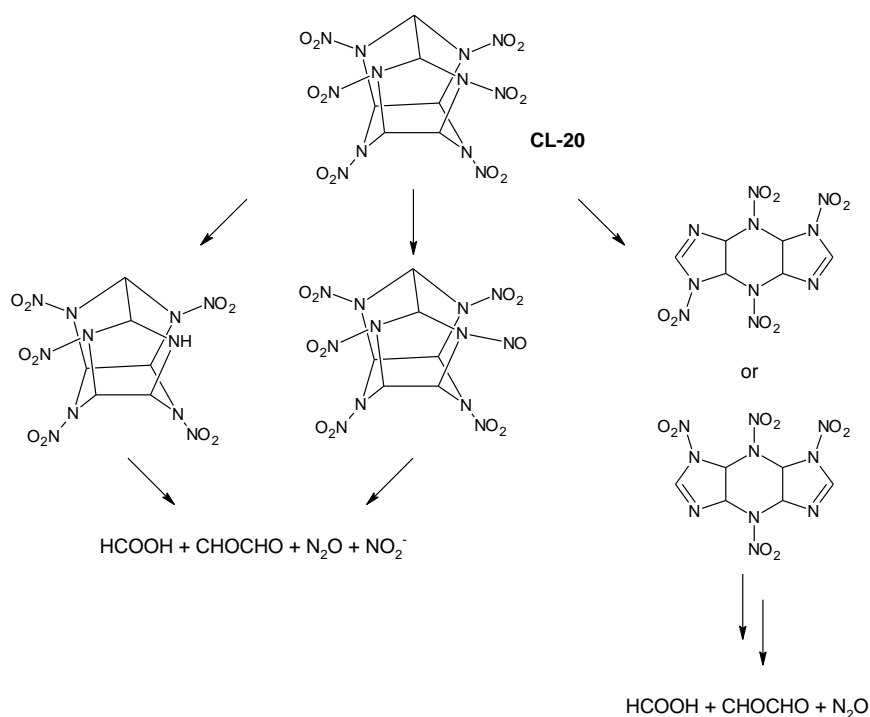


Figure 2.26 Proposed biotic degradation pathways for CL-20 (based on [67][118])

For the case of the insensitive explosives like DNAN, NQ and NTO, there is interest about their environmental fate. Studies performed in static and soil columns in soil present in UK [105, 122], showed that when a formulation of these three compounds was tested, both DNAN and NTO start to biodegrade within one day, and were completely degraded after sixty days, while NQ was only slightly biodegraded after the same period. This also suggests no adverse interactions between the three compounds in terms of biodegradation. These results are partially in accordance with some

studies [123] in which the biodegradation of DNAN, NQ and NTO as part of formulations (IMX-101 and IMX-104) was determined in two types of soil through metagenomic analysis in aerobic and anaerobic conditions, being the anaerobic decomposition faster. For the latter, the presence of RDX in the formulations might have affected the degradation rate for DNAN and NTO, and the researchers question if these effects might have been present also in the case of formulations containing TNT.

Several groups have proposed the biotransformation of NTO in both aerobic and anaerobic conditions, with a description of the possible intermediates: the NTO molecule is first biotransformed into 3-amino-1,2,4-triazol-5-one (ATO) at pH 6, and then this intermediate is mineralized at pH 8. The sequential anaerobic-aerobic biodegradation of NTO in a bioreactor has been studied [124], showing the conversion of the nitrogen atoms of ATO into inorganic species like ammonium and nitrate, and noted that in the case of nitroaromatic cases and other explosives, the difficulty for the nitro group to be oxidized explains their persistence in aerobic conditions compared to anaerobic conditions. This case is the opposite for amines, which are more easily degraded in aerobic conditions and are recalcitrant under anaerobic degradation.

The aquatic toxicity (towards *Ceriodaphnia dubia*) of IMX-101 formulation was studied before and after photodegradation [125], finding that without photodegradation, DNAN was more toxic than the other components of the formulation, though the total toxicity of IMX-101 is lower than that reported for TNT. After the photodegradation, it was found that it was NQ the most toxic constituent, which shows how the toxicity and environmental interactions of a formulation are really complex not only in terms of the given toxicities of their components, but also because of the toxicity of the degradation products generated through the different processes. About the higher water toxicity of NQ after irradiation, Becher and her group found evidence of the formation of cyanoguanidine, and urea among others [126], depending of the wavelength and exposure time. This same research showed that for NTO, the degradation of the triazole is independent of the wavelength and the exposure time, and has as final products ammonia, carbonate, and carbon dioxide, which indicates that at some point of the degradation, a ring cleavage occurs.

On the other hand, Halasz and her team [43] studied the photochemical degradation of IMX-101 in water, and found different degradation products when the components were together, indicating that the degradation products could react with each other or with the original compounds, resulting

in new compounds with different toxicities. Such is the case of DNAN, which in the presence of NQ and NTO produces methoxynitrophenols by nitration of methoxyphenol after denitration. These compounds were not expected, as the common photodegradation products for DNAN found are methoxynitroanilines (MENA) [127].

2.3.5 Isotope Analysis for Biodegradability studies

The isotope analysis follows specific atoms of certain molecules during chemical or biological processes. This allows, for example, to elucidate the degradation rate of a material inside the body of a living being, to detect the release of contaminants in an industrial process, or to verify the origin of a specific sample in origin denomination claims.

In the case of the technique known as Compound Stable Isotope Analysis (CSIA), it quantifies the isotopic composition of a sample allowing the distinction of organic compounds, identify the reactions that transform the studied compound, even clarifying details about the mechanism [128]. Usually, this methodology uses the differences in isotopic mass as revealed by mass spectrometry to evaluate how the sample gets enriched or depleted of the heavier isotopes.

Some studies “label” the molecules with isotopes of some elements to replace the most common isotope: for example, replacing one of the carbon atoms of a molecule with ^{14}C or with ^{13}C . The substitution of these atoms is usually done by synthesis of the final molecule from reagents that already possess the markers [128]. Nowadays, the sensitivity of the mass spectrometers can detect changes in the isotopic abundance in a reliable way, and for some of the isotopes, it is enough to have an excess of 0.5 atom percentage above the natural abundance for it to be detected and quantified [129].

Once the target molecule is marked, different techniques can be used to detect the isotopes during its chemical transformations: for example, in the substitution of carbon atoms with heavier isotopes, the ^{14}C isotopes could be detected by their radioactivity, while the ^{13}C could be detected by nuclear magnetic resonance (NMR). The technique to be used would depend on its detection limit and sensitivity towards the marker, as well as the availability of the needed isotopes.

In the Table 2.3 are shown some examples of isotopes used for the isotope analysis and the usual techniques associated. For example, the group of Limam [130] studied the biodegradation of

phenol and bisphenol A by composting ^{13}C -labeled versions of the molecules, injecting them in the composting systems and then analyzed the gases produced by isotope-ratio mass spectrometry. The use of slightly radioactive isotopes, also known as “radiotracers”, has focused especially on the utility of ^{14}C as a molecular marker, by synthesis of molecules of energetic materials in which some of the lighter carbons are substituted by heavier, radioactive carbons. This allows to trace the diffusion and degradation of the molecules, for example RDX [131, 132].

Table 2.3 Examples of biodegradation studies using isotopes as molecular markers.

| Original isotope | Isotope | Abundance % ^a [128, 129] | Detection Technique | Study detail |
|------------------|---------------------------------|-------------------------------------|-------------------------|---|
| ^{12}C | ^{14}C | < 1 ppb | Radioactivity detection | ^{14}C -CL-20 in sandy soils [10] |
| | ^{13}C | 1.11 | NMR | ^{13}C -TNT used by anaerobic bacteria [133] |
| ^1H | ^2H (or ^2D) | 0.015 | NMR (indirect) | Propane and butane anaerobic degradation by marine bacteria [134] |
| | ^3H | traces | IRMS | Presence of TNT and degradation into DNT in groundwater [135] |
| ^{14}N | ^{15}N | 0.366 | IRMS, NMR | ^{15}N -RDX in coastal marine habitat [136] |

a: Expressed as the ratio of the natural abundance of the heavier isotope to the natural abundance of the lighter isotope.

Another example is the study of the mineralization of RDX in a simulated coastal marine habitat, and the detection of dissolved inorganic nitrogen species like ammonia, nitrate and gaseous nitrogen, by introduction of RDX labelled with ^{15}N , and it was found that after 21 days, 42% of the total ^{15}N had been converted to $^{15}\text{N}_2$ [136]. Other studies have, to followed the biodegradation of RDX in soil [137], by adding a known quantity of isotopically enriched sample of ^{15}N -RDX to the soil and studying the amount of heavy nitrogen by elemental analysis. A similar approach can be used to assess the effect of the biodegradation of RDX on underground waters, [138] concluding that the biodegradation rate of the explosive decreased with depth, implying the possibility of more extended pollution of this material in the presence of underground rivers or water systems.

The presence of a higher atomic mass isotope might affect some of the reactive properties of the molecule, in an effect known as the Primary or Kinetic Isotope Effect, or KIE, which occurs in the

bond containing the heavy isotope, being the formation or breakdown of this bond a rate-determining step of the studied reaction [129].

In a study about the thermal decomposition of GAP, a comparison was made between the decomposition of normal GAP versus a semi-deuterated version of the GAP by heating them in a thermogravimetric apparatus (TGA) and analyzing the products by FTIR and MS. The differences in the mass/charge signals between the normal molecule and the deuterated one on the mass spectrometer allowed the researchers to elucidate the fragments that are formed in the initial stages of the decomposition of GAP [139, 140]. In this case, the weight difference between the normal GAP and the semi-deuterated one was about 2%.

It has been established in various studies that the biodegradation processes of various energetic materials involve the transformation of nitrogen into nitrate groups, and the detection of this ion helps to track the extent of the degradation of energetic materials, especially the formation of polluting “plumes”. Nevertheless, as the presence of nitrate can be caused by different sources, like the natural nitrogen cycle, the tracking of the stable isotopes of nitrogen is a strategy that has proved to help differentiate between the native nitrogen and the anthropogenic nitrogen that would turn into nitrates. Projects like the one of Bordeleau and her team [141, 142] used the isotopic ratios of ^{15}N and ^{18}O to trace back the presence of NG, NC and RDX in groundwater near military training ranges, and found that for some of the places studied, the levels of nitrate in those waters were higher than allowed by the norm, and that in all the cases the presence of nitrate was not due to the native nitrogen but to the use of energetic materials.

In summary, while there is an interest in the environmental effects of energetic materials, most research has been done on RDX, HMX, and above all, TNT, whose negative environmental impacts have been thoroughly assessed. Nevertheless, the environmental research in energetic materials has been done after these compounds are widely used; instead of assessing the biodegradation, and environmental impact from the beginning of their development.

The field of energetic materials is always looking for substances with a better performance, but the environmental impacts were not considered until the second half of the 20th century. For example, the research on GAP has focused exclusively on the improvement of its performance as a binder or plasticizer, but not on the environmental effects of the resulting formulations. The development

of “greener” energetic materials has become more frequent, but these efforts usually focus on either cleaner synthetic methods or on the reduction or avoidance of accumulation of these compounds in the environment.

The biodegradation pathways of polymers containing tetrazole groups and GAP is not clear. This type of research is necessary to better understand the possible environmental effects associated with nitrogen-rich materials containing tetrazoles and triazoles, which would allow a better decision making towards the remediation, recycling, or elimination of said materials.

CHAPTER 3 METHODOLOGY AND EXPERIMENTAL DESIGN

In this project, various polymers with energetic characteristics were composted up to 18 days at 55 °C: two polyvinyl tetrazole polymers and two polymers of crosslinked GAP. All the polymeric samples were characterized before and after the composting experiments, through NMR spectroscopy (^1H and ^{13}C), infrared spectroscopy (FTIR), soluble fraction extraction, differential scanning calorimetry (DSC), energy dispersive X-Ray spectroscopy (EDS), and dynamic mechanical analysis (DMA) for the GAP crosslinked samples.

Also, a polymer with isotope marking was prepared: a poly vinyl tetrazole- co- poly acrylo nitrile (PVT-PAN) marked on the tetrazole ring (by using $1\text{-}^{15}\text{N-NaN}_3$ on the cycloaddition reaction). It was composted for 6 days and then analyzed by $^{15}\text{N-NMR}$ to evaluate possible changes in the tetrazole ring during the earlier stages of the biodegradation.

3.1 Experimental Constraints and Limitations

The experimental design of this project had to consider several constraints or limitations related either to the samples and their preparation, or to the experimental techniques and facilities:

1. Low solubility of the polymers
2. High molecular weight of the Poly Acrylonitrile used
3. Laboratory Safety
4. Economic factors

3.1.1 Low solubility of the polymers after solvent casting:

After the solvent casting preparation of the samples (PVT and PVT-PAN), a decrease of the solubility was found. This hindered some of the analyses, as was the case of the NMR experiments, that had to be performed in Solid-State (SS NMR) instead of Liquid NMR. This requires more sample, longer acquisition times, and it increases the cost of the analyses.

3.1.2 High molecular mass of PAN polymers:

The selected starting polymer for the PVT and PVT-PAN polymers was polyacrylonitrile which had a high molecular weight. This precluded to obtain the molecular mass of the samples of PVT and PVT-PAN as the Gel Permeation Chromatography (GPC) analyses did not show any information, due to the chromatographic columns getting obstructed. The Matrix-Assisted Laser Desorption/Ionization-Time of Flight (MALDI-TOF) technique was also considered for the determination of the molecular weights, but it was discarded as per recommendation of the personnel in charge of this technique at Université de Montréal, as the low solubility and high molecular mass of the samples made them not suitable for this technique.

3.1.3 Laboratory Safety

The synthesis and manipulation of energetic materials require paying special attention to the safety in all the stages of the experiments. For example, the syntheses in the laboratory were performed in small-scale batches, because the use of bigger reactors would imply the risk of hotspots forming in the polymer mixture. Another safety concern that resulted in small-scale experiments was the use of NaN_3 , a substance of known toxicity that during the syntheses could generate small quantities of hydrazoic acid HN_3 which is highly explosive and also toxic.

In terms of equipment and analyses, it has to be noted that the thermal analyses were done by DSC and DMA, as the Thermogravimetric Analysis (TGA) was not possible because of the risk of heating a sample of energetic material that would affect the integrity of the equipment of other research groups.

3.1.4 Economic factors

One of the most important criteria for the selection of the polymers to study was the low cost of preparation, which would be an advantage in the case that the reactions would be scaled-up in

industrial setups in the future. This preference for low cost of the preparation implied the use of reagents and techniques that were simple and that would result in high yields.

Another economic constraint was the costs of NMR and SS NMR analyses, especially in the case of the latter, where the acquisition times are long. For this reason, the NMR analyses were not performed for all of the samples but only at the beginning, the middle-point, and the end of the composting experiments.

One of the most important economic constraints for this project was the use of “isotopic labels”. Several options were considered to modify certain polymers with isotopes, and finally the chosen compound was $1\text{-}^{15}\text{N-NaN}_3$, a salt where only one of the three nitrogen atoms of the azide group is a ^{15}N isotope. Even though the labelling process was simple, and it required no change in the synthesis procedure. However, the high cost of the $1\text{-}^{15}\text{N-NaN}_3$ influenced the amount of samples to be prepared and the composting time used, as it was desired to remain a big portion of the original samples, instead of losing them into the ground.

3.2 Experimental Design

The methodology of the present project comprises various stages:

1. Synthesis and modification of polymeric samples
2. Characterization of the polymeric samples
3. Biodegradation experiments

For the synthesis and modification of polymers, four different polymers were prepared, and by the study of the differences on the biodegradation, the effects of specific structural features were analyzed.

A series of polymers were synthesized in the lab, with different functional groups linked to the tetrazole moiety or to the polymeric backbone. Of the prepared polymers, only four were used for the composting experiments, and one of these four polymers was also prepared with an ^{15}N isotope marker and subjected to composting.

The composting experiments were based on the modification of the ASTM protocols D5988-12 and D5338-98 proposed by Cossu [143], and a experiment design scheme is shown in Figure 3.1

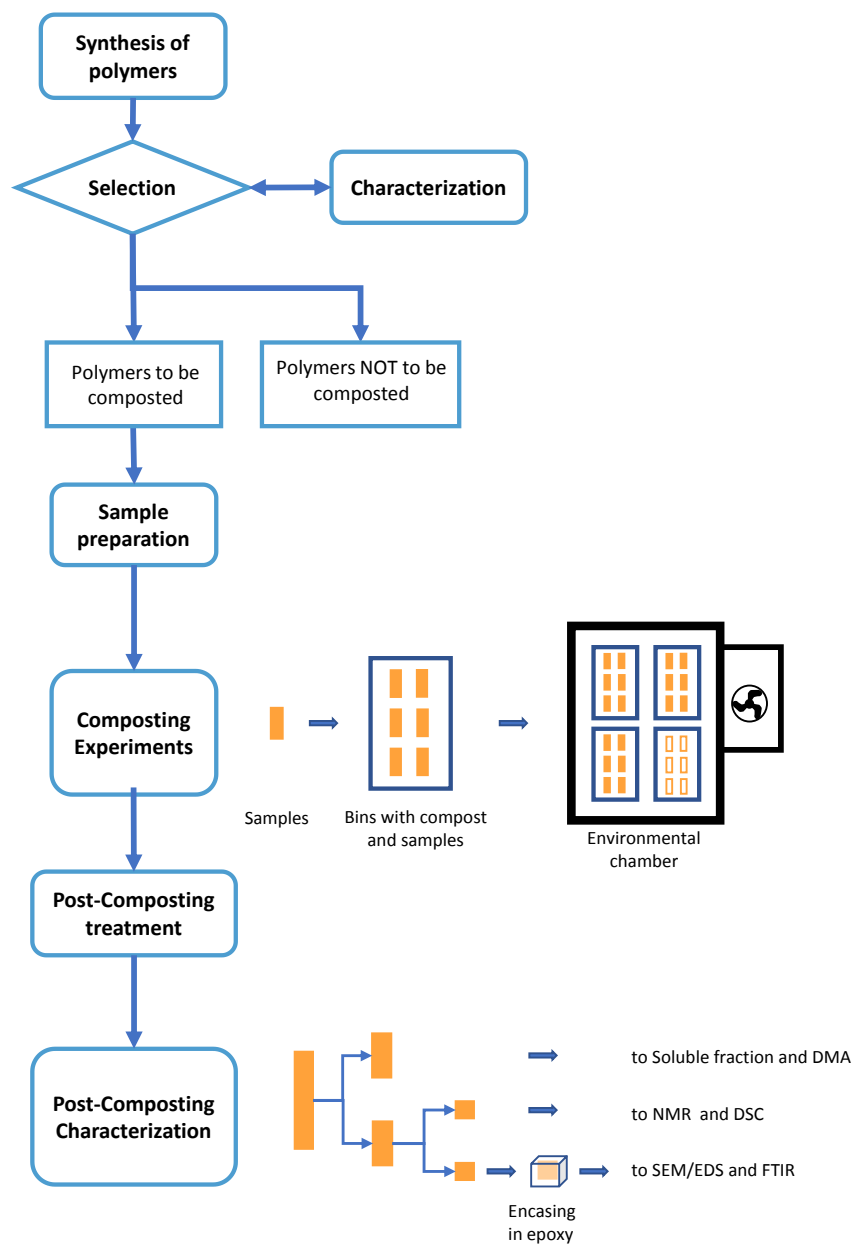


Figure 3.1 Scheme of the experimental methodology

During the first stage of this project, ten polymers were prepared, and only four of them were selected for the composting experiment, based in criteria of purity, simplicity of synthesis and

Synthesis

10 polymers were prepared

Selection criteria:

- High yield
- High purity
- Easy synthesis

4 polymers were selected

Sample Preparation

- Solvent casting for PVT and PVT-PAN
- In-mold crosslinking for GAP-BPM and GAP-DCHD

Composting Experiments:

For each polymer:

- 3 bins: 6 triplicates for days 3 to 18 (6 samples/bin)
- 1 bin with PLLA witness for days 9 and 18 (white samples)

Post Composting Characterization:

- Samples were cut in half (Soluble fraction and DMA)
- Remaining half was cut again: one quarter for NMR and DSC and the other was encased in epoxy resin (SEM/EDS and FTIR)

experimental yield. In a later stage of the project, one of these four polymers was prepared with nitrogen-15 isotopic labelling and subjected to another composting experiment. In

Table 3.1 are shown the experimental conditions for the five polymers that were composted, and the variables that were considered.

Table 3.1 Experimental conditions and variables for the composting experiments

| | | |
|---|---|--|
| Composted Polymers | 2 Tetrazole polymers | PVT, PVT-PAN |
| | 2 Triazole Crosslinked | GAP-BPM, GAP-DCHD |
| | 1 Labelled polymer | ¹⁵ N-PVT |
| Polymeric references | 1 | Biodegradable polymer to confirm microbial activity (PLLA 4032D) |
| Days for the composting test (non-labelled samples) | 18 days (measurements every 3 days) | Measurements on days: 0, 3, 6, 9, 12, 15 and 18 for the samples Measurements on days: 0, 9 and 18 for the references |
| Days for the composting test (¹⁵N-labelled samples) | 6 days (measurements every 3 days) | |
| Total number of samples | 93 polymer samples | 5 polymer types (4 non labelled and 1 labelled) 7 measurements x triplicates for non-labelled = 84 samples 3 measurements x triplicates for ¹⁵ N-labelled = 9 samples |
| | Monitored conditions during the composting | |
| | pH | Between 6 and 8 |
| | Temperature | Temperature at 55 °C |
| | Soil Water Content | 60% of Water retention capacity |
| | Humidity | 60% |

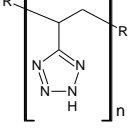
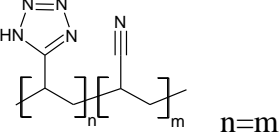
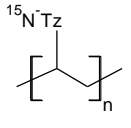
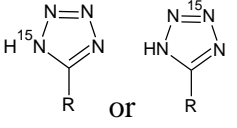
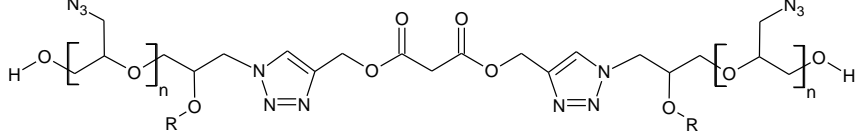
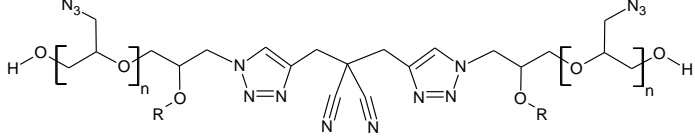



In Table 3.2 are listed the various characterization techniques used to assess the purity of the prepared polymers, and to gather information about their composition before and after the composting experiments.

Table 3.2 Techniques used for the characterization of the samples.

| Characterization Technique | Expected Evidence |
|---|--|
| <ul style="list-style-type: none"> • Mass Loss | Preliminary evidence of decomposition. |
| <ul style="list-style-type: none"> • Soluble fraction (Soxhlet extraction) | Formation of small fragments during decomposition. Extracts were obtained for further analysis. |
| <ul style="list-style-type: none"> • Solid State ^1H – NMR (Nuclear Magnetic Resonance) | Changes in functional groups containing hydrogen (backbone and pending groups). |
| <ul style="list-style-type: none"> • Solid State ^{13}C – NMR | Changes in backbone and triazoles groups. |
| <ul style="list-style-type: none"> • Solid State ^{15}N - NMR (only for the isotopically labelled samples) | Changes in the tetrazole groups in the early stages of composting. |
| <ul style="list-style-type: none"> • FTIR (Fourier-transformed Infrared Spectroscopy) direct ATR mode | Identity and purity of compounds after their synthesis. |
| <ul style="list-style-type: none"> • FTIR (Microscopy in ATR mode) | Changes in the structure at different depths of the sample. |
| <ul style="list-style-type: none"> • SEM (Scanning Electronic Microscopy) | Microscopic evidence of biodegradation: presence of compost particles, changes in texture, etc. |
| <ul style="list-style-type: none"> • EDS (Energy-Dispersive X-Ray Spectroscopy) | Variations on the elemental composition. |
| <ul style="list-style-type: none"> • DSC (Differential Scanning Calorimetry) | Variations in Thermochemical properties: glass transition temperature (T_g), decomposition temperature (T_{dec}) and decomposition energy released (E_{dec}) |
| <ul style="list-style-type: none"> • DMA (Dynamic Mechanical Analysis) | Variations in mechanical properties: Storage Modulus (E'), Loss Modulus (E''), and indirect measurement of glass transition temperature (T_g) |

3.2.1 Synthesis of the Polymers

Table 3.3 Chemical structure of the synthesized polymers.

| Polymer | Structure |
|---|--|
| Poly Vinyl Tetrazole (PVT) |  |
| Poly Vinyl Tetrazole - co- acrylonitrile (PVT-PAN) 1:1 |  <p style="text-align: center;">$n=m$</p> |
| ¹⁵ N Labeled PVT (¹⁵ PVT) |  $^{15}\text{N-Tz} =$  |
| Crosslinked GAP with Bis propargyl malonate (BPM) |  |
| Crosslinked GAP with 4,4'-Dicyanohepta-1,6-diyne (DCHD) |  |
| Alkylated Polyvinyl tetrazoles |  |
| t-Butyl Poly Vinyl Tetrazole, tBu-PVT | Poly Allyl Vinyl Tetrazole, Allyl-PVT |
| Copolymers Allyl-Vinyl |  |
| Poly Acrylonitrile-co-Allyl Chloride PAN-PAC | Poly Vinyl Tetrazole-co-Allyl Azide PVT-PAAz |
| Other polymers |  |

3.2.2 Reagents for the synthesis

Table 3.4 Reagents to be used for synthesis and polymerization.

| Substance | MW (g/mol) | Source | Section |
|---|---------------------|---|---|
| Polymers | | | |
| Poly Acrylo Nitrile (PAN) | 150 000 | Sigma-Aldrich (CA) | 3.2.3.1, 3.2.3.2, 3.2.3.13 |
| Glycidyl Azide Polymer Plasticizer (GAP-700) | M _n ~700 | Supplied by General Dynamics Ordnance and Tactical Systems (Valleyfield, CA), originally produced by 3M | 3.2.3.11, 3.2.3.12 |
| Barex© (PAN-co-PMA) | NA | Good Fellow | 3.2.3.3 |
| Poly Lactic Acid PLA 4032D | NA | Nature Works | 3.2.5.6 |
| PVC | 43 000 | Aldrich (CA) | 3.2.3.6 |
| Crosslinking and curing agents | | | |
| Bis propargyl malonate (BPM) | 180.16 | Prepared in the lab | 3.2.3.11 |
| 4,4'-Dicyanohepta-1,6-diyne (DCHD) | 142.16 | Prepared in the lab | 3.2.3.12 |
| Molecular Labelling | | | |
| Sodium azide-1- ¹⁵ N | 66.00 | ACP Chemicals Inc. | 3.2.3.13 |
| Salts | | | |
| Magnesium Sulfate anhydrous MgSO ₄ | 120.36 | Fisher Chemicals (CA) | 3.2.3.9 |
| Ammonium Chloride NH ₄ Cl | 53.49 | Sigma-Aldrich (CA) | 3.2.3.1, 3.2.3.2, 3.2.3.3, 3.2.3.8 |
| Sodium Azide, NaN ₃ | 65.01 | Sigma-Aldrich (CA) | 3.2.3.1, 3.2.3.2, 3.2.3.3, 3.2.3.6, 3.2.3.8 |

| | | | |
|-------------------------------|--------|------------|----------------------|
| Potassium Carbonate K_2CO_3 | 138.20 | Alfa Aesar | 3.2.3.5, 3.2.3.10 |
|-------------------------------|--------|------------|----------------------|

Table 3.3 Reagents to be used for synthesis and polymerization (Continued)

| Substance | MW (g/mol) | Source | Section |
|---|---------------|-----------------------|---|
| Other substances | | | |
| Hydrochloric acid, HCl | 36.55 | Sigma-Aldrich (CA) | 3.2.3.1, 3.2.3.2, 3.2.3.3, 3.2.3.6, 3.2.3.8 |
| p-Toluenesulphonic acid (PTSA, anhydrous) | 172.20 | Sigma-Aldrich (CA) | 3.2.3.9 |
| Malonic acid | 104.06 | Sigma-Aldrich (CA) | 3.2.3.9 |
| Propargyl alcohol | 56.06 | Aldrich (CA) | 3.2.3.9 |
| Tert-Butanol | 74.12 | Sigma-Aldrich (CA) | 3.2.3.4 |
| Malononitrile | 66.06 | Aldrich (CA) | 3.2.3.10 |
| Propargyl bromide | 118.96 | Alfa Aesar | 3.2.3.10 |
| Sulfuric acid H_2SO_4 | 98.08 | Fisher Chemicals (CA) | 3.2.3.4, |
| Allyl bromide | 120.98 | Sigma-Aldrich (CA) | 3.2.3.5 |
| Allyl chloride | 76.52 | Sigma-Aldrich (CA) | 3.2.3.7 |
| Acrylonitrile | 53.06 | Sigma-Aldrich (CA) | 3.2.3.7 |
| Solvents | | | |
| Toluene | 92.14 | Laboratoire MAT | 3.2.3.9, 3.2.3.10 |
| Dimethyl formamide (DMF) | 73.09 | Sigma-Aldrich (CA) | 3.2.3.1, 3.2.3.2, 3.2.3.3, 3.2.3.5, 3.2.3.8 |
| Dichloromethane | 84.93 | Fisher Chemicals (CA) | 3.2.5.8.1 |

| | | | |
|------------|--------|-----------------------|---------------------------------|
| Methanol | 32.04 | Fisher Chemicals (CA) | 3.2.3.1, 3.2.3.2, 3.2.3.5 |
| Chloroform | 119.37 | Fisher Chemicals (CA) | 3.2.3.4, |

3.2.3 Synthesis and preparation of samples

3.2.3.1 Synthesis of Poly Vinyl-Tetrazole PVT [28]

In a 250 mL flask, PAN (5.3 g, 100 mmoles of acrylonitrile groups) is added to 100 mL of DMF at 50 °C. When all the solid is dissolved, NaN₃ (6.5 g, 100 mmoles) and NH₄Cl (5.35 g, 100 mmoles) are added. The mixture is heated at 105 °C for 24 hours, and then the cooled mixture is added slowly to 300 mL of 0.5 M HCl. The resulting solid is taken out of the mixture as it forms. The solid is washed twice with 50 mL of distilled water and left to dry at room temperature for 4 days.

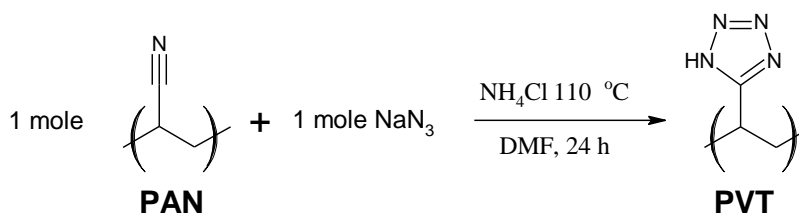


Figure 3.2 Reaction scheme for the synthesis of PVT

3.2.3.2 Synthesis of Poly Vinyl-Tetrazole-co- Acrylonitrile PVT-PAN 1:1

In a 250 mL flask, PAN (5.3 g, 100 mmoles of acrylonitrile groups) is added to 100 mL of DMF at 50 °C. When all the solid is dissolved, NaN₃ (3.25 g, 50 mmoles) and NH₄Cl (5.35 g, 100 mmoles) are added. The mixture is heated at 105 °C for 24 hours, and then the cooled mixture is added slowly to 300 mL of 0.5 M HCl. The resulting solid is taken out of the mixture as it forms. The solid is washed twice with 50 mL of distilled water and left to dry at room temperature for 4 days.

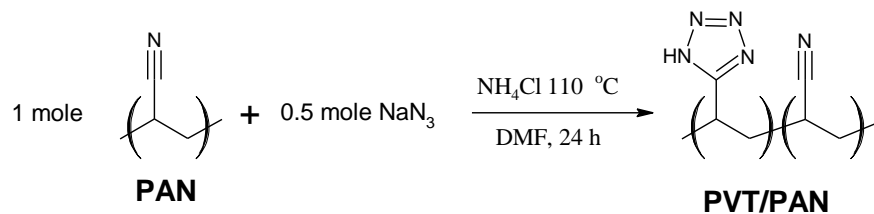


Figure 3.3 Reaction scheme for the synthesis of PVT-PAN

3.2.3.3 Synthesis of Poly Vinyl-Tetrazole-co-Methyl Acrylate, PVT-PMA

In a 250 mL flask, 130 mL of DMF are added and heated at 100 °C. To the hot solvent, 6.0 of poly acrylonitrile-co-methyl acrylate (43 mmoles) were added little by little until total dissolution. To this solution, 6.5 g of NaN₃ (100 mmoles) and 5.35 g of NH₄Cl (100 mmoles) were added, and the mixture was heated under reflux for 24 hours. Then, the mixture was allowed to cool down to room temperature and poured to a mixture of 100 mL HCl 1 M and 300 mL water. The solid formed was washed twice with 100 mL deionized water and left to air dry.

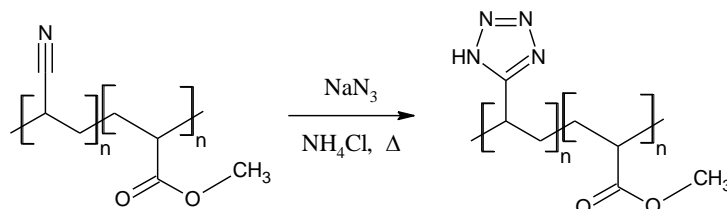


Figure 3.4 Reaction scheme for the synthesis of PVT-PMA

3.2.3.4 Synthesis of t-Butyl Poly Vinyl Tetrazole, tBu-PVT

The synthesis was adapted from the procedure described by Gaponik [30]. In a 100 mL flask with 40 mL of CHCl₃, were added 1.92 g of ground PVT (20 mmoles), 6.7 g of tert-butanol (90 mmoles), and 2 mL of concentrated H₂SO₄. An addition funnel was added on top of the flask, and a condenser on top of the funnel. The mixture was heated under reflux, and every hour the valve of the funnel was open a little bit to reincorporate the chloroform while separating the water (as it would happen in a Dean-Stark setup). After 5 hours of reflux, the mixture was allowed to cool down and the solvent was distilled out of the flask. To the suspension left on the flask, 20 mL of acetone were added, and the resulting solid was filtered and dried.

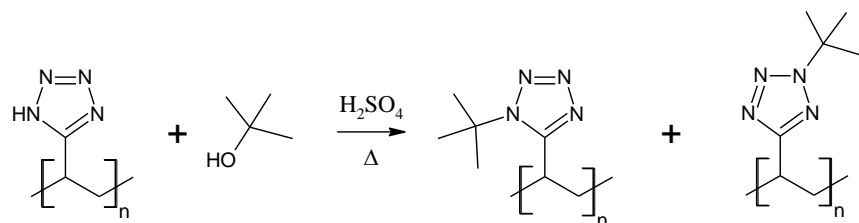


Figure 3.5 Reaction scheme for the synthesis of tBu-PVT

3.2.3.5 Synthesis of Poly Allyl Vinyl Tetrazole, Allyl-PVT

In a 100 mL flask with magnetic stirrer, 1.92 g of PVT (20 mmoles) were dissolved in 40 mL of DMF at 40-50 °C. To this solution, 2.76 g of K_2CO_3 (20 mmoles) and 2.66 g of allyl bromide (22 mmoles) were added. A condenser in reflux position was attached to the flask, and the mixture was allowed to react at 45 °C for 4 hours. The solution was cooled to room temperature and poured over water. The solid was separated as it formed, washed with deionized water (3 x 100 mL) and with methanol (2 x 50 mL) and then dried under vacuum at 65 °C for 24 hours.

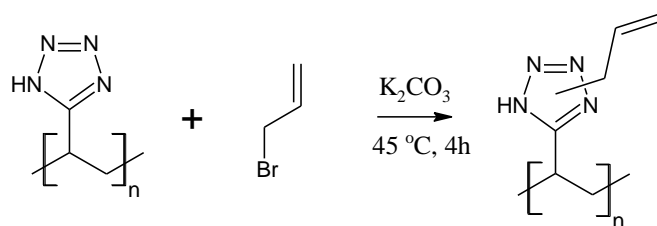


Figure 3.6 Reaction scheme for the synthesis of PVT-Allyl

3.2.3.6 Synthesis of Poly Vinyl Azide, PVAz

The procedure was adapted from the one reported by Gilbert [37] and Ouerghui [38]. In a 250 mL flask, 125 mL of DMF were heated at 55 °C with a magnetic stirrer. Then, 5 g (80 mmoles of vinyl chloride groups) of poly vinyl chloride PVC were added and stirred until all the solid was dissolved. To this solution, 5 g (78 mmoles) of NaN_3 were added, and a condenser was put over the flask. The reaction mixture was heated under reflux for 24 hours, then cooled down and precipitated over 400 mL of water with 50 mL HCl 10%. The obtained solid was washed with deionized water (3 x 100

mL) and with methanol (2 x 50 mL). The solid was dried in the oven at 60 °C for 24 hours and then dissolved in acetone for its storage.

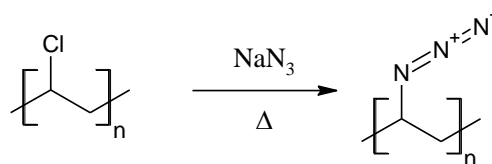


Figure 3.7 Reaction scheme for the synthesis of PVAz

3.2.3.7 Synthesis of Poly Acrylonitrile-co-Allyl Chloride PAN-PAC

In a 250 mL flask with 80 mL of water with a magnetic stirrer, 9 g of acrylonitrile (170 mmoles of acrylonitrile groups), 1 g of allyl chloride (13 mmoles), 0.4 g of sodium lauryl sulfate (1.3 mmoles) and 0.15 g of potassium persulfate (0.55 mmoles) were added. A condenser was placed over the flask and the mixture was heated at 70 °C for 2 hours and then at 60 °C for 22 hours. The reaction mixture was cooled down to room temperature and dissolved in a mixture of 33 mL DMF and 65 mL MeCN and stored in the refrigerator for 24 hours. The solid formed was filtered, washed with hexane, and dried under low vacuum at 60 °C for 5 days [144].

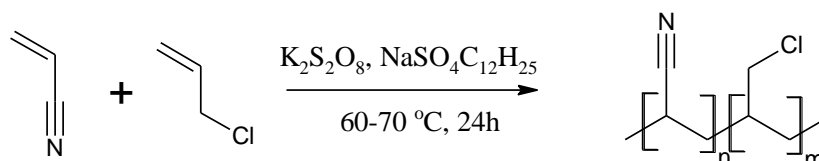


Figure 3.8 Reaction scheme for the synthesis of Poly Acrylonitrile-co-Allyl Chloride PAN-PAC

3.2.3.8 Synthesis of Poly Vinyl Tetrazole-co-Allyl Azide PVT-PAAz

In a 250 mL flask with 100 mL of DMF and a magnetic stirrer, 4.5 g of PAN-PAC (4.6 mmoles), 5.5 g of NaN₃ (85 mmoles) and 4.5 g of NH₄Cl (85 mmoles) were added, and a condenser was attached on top of the flask. The mixture was heated under reflux at 105 °C for 20 hours and cooled down to room temperature. The cool mixture was poured over a solution of 200 mL of water with 50 mL HCl 1M. The solid was separated as it formed. The solid was washed with water (3 x 50

mL) and with methanol (3 x 25 mL) and left to air-dry in the fume hood for 5 days before being dried in the oven under low vacuum at 100 °C.

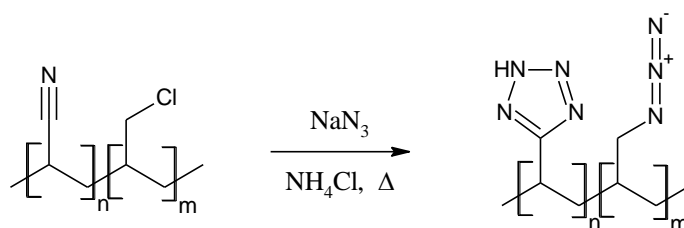


Figure 3.9 Reaction scheme for the synthesis of Poly Vinyl Tetrazole-co-Allyl Azide PVT-PAAz

3.2.3.9 Synthesis of Bispropargyl Malonate BPM

The synthesis of BPM is a modification of the procedures described by Keicher [55]. Around 100 mmoles (10.4 g) of malonic acid are dissolved in 100 mL of anhydrous toluene and added to a 250 mL flask with a magnetic stirrer. Then, a quantity of propargyl alcohol between 240 and 300 mmoles is added. To this mixture, p-toluenesulphonic acid (1 mmol, 172 mg) is added. The reaction mixture is heated at 110 °C, and both a condenser and a Dean-Stark apparatus are connected to the flask. The reaction is stopped when there is no more water being collected in the Dean-Stark trap.

The reaction mixture is cooled down to 30 °C and the acid excess is removed by washing with a saturated solution of Na₂CO₃ in a separation funnel. The aqueous phase is extracted three times with 50 mL of ethyl acetate and the extracts are added to the organic phase. After this, all the organic phases are collected and dried over MgSO₄, and the solvents are separated by distillation under vacuum.

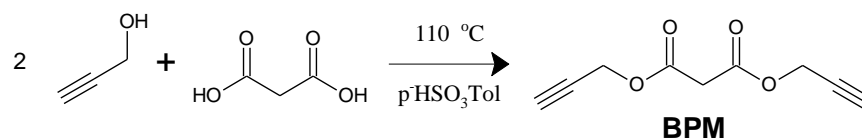


Figure 3.10 Reaction scheme for the synthesis of BPM

3.2.3.10 Synthesis of 4,4'-Dicyanohepta-1,6-diyne DCHD

4,4'-Dicyanohepta-1,6-diyne was synthesized from a procedure adapted from the one described by Schmitt and his group [145]. A solution of malononitrile (6.889 g, 104 mmol) in 100 mL DMF was prepared and K_2CO_3 (35g, 253 mmol) was added in one portion. The resulting slurry was cooled in an ice bath to $0^\circ C$ under inert atmosphere (N_2). Freshly distilled propargyl bromide (30 g, 252 mmol) was added gradually, over 30 minutes, while the temperature was maintained at $0^\circ C$. After the addition, the mixture was allowed to reach room temperature and left to react for another 6 hours. To the resulting suspension was added 500 mL of water to dissolve the solids, and the solution was extracted with toluene (2x150 mL). The toluene layer was washed with water (2x300 mL), dried with anhydrous sodium sulfate and filtered through a silica bed. The resulting clear solution was concentrated in vacuum and the product was precipitated using hexane.

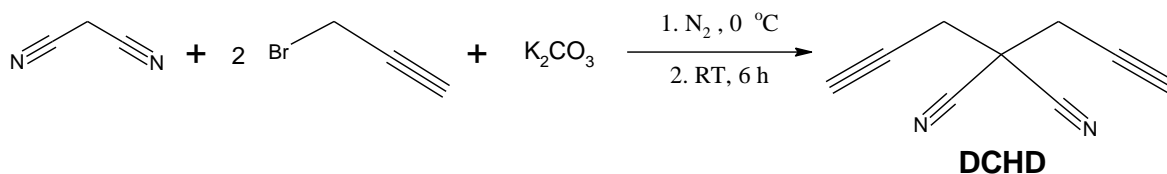


Figure 3.11 Reaction scheme for the synthesis of DCHD

3.2.3.11 Preparation of GAP crosslinked with BPM

A mixture of BPM and GAP (60 g of polymer with an alkyne/azide molar proportion of 0.2) was prepared by adding the powdered BPM (9.23 g) to the liquid GAP polymer (50.77 g) at room temperature. The mixture was stirred for approximately one hour until a homogeneous liquid mixture was obtained. Pre-cured samples were then kept in a freezer to halt the advancement of the curing reaction until testing. The pre-cured samples were poured into silicon molds to produce 24 samples and put in the oven at $60^\circ C$ during 48 hours with low vacuum. The cured samples were cooled down to room temperature and taken out of the molds. The samples were kept in sealed plastic bags, protected from sunlight and humidity until used.

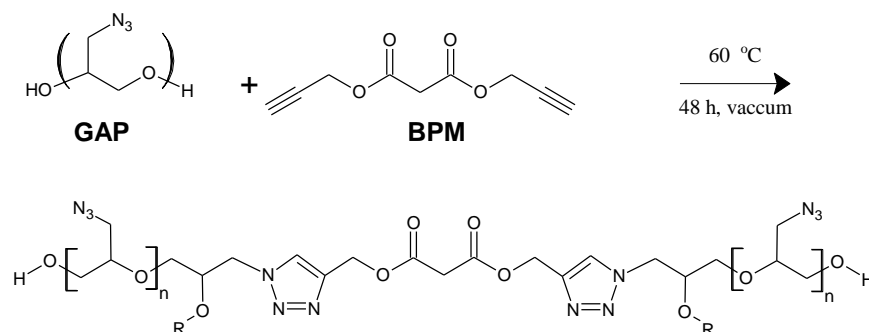


Figure 3.12 Reaction of the crosslinking of GAP with BPM

3.2.3.12 Preparation of GAP crosslinked with DCHD

A mixture of DCHD and GAP (60 g of polymer with an alkyne/azide molar proportion of 0.2) was prepared by adding the powdered DCHD (7.54 g) to the liquid GAP polymer (52.46 g) at room temperature. The mixture was stirred for approximately one hour until a homogeneous liquid mixture was obtained. Pre-cured samples were then kept in a freezer to halt the advancement of the curing reaction until testing. The pre-cured samples were poured into silicon molds to produce 24 samples and put on the oven at 60 °C during 48 hours with low vacuum. The cured samples were cooled down to room temperature and taken out of the molds. The samples were kept on sealed plastic bags, protected from sunlight and humidity until used.

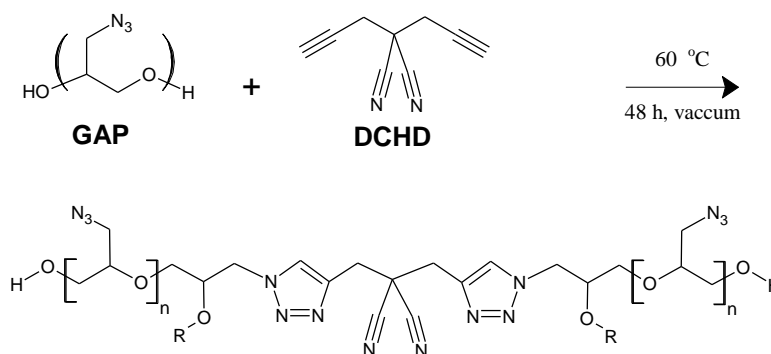


Figure 3.13 Reaction of the crosslinking of GAP with DCHD

3.2.3.13 Synthesis of Isotope-Marked Polymer 1-¹⁵N PVT

The synthesis of the isotope-marked polymer 1-¹⁵N PVT was performed in the same way as the synthesis of the PVT polymer described in section 2.2.3.1, using for this synthesis 5.62 g of PAN, 5.67 g of NH₄Cl and 7.0 g of 1-¹⁵N NaN₃ 98%.

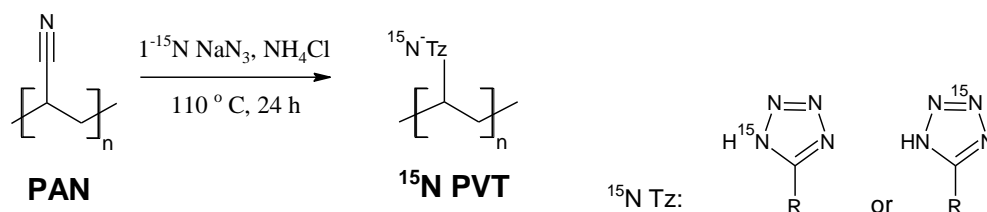


Figure 3.14 Reaction scheme for the synthesis of isotope-marked PVT (1-¹⁵N PVT)

3.2.4 Polymer Characterization

The polymers prepared were characterized before and after the composting. In the case of PVT and PVT-PAN, the polymers were characterized also before and after the solvent casting procedure used for the sample preparation.

3.2.4.1 Nuclear Magnetic Resonance, NMR

The samples were analyzed at the Centre Régional de Résonance Magnétique Nucléaire of the Chemistry Department of Université de Montréal

The Solid-State NMR experiments were carried out at room temperature on a Bruker Avance spectrometer operating at 14T (600 MHz ¹H frequency), with a 4 mm MAS (Magic Angle Spinning) probe.

For the PVT and PVT-PAN samples, ¹³C CPMAS experiments were performed with a spinning rate of 10.5 kHz, a contact time of 1.5 ms (¹³C radiofrequency field of 55 kHz), a repetition time of 0.5 seconds and a ¹H decoupling procedure using a radiofrequency field of 71 kHz. A total of 13000 scans were accumulated.

For the GAP-BPM and GAP-DHCD samples, ¹³C SPE (Single Pulse Excitation) experiments were performed with a spinning rate of 6 kHz, a repetition time of 10 seconds and the ¹H decoupling was performed with a radiofrequency field of 71 kHz. A total of 1024 scans were accumulated.

On the other hand, the liquid experiments were performed in one of the following equipments: a) Bruker AVANCE III 400 MHz, with a Prodigy probe CPBBO or b) Bruker AVANCE II 700 MHz Cryoprobe CPDCH, and the experimental conditions for the ^1H spectra were: angle $90^\circ = 11\text{-}12\ \mu\text{sec}$, and for the ^{13}C spectra: angle $90^\circ = 10\text{-}11.8\ \mu\text{sec}$.

For the solid-state ^{15}N NMR experiment, a ^{15}N CPMAS experiment was performed at $35\ ^\circ\text{C}$, with a spin rate of 12 kHz, a contact time of 1.5 ms, a repetition time of 6 s, and 700 scans were accumulated.

3.2.4.2 Sample preparation for FTIR and SEM-EDS

For the FTIR Microscopy and the SEM-EDS analysis, the samples were prepared as follows: from each sample, a piece about 1 cm width, 0.5 cm length and variable thickness was cut from the geometric center. These subsamples were encased inside epoxy resin, cured for 48 hours, and the cured encased subsample was sanded through a series of sandpapers (grits of 280 and 400) and then polished using polishing sheets of 12 microns and 3 microns. A scheme of the sample preparation is shown in Figure 3.15. Another possible method for the preparation of the samples is microtomy, but it generates a smaller sample, in which there might be less space for finding an unobstructed path for the microscopic analysis performed.

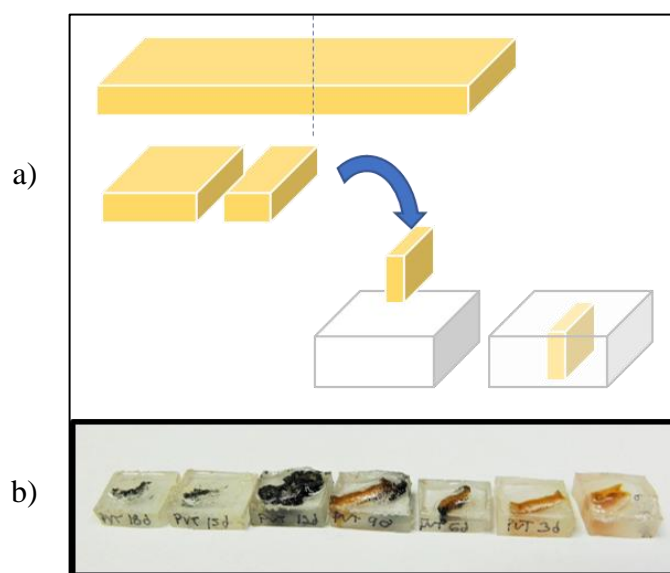


Figure 3.15 Preparation of the samples for FTIR Microscopy and EDS a) Scheme of the sample cut for resin encasing b) final samples after sanding and polishing (PVT samples shown)

3.2.4.3 Infrared Spectroscopy, FTIR

The FTIR analysis was performed by two methods: regular FTIR analysis for the powder samples before the solvent casting and the extracts; and “FTIR Microscopy” for the composted samples.

The FTIR Microscopy analyses were performed in the Vibrational Spectroscopy Laboratory of the Materials Characterisation Laboratory (LCM), of the Department of Chemistry of Université de Montréal with a Gigilab FTS-7000e FTIR microscope equipped with a micro-ATR accessory and a MCT infrared detector for the measurements. The measurements parameters for the analysis: 256 scans with a spectral resolution of 4 cm^{-1} ; and a spectral range of $700\text{-}4000\text{ cm}^{-1}$ using a Varian acquisition software of the instrument. The spectra were taken on the samples prepared as explained in section 3.2.4.2, perpendicular to the surface of the sample at “depths” of $0\mu\text{m}$, $150\mu\text{m}$, $300\mu\text{m}$ and $450\mu\text{m}$.

The rest of the FTIR analyses were performed at the Electrospinning and Film Characterization Laboratory of the Chemical Engineering of Polytechnique in a Spectrum 65 apparatus from Perkin Elmer, with an ATR Pike, and a Zn/Se crystal.

3.2.4.4 SEM and EDS (Energy-Dispersive X-Ray Spectroscopy)

The analysis of Scanning Electronic Microscopy (SEM) was made at the CREPEC Laboratory of Morphology of the Chemical Engineering Department at Polytechnique in a Hitachi TM3030 Plus equipment with no chromium deposition, at 5kV Mix of SE and BSE. The samples were prepared as explained in section 3.2.4.2. Pictures of the samples were taken at the following magnifications: 30x, 150x, 500x and 1000x. Two sets of images were taken for each sample: one on the geometric center of the sample (noted as “Middle”) and another near the interphase between the sample and the epoxy matrix (noted as “Side”).

The elemental analysis was performed by EDS at a magnification of 500x using a Bruker Quantax 70 software on the same equipment. The region for the elemental analysis was chosen from a

preliminary EDS analysis at a magnification of 30x by mapping the distribution of the elements, to ensure the presence of the energetic polymer, instead of the epoxy matrix or any compost residue.

3.2.4.5 Differential Scanning Calorimetry, DSC

The DSC analysis were performed in the Chemical Engineering Department at Polytechnique with a Q1000 equipment from T.A. Instruments with a cooling system RCS90 and, an autolid and autosampler. For the analysis, 1 mg of sample was put in a hermetic aluminium pan. Starting at 35 °C it was cooled to -90 °C at a rate of 5 °C/min, then it was heated to 40 °C at a rate of 10 °C/min, and finally heating to 300 °C at a rate of 3 °C/min.

3.2.4.6 Dynamic Mechanical Analysis, DMA

The DMA analysis were performed at General Dynamics Ordnance and Tactical Systems Canada laboratories located in Valleyfield, Québec with a DMA 850 equipment from T.A. Instruments. The analysis was run using a single cantilever clamp under the mode of constant strain temperature sweep, using an amplitude of 20 µm and a frequency of 1 Hz. The temperature ramp used a heating rate of 3 °C/min. The nominal sample size was: 12.00 mm x 3.00 mm x 35.00 mm (rectangular)

3.2.5 Biodegradability Experiments

The biodegradability tests were performed by following a protocol originally developed for polylactic acid (PLA) degradation (see Annex 1). This protocol is based upon the ASTM norms ASTM D5988-12 and D5338-98 and has been adapted by following the modifications suggested by Cossu C. and Lavoie J. [146].

The essays were performed using a composting material, assuming that the degradation would only be feasible in the presence of microbial flora in humid conditions; this assumption contrasting with what is signaled on the PLA protocol. The microbial community on the compost was not characterized. The compost used was Sea Compost from the brand MiracleGro, reporting the characteristics shown in Table 3.5. As a positive control, samples of PLLA 4032D were used.

Table 3.5 Compost composition as reported by the manufacturer.

| Species | Weight percentage |
|---|--------------------------|
| Total Nitrogen | 0.11 |
| Available Phosphate (as P ₂ O ₅) | 0.10 |
| Soluble Potash (as K ₂ O) | 0.12 |
| Calcium | 0.02 |
| Organic matter | 5 |
| Maximum moisture | 60 |

3.2.5.1 Compost preparation

The protocol for the preparation of the composting media was established at École Polytechnique de Montréal by CIRAIG, for the case of studies on the degradation of PLA [143]. For this matter, the large inert impurities of the compost were discarded, and the compost was air-dried for three days to facilitate the manipulation. The air-dried compost was sieved through two screens (5 mm and 4 mm). The aggregated material was crushed on a mortar to get a uniform density. All the sieved sub samples of compost were mixed together to ensure the uniformity of the compost material for all the essays conducted. The processed compost was stored in air-tight buckets and kept away from sunlight until its use.

3.2.5.2 Water Retention Capacity, WRC

The maximum water retention capacity (WRC) was measured according to the protocol developed by CIRAIG [147]:

$$\text{WRC} = [(P_2 - P_1) - (P_3 - P_1)] / (P_3 - P_1) \quad \text{Equation 1}$$

where P₁ is the weight of the aluminum vessel used for the weighting, P₂ is the total weight of the saturated compost sample plus the weight of the aluminum vessel, and P₃ is the weight of the dry compost plus the weight of the aluminum vessel.

3.2.5.3 Initial Water Content, IWC

The initial humidity of the compost was evaluated by the same protocol used for the water retention capacity described in equation 1 by measuring the weight of the humid compost, then drying it on the oven at 105°C for 24 hours and then measuring the weight of the dry compost. In this case, P2 becomes the total weight of the original compost (not saturated with water) plus the weight of the aluminum vessel.

3.2.5.4 Evaluation of the pH of the compost

The pH of the compost was kept between 6 and 8 to guarantee adequate conditions for the biodegradation [148, 149]. If the pH of the compost is below 6, the microbial flora can be atypical, and on the other hand, if the pH is higher than 8, it is possible to have retention of the CO₂ formed during the biodegradation process. The measurement of the pH was done by following the protocol established by the Centre d'Expertise en Analyse Environnementale du Québec [60]

3.2.5.5 Evaluation of the Humidity of the Compost

To ensure that the water content for the composting experiments was kept at 60% of the WRC value, the mass of the experimental bins (including lid, soil, and samples) was measured every two days. The amount of water to be added was the difference between the experimental soil mass and the expected soil mass at 60% WRC (M^*). Equation 2 was obtained by including these conditions in Equation 1

$$M^* = \frac{(1+0.6 \text{ WRC})}{(1+\text{IWC})} M_{\text{soil}}^{\circ} \quad \text{Equation 2}$$

M^* = Mass in grams of soil expected or ideal for soil with a water content of 60% WRC

WRC = Water Retention Capacity (as calculated in section 3.2.5.2)

IWC = Initial Water Content (as calculated in section 3.2.5.3)

M_{soil}° = Initial mass in grams of soil (experimental)

3.2.5.6 Sample Preparation

For both PVT and PVT-PAN, the composting samples were prepared by solvent casting as follows: a solution of the polymer was prepared by dissolving 6 g of polymer in 50 mL of hot DMF with agitation. The solution was let cool to room temperature, and then aliquots of 2-3 mL were poured on a silicon mold and heated on an oven at 90 °C under light vacuum. When the solvent was mostly evaporated, another aliquot was added, and the process was repeated until the final mass of the samples was 2-3 g. The samples were left at 80 °C under vacuum for 12 hours, then cooled down to room temperature and stored in airtight bags until the composting experiment.

The samples of GAP crosslinked with BPM or with DCHD were used without any further preparation after their unmolding.

3.2.5.7 Sample Composting Experiment

The composting experiments for each of the studied polymers were performed as follows:

Four plastic bins were filled with processed compost, until a height of 4 cm. Two triplicates of samples were put in three of the four plastic bins, each sample separated from the others. In the fourth bin, two triplicates of PLLA were put, as a biotic witness. Then all the samples were covered with processed compost until the total height was 8 cm from the bottom of the bins, and each bin was covered with its respective lid.

The bins were put in an environmental chamber Model LH-10 from Associated Environmental Systems, at the conditions established in During the first stage of this project, ten polymers were prepared, and only four of them were selected for the composting experiment, based in criteria of purity, simplicity of synthesis and experimental yield. In a later stage of the project, one of these four polymers was prepared with nitrogen-15 isotopic labelling and subjected to another composting experiment. In

Table 3.1 are shown the experimental conditions for the five polymers that were composted, and the variables that were considered.

Table 3.1. Every two days, all the bins were taken out of the environmental chamber and let cool to room temperature. The total weight of each bin was taken, including the lid, the samples and the compost, and the water content was corrected back to the chosen value (60% of Water Retention Capacity, WRC) by adding water, according to the calculations shown in section 3.2.5.5. The bins were then returned to the environmental chamber in such a manner that their positions inside were changed each time, to guarantee a homogeneous distribution of air and humidity inside the chamber.

Every three days, after adding the amount of water needed for a 60% WRC, a triplicate was taken out, by removing one sample from each of the three experimental bins in random order and position. The pH was also measured every 3 days as established in section 3.2.5.4. The total weight of the bin (including lid, compost, and samples) was measured to register the new weight of the bin at 60% WRC. A triplicate of the biotic witness was taken from the fourth bin only on days 9 and 18.

All the samples and the biotic witnesses were then washed manually with distilled water to remove as much compost particles as possible. Then the samples were dried with a paper towel and left to soak in 95% ethanol to remove any bacteria or fungi present. After 5-10 minutes, the samples were taken out of the ethanol and air dried to remove any rest of ethanol. The dry samples were stored in a dry place in airtight plastic bags away from sunlight until being analyzed.

3.2.5.8 Post-composting Characterization

3.2.5.8.1 Soluble Fraction

To evaluate the amount of crosslinking or reticulation on the samples before and after the degradation, a Soxhlet extraction of a subsample (1-2 g.) with 400 mL CH_2Cl_2 was performed for 24 hours. The soluble fraction (Xs) of the sample represents the mass fraction of the sample formed by small chains of polymer, which can be caused by the breakdown of the polymeric matrix.

$$X_s = \frac{M_{f+e} - M_f}{M_i} \quad \text{Equation 3}$$

M_{f+e} = Total mass in grams of the flask and extract after extraction

M_f = Mass in grams of dry flask

M_i = Initial mass in grams of polymeric sample

3.2.5.8.2 Chemical Characterization of the composted samples

The samples were characterized by FTIR, SEM-EDS and DSC, as was explained in the sections 3.2.4.3, 3.2.4.4 and 3.2.4.5 respectively.

3.2.5.8.3 Characterization of the composted samples by NMR Spectroscopy

For the NMR analyses, all the samples were analyzed on the solid state, under the conditions stated on section 3.2.4.1 for ^1H and ^{13}C . The extracts obtained from the soluble fraction determination (section 3.2.5.8.1) were also analyzed by ^1H and ^{13}C liquid NMR. The samples of the ^{15}N isotope-labeled PVT-PAN were analyzed only by ^{15}N NMR.

CHAPTER 4 RESULTS

4.1 Physical Properties of Synthesized Polymers

4.1.1 Experimental yields of Synthesis

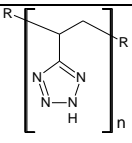
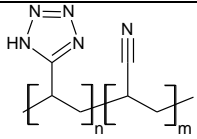
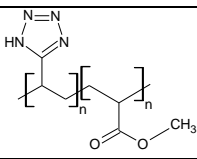
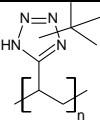
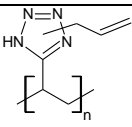
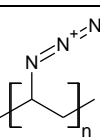
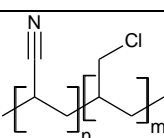
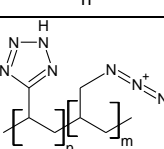
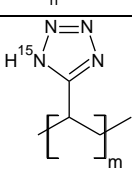
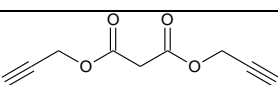
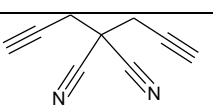
Given that the main goal of this research was the study of the biodegradation of energetic polymers by composting, it was necessary to have polymers of high purity, using synthesis methods that would be easy to perform to produce insensitive materials in high yields. In Table 4.1 are shown the highest yields of synthesis obtained for the different polymers prepared.

Both PVT and PVT-PAN complied with all these requirements, and while the yield of the dried polymers could have been higher, the solids after the synthesis and purification were very pure, and the additional mass found was due to the presence of residual solvent (DMF). This was also the case with the $1\text{-}^{15}\text{N}$ PVT sample, but as DMF was the solvent used for the solvent casting, it was not considered necessary to further purify nor dry the samples prior to solvent casting.

In the case of the PVT-PMA polymer, even though the synthesis was easy, it was not used for the composting experiments because during the preliminary tests, the purification of the samples was complicated by the hydrolysis of the ester group, and it was theorized that this process would also complicate the analysis of the composted samples by NMR.

The alkylated tetrazole polymers, tBu-PVT and allyl-PVT were proposed because of the easiness of their preparation and because it would be interesting to see the differences in the biodegradation behavior of the tetrazole group due to different substituents. Nevertheless, the purity of the synthesis was low, and in the case of the allyl compound, the attempted purification produced secondary reactions and crosslinking on the allyl group, decreasing the solubility of the sample, which would have hindered the solvent casting. For the tBu-PVT, the preliminary NMR analysis were very difficult due to the low solubility of the polymer, and the ^{13}C -NMR tests showed that the position of the tert-butyl group made it impossible to distinguish the tetrazole signal in liquid NMR (around 150-160 ppm), which would have complicated the analysis by Solid-State NMR.

Table 4.1 Experimental yields of the polymers prepared.

| Compound | Conditions | Yield | Composted |
|------------------------|--|--------------------------------------|-------------------|
| PVT |  100 °C, 24h 110 °C, 24h | 64% ^a 77% ^a | Yes |
| PVT-PAN |  100 °C, 24h 110 °C, 24h | 87% ^a 93 % | Yes |
| PVT-PMA |  100 °C, 24h 110 °C, 24h | 76% 94% (impure) | No |
| tBu-PVT |  80 °C, 2h CHCl ₃ reflux, 5h 80 °C, 24h | 71% (impure) 92% (impure) 66% | No |
| Allyl-PVT |  45 °C, 4h | 53% | No |
| PVAz |  65 °C, 24h (N ₃ :Cl 1:2) 100 °C, 2h | 91% (impure) 70% (impure) | No |
| PAN-PAC |  70 °C (2h), 60 °C, 22h | 56% ^b | No |
| PVT-PAAz |  105 °C, 20h | >98% ^b | No |
| 1- ¹⁵ N PVT |  110 °C, 24h | >100% ^c | Yes |
| BPM |  110 °C, 4h | 71% [150] | Yes (as GAP-BPM) |
| DCHD |  0 °C to RT, 6h | 74% [150] | Yes (as GAP-DCHD) |

^a calculated from the solid after several days of high vacuum drying.^b assuming a molar nitrile:allyl ratio of 13:1^c pure product (excess of solvent).

On the other hand, the poly vinyl azide sample, PVAz was the first polymer attempted, and even though its synthesis was easy, the resulting polymer had low purity, due to an incomplete substitution reaction. This resulted in the presence of both chlorine and azide groups on the polymer. Another cause of the low purity of this sample was the fact that as both groups were on a secondary carbon, there was a competition between the substitution and the elimination reactions. The elimination reaction resulted in double bonds in the polymer backbone, that over time could react and produce undesired crosslinking of the polymer, decreasing its solubility, as was observed by the formation of a precipitate on the stored solutions of the polymer in acetone.

In Table 4.2 are shown the analyses run for each of the compounds. The FTIR analyses were performed on the polymers that were composted, or to verify the purity of some samples. The NMR were run on the composted samples, and also in the reagents for the crosslinked samples, to help in the identification after the composting. The DSC analyses were only run on the polymers that were to be composted, and the DMA was only performed in the GAP-crosslinked polymers to find evidence of biodegradation. The rest of the polymers were not analyzed, due to their low purity or yield.

Table 4.2 Characterization tests run in the prepared samples.

| | Compound | Composting | NMR | FTIR | DSC | DMA |
|---|------------------------|-------------------|------------|-------------|------------|------------|
| Poly Vinyl Tetrazole and derivatives | PVT | X | X | X | X | |
| | PVT-PAN | X | X | X | X | |
| | PVT-PMA | | | X | | |
| | tBu-PVT | | | | | |
| | Allyl-PVT | | | | | |
| | PVT-PAAz | | | | | |
| | 1- ¹⁵ N PVT | X | | | | X |
| Other polymers | PAN-PAC | | | | | |
| | PVAz | | | X | | |
| | GAP | | X | | X | |
| Crosslinkers | BPM | | X | | | |
| | DCHD | | X | | | |
| Crosslinked GAP | GAP-BPM | X | X | X | X | X |
| | GAP-DCHD | X | X | X | X | X |

4.1.2 NMR analysis: ^1H -NMR and ^{13}C -NMR

In this section are presented the NMR spectra of the compounds used for this project, and the expected chemical shifts in liquid state experiments for proton and carbon can be seen in Table 4.3 and

Table 4.4 respectively. The ^1H -NMR spectra for the samples were difficult to obtain, due to the exceptionally low solubility of the polymer after the solvent casting process. After several attempts, it was decided to focus the attention on the carbon spectra.

In the case of the ^{13}C -NMR, it was preferred to perform Solid State experiments, which have the disadvantage of presenting broader signals, which can result in overlapping signals that would appear separated on liquid NMR experiments.

Table 4.3 Expected ^1H -NMR chemical shifts in liquid state.

| Signal (ppm) | Interpretation | Reference |
|------------------|-----------------------------------|-----------|
| 2.74, 2.89, 7.96 | DMF impurities | [151] |
| ~2.03 | -CH ₂ - β to CN in PAN | [31] |
| ~3.14 | -CH- α to CN in PAN | [31] |
| ~7.9, 9.5 | NH in tetrazole group | [31, 152] |
| 7.75, ~8.6 | CH on the triazole ring | [62, 152] |

Table 4.4 Expected ^{13}C -NMR chemical shifts.

| Signal (ppm) | Interpretation | Reference |
|----------------------|------------------|-----------|
| 30.73, 35.74, 162.29 | DMF impurities | [151] |
| 120 | CN PAN | [29] |
| 27, 33 | C from PAN Chain | [29] |
| 38 | C from PVT Chain | [29] |
| 129.9 | Triazole | [62] |
| 158 | Tetrazole | [29] |

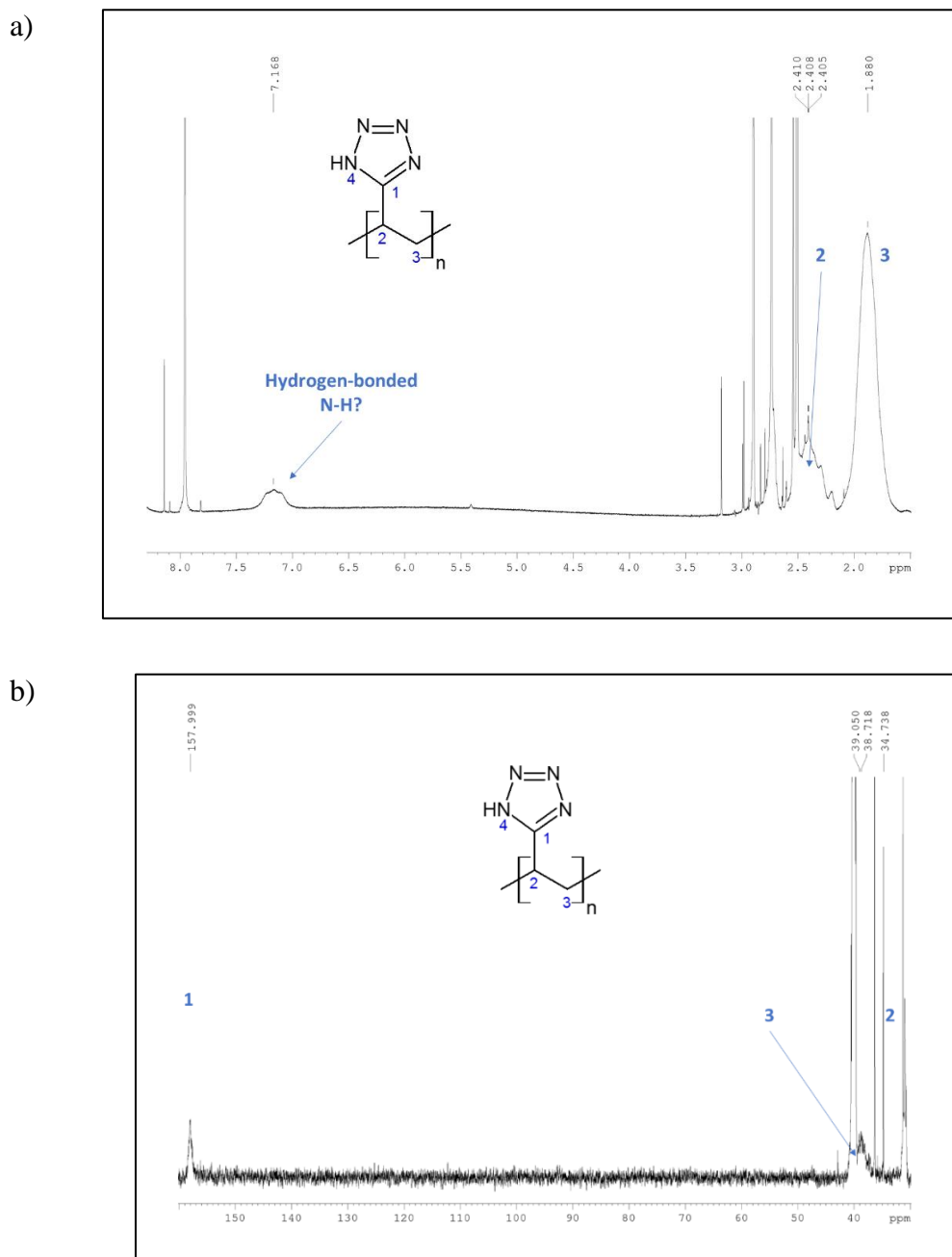


Figure 4.1 Spectra of PVT a) ^1H -NMR b) ^{13}C -NMR

In Figure 4.1 are shown the NMR spectra for PVT. In the ^1H -NMR it can be seen the signals for the protons in the backbone, and while the proton of the tetrazole was expected to appear in the spectrum, it was not clear from the experiments run. One of the possible explanations for this is that the proton is very labile, as the tetrazole ring exhibits tautomerization from the resonance of

the different electronic pairs in the ring. Another possibility is that the N-H groups are not free, but are actually participating in hydrogen-bonds, either with a neighbor tetrazole ring, or with molecules of DMF trapped in the polymeric matrix during the solvent-casting preparation. This would explain the broad multiplet found at 7.15 ppm.

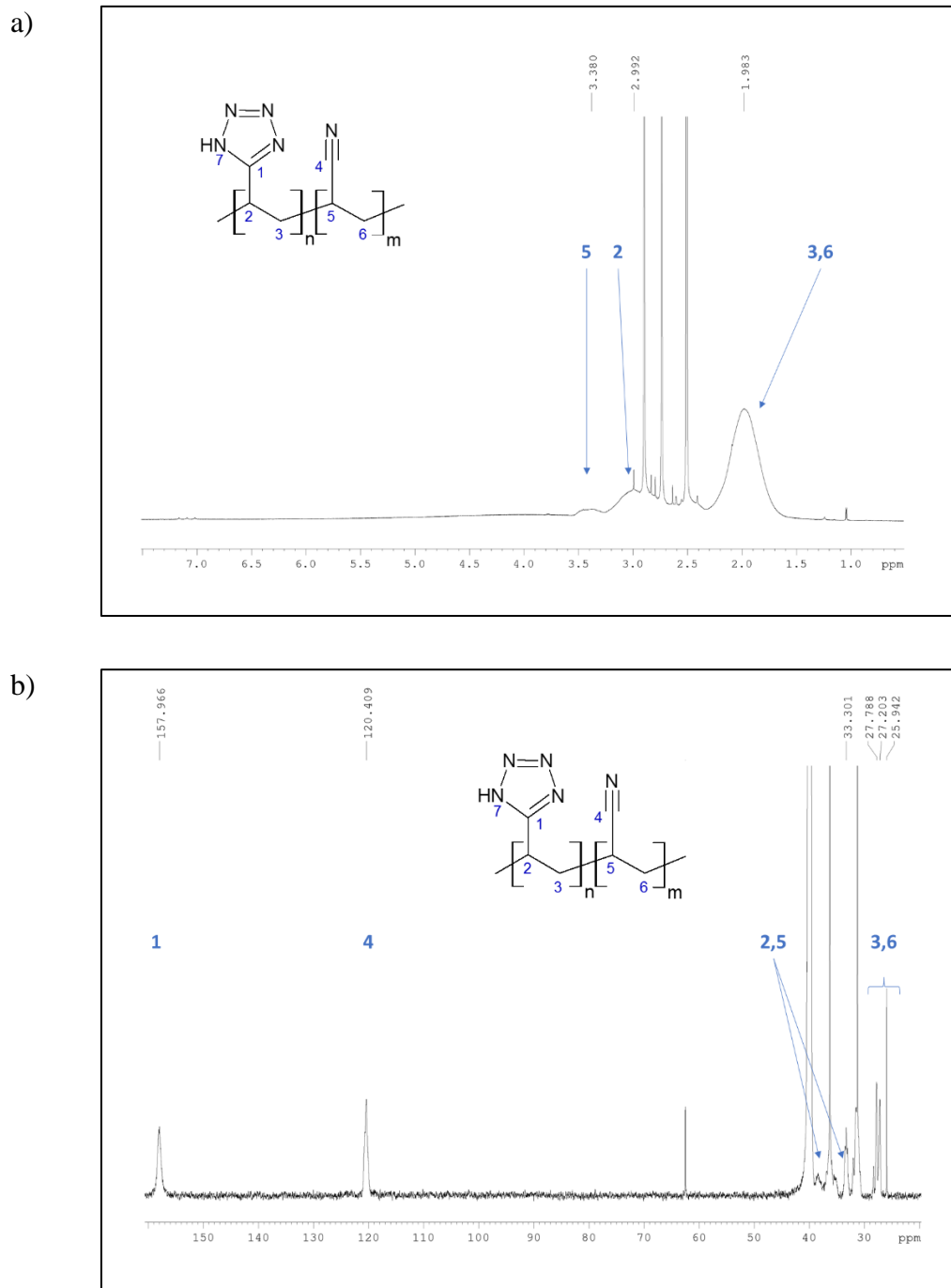


Figure 4.2 Spectra of PVT-PAN a) ^1H -NMR b) ^{13}C -NMR

On the other hand, the ^{13}C -NMR clearly shows a signal at 158 ppm which can be attributed to the tetrazole carbon. This confirms the azidation of the nitrile groups on the starting material, and the absence of signals for the nitrile group at ~ 120 ppm supposes a polymer formed with a high degree of purity.

The spectra of PVT-PAN are presented in Figure 4.2. The signals for the protons in the backbone become broader and more complicated, as the azidation of the polyacrylonitrile is expected to be random, giving rise to different combinations of vicinal groups. The signal at 3.5 ppm corresponds to the methine proton located next to the nitrile group at the “alpha” carbon, which as expected, should appear for the PVT-PAN samples but not for the PVT ones, suggesting the partial azidation for the former and the total azidation of the latter.

Regarding the ^{13}C -NMR, the spectrum shows the signals already discussed for the PVT, including the tetrazole signal, plus a signal at 120 ppm, which corresponds to the chemical shift of the nitrile groups of the starting material that were not azidated. This also confirms the different identities of both polymeric samples.

For the analysis of the GAP-BPM and GAP-DCHD samples, it was necessary first to differentiate the signals of the glycidyl azide polymer, so a series of spectra were taken. In Figure 4.3 are shown the ^1H -NMR and ^{13}C -NMR spectra for GAP with their interpretation, and in Figure 4.4 it is presented the HSQC (“heteronuclear single quantum correlation”) spectrum of GAP, which correlates the chemical shifts in the ^{13}C and ^1H -NMR spectra shown in Figure 4.3. This type of correlation spectroscopy shows the “one-bond couplings” existing between carbon atoms and their associated hydrogens [153]. For interpretation purposes, the x-axis on the HSQC spectrum is the ^1H -NMR spectrum shown in Figure 4.3a, while the y-axis on the HSQC corresponds with the ^{13}C -NMR shown in Figure 4.3b. As it can be seen from the HSQC, each carbon has a variety of proton signals associated, which is expected for a resin that would contain oligomeric chains of different lengths, and different tacticities.

From the HSQC analysis, the signal at 3.5 ppm in the ^1H -NMR correspond to the signal at 57.9 ppm in the ^{13}C -NMR, and it can be assigned to a $\text{CH}_2\text{-OH}$ group, as an end group for the polymer.

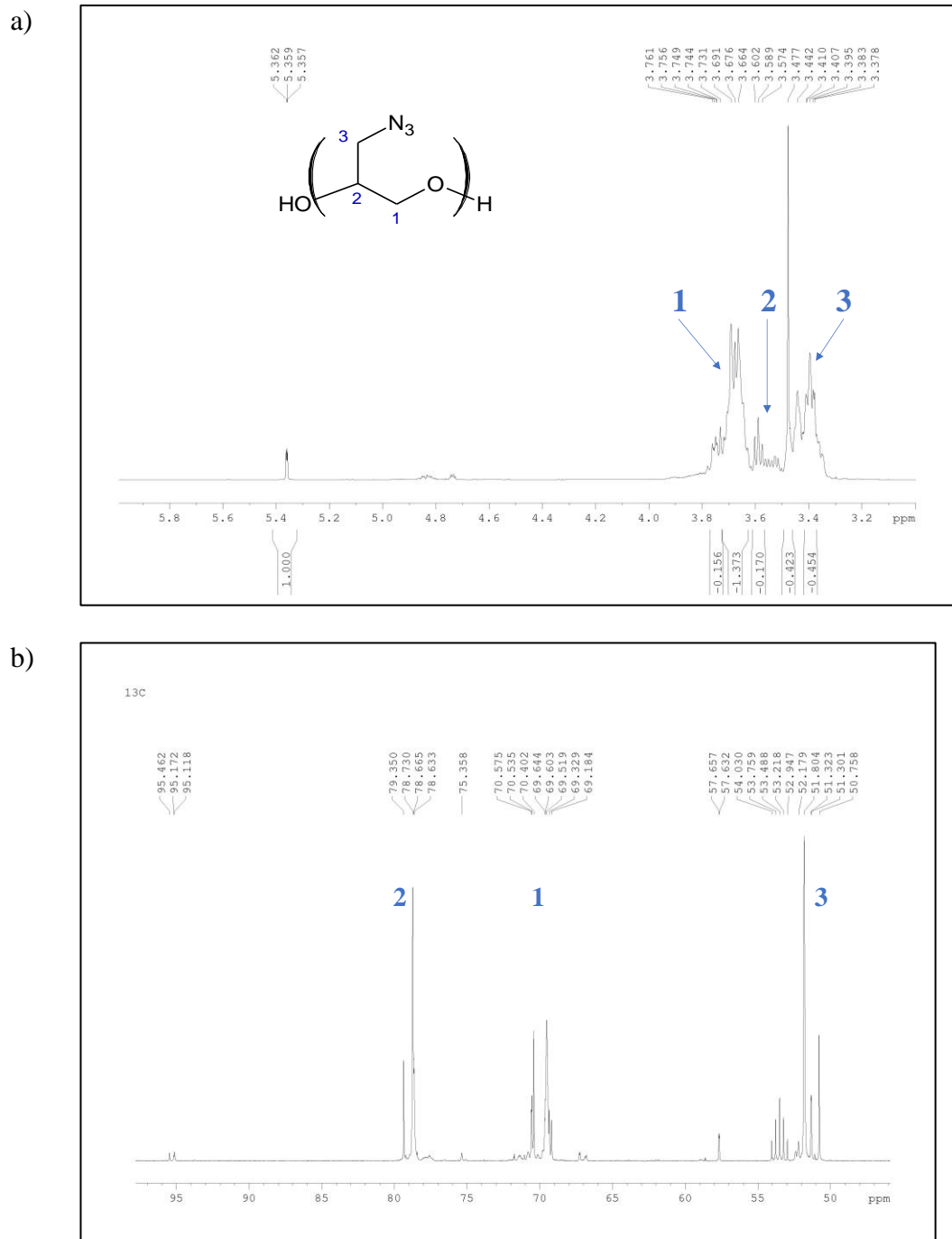


Figure 4.3 Spectra of GAP a) $^1\text{H-NMR}$ b) $^{13}\text{C-NMR}$

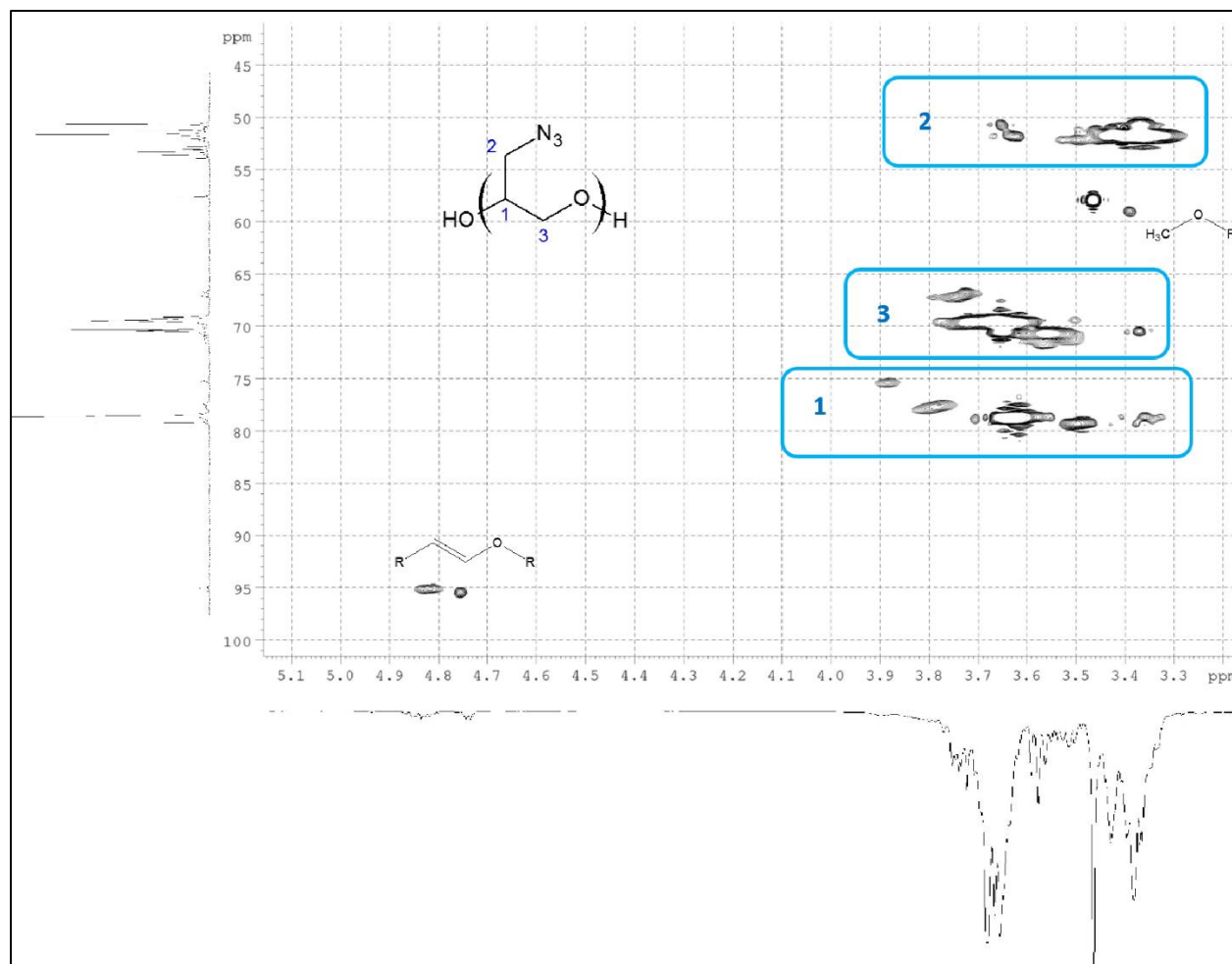
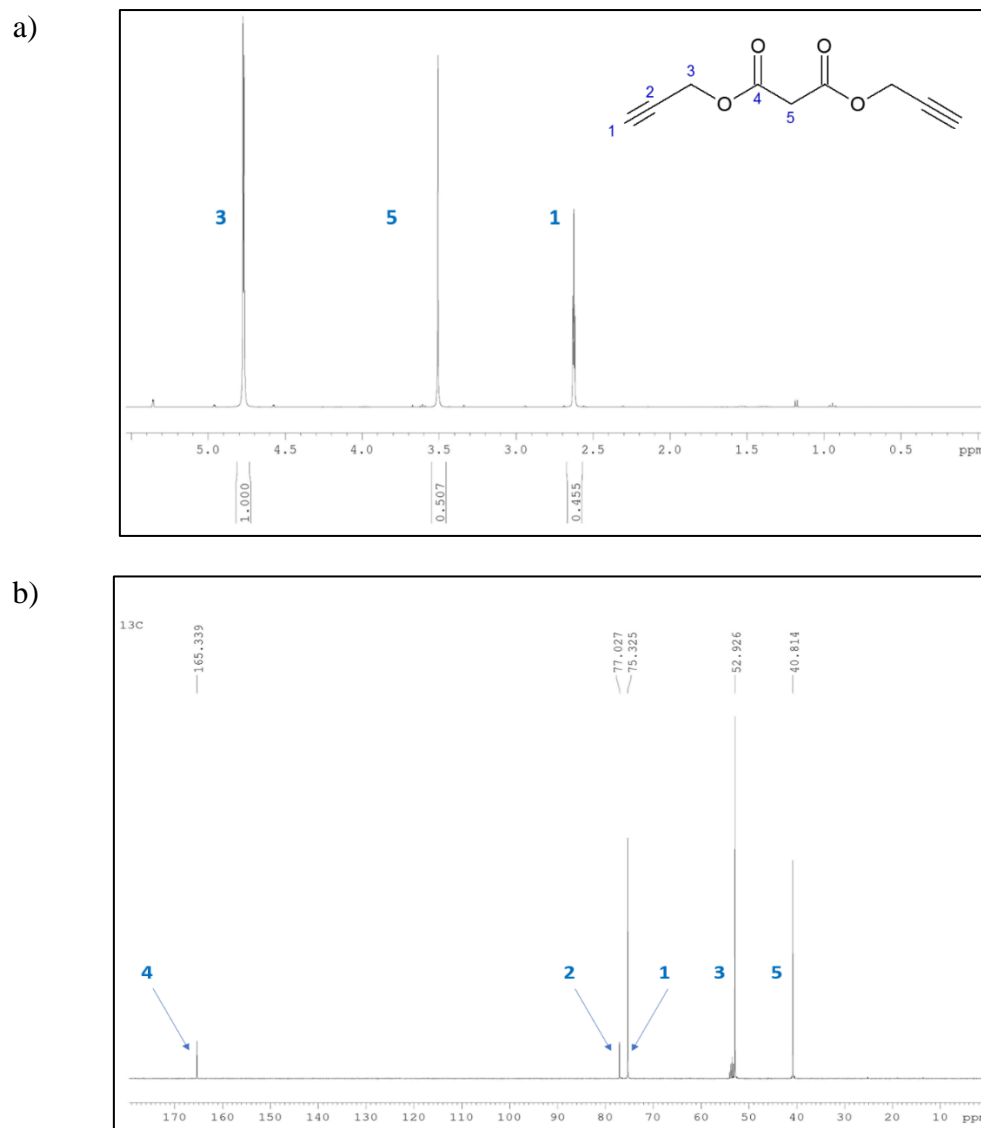


Figure 4.4 Spectrum HSQC of GAP (X-axis: ^1H -NMR, Y-axis: ^{13}C -NMR)

The spectra of BPM and DCHD are shown in Figure 4.5 and Figure 4.6 respectively and were taken to help identify different groups during the analysis of the spectra of GAP crosslinked with these substances. For example, it is expected that the signals for the alkynes disappear as they would become part of the triazole groups, unless the reaction is not complete. Also, the nitrile groups in DCHD should appear; same for the carbonyl signals in BPM, unless any of these groups would suffer some change during the composting (for example, hydrolysis of the esters).



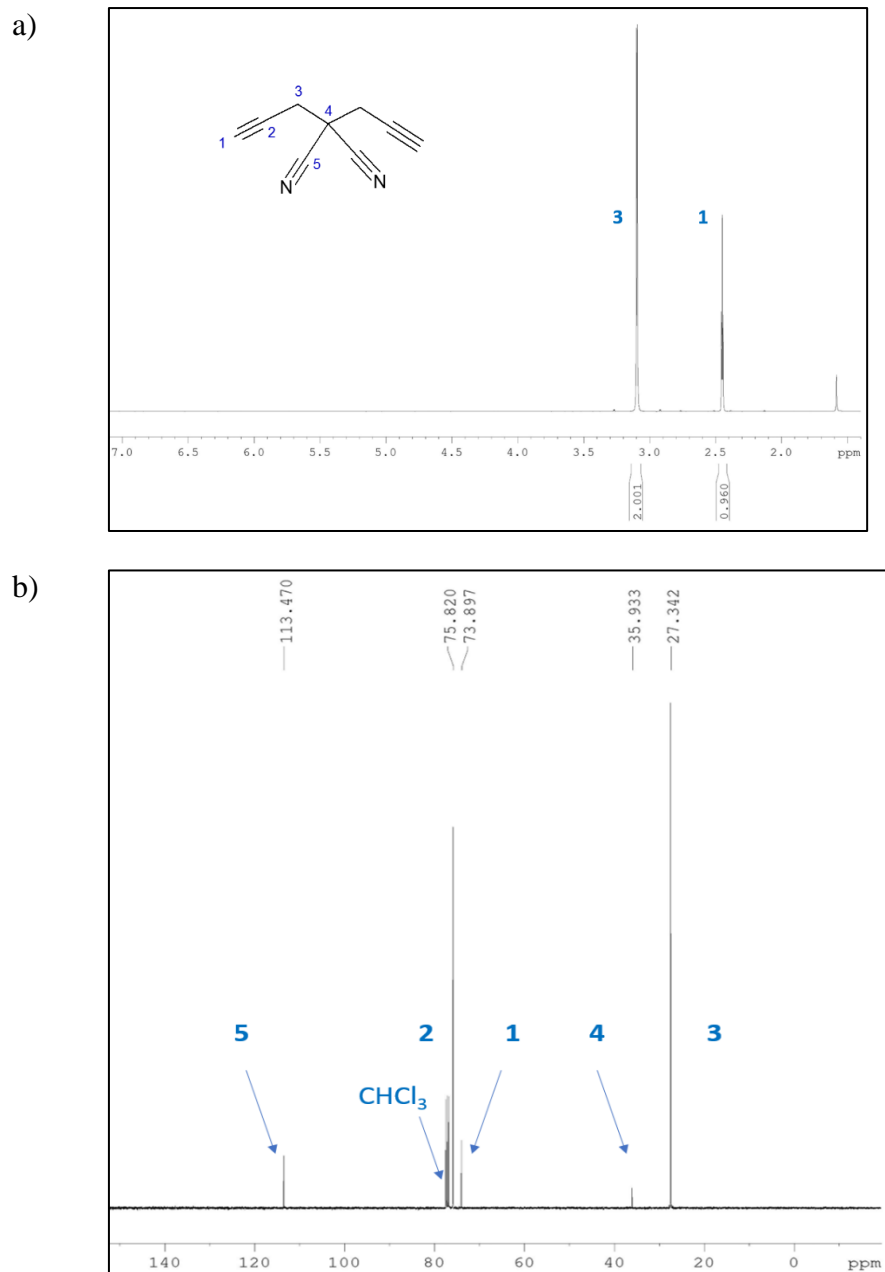


Figure 4.6 Spectra of DCHD a) $^1\text{H-NMR}$ b) $^{13}\text{C-NMR}$

4.1.3 FTIR

The expected bands for the different compounds analyzed can be seen on the following table

Table 4.5 Expected FTIR bands

| Expected Bands (cm ⁻¹) | Group | Reference |
|--|---|----------------------|
| 1430 (CHO), 1680 (amide) | DMF impurities | [153] |
| 736, 1020-1025, 1038-1147 1265-1320 1650 (C=N stretching) 2490-3130 (broad) | Tetrazole | [28, 29, 31, 154] |
| 2243 (stretching) | -C≡N | [28, 29, 31] |
| 2930, 2850 (stretching) 1450 (bending) | Alkyl protons (-CH ₂ - and -CH-) | [28, 31] |
| 650-1000 (C-H bending) 1640-1670 >3000 (stretching) | Double bonds (crosslinking or elimination) | [153] |
| 1730 | C=O Esters | [62] |
| 2122 (C≡C stretching) 3285 (C-H stretching) | Triple bonds (unreacted BPM, DCHD) | [56, 153] |

The products analyzed by FTIR were those with a good synthesis yield: PVT and PVT-PAN. The analyses of PVAz and PVT-PMA confirmed that the products had low purity. In the case of PVAz, this low purity is due to the presence of double bonds related to elimination reactions. For the case of PVT-PMA, it was considered that from a real-life perspective, an energetic formulation with this compound might be unstable due to the presence of carboxylate groups that might be incompatible with other components.

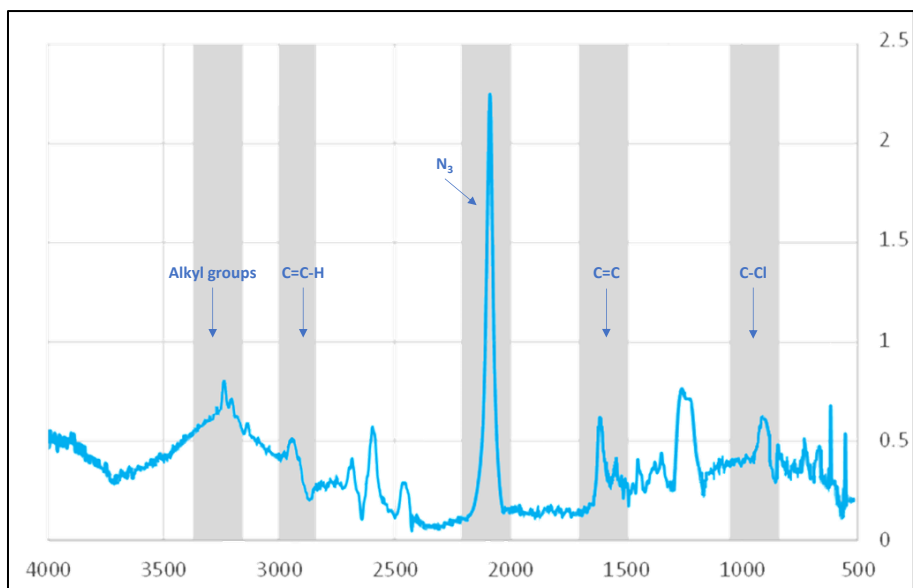


Figure 4.7 FTIR Spectrum for PVAz

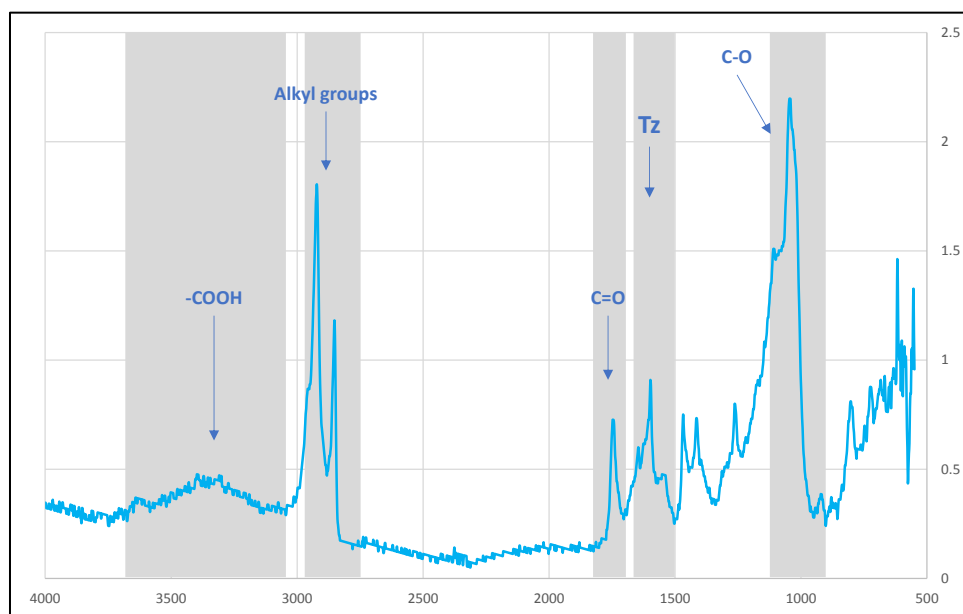


Figure 4.8 FTIR Spectrum for PVT-PMA

In the Figure 4.9 are shown the FTIR spectra for PAN, PVT, and PVT-PAN, to better understand the changes that the polyacrylonitrile chain suffered during the azidation. The most notable change is the decrease in intensity of the nitrile signal around 2240 cm^{-1} , being one of the most important

signals for PAN, together with the alkane stretching signal around 1400 cm^{-1} . As it can be seen, this signal for the nitrile group is present also in the PVT-PAN polymer, but in a lower degree.

The next key signal is the C=N stretching signal from the tetrazole rings, found at 1636 cm^{-1} for both PVT and PVT-PAN, but absent in the PAN, confirming the azidation of the nitrile groups. And finally, the broad signal centered at 3100 cm^{-1} , which was attributed to the sum of the N-N stretching of the tetrazole ring, broadened by the presence of the alkane signal before 3000 cm^{-1} , plus the lability of the proton of the tetrazole ring, due to tautomerism.

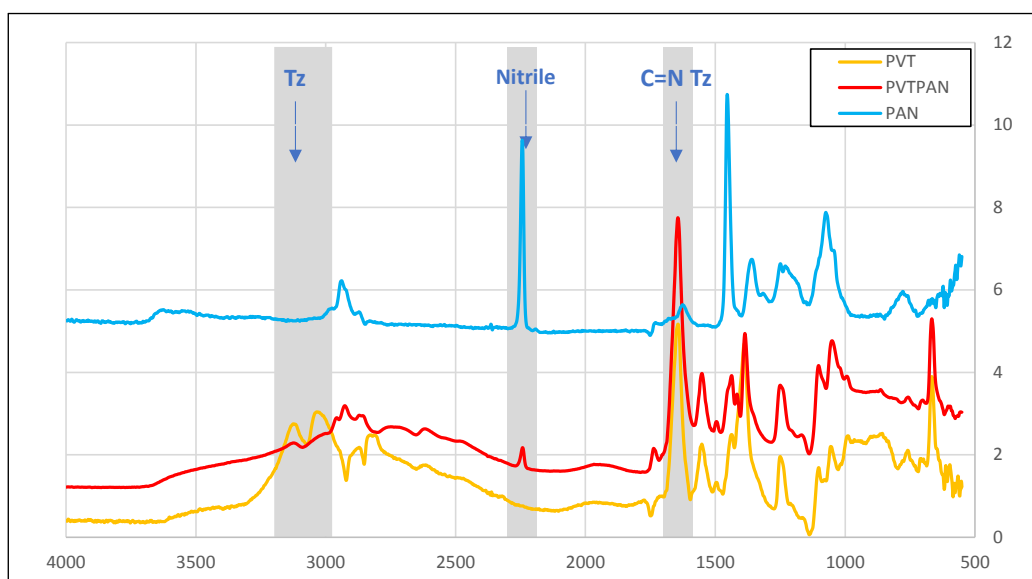


Figure 4.9 FTIR Spectra for PAN, PVT, and PVT-PAN

4.2 Thermal and Mechanical Properties of Synthesized Polymers

4.2.1 DSC

In the DSC curve for PVAz, shown in Figure 4.10, the decomposition peak at $208\text{ }^{\circ}\text{C}$ is due to the decomposition of the azide group with the release of N_2 [38], while the peak at $252\text{ }^{\circ}\text{C}$ might be caused by the release of chlorine atoms (either as HCl or as Cl_2). As it can be seen, the polymer contains a high proportion of chlorine, signaling an incomplete azidation, which was the case after several synthesis attempts.

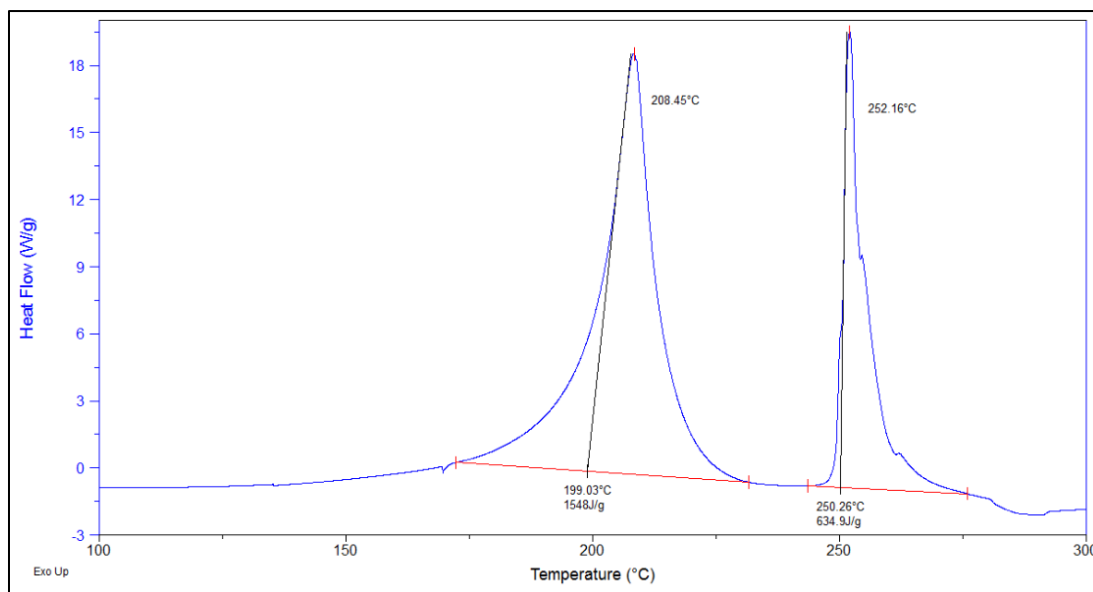


Figure 4.10 DSC decomposition curve for PVAz

As was reported by Huang [28], the DSC of PVT can present a broad endothermic peak below 100 °C, due to the evaporation of water. It is also typical for the prepared samples to have a melting point signal around 180 °C, happening exactly at the onset of decomposition, which would suggest a faster decomposition in the molten state; while the peak linked to the decomposition of the tetrazole rings is found between 215 °C and 285 °C. This can be seen in Figure 4.11, where the presence of two signals for the decomposition of the tetrazole group might be due to complex reactions between the by-products of the decomposition of the tetrazole groups.

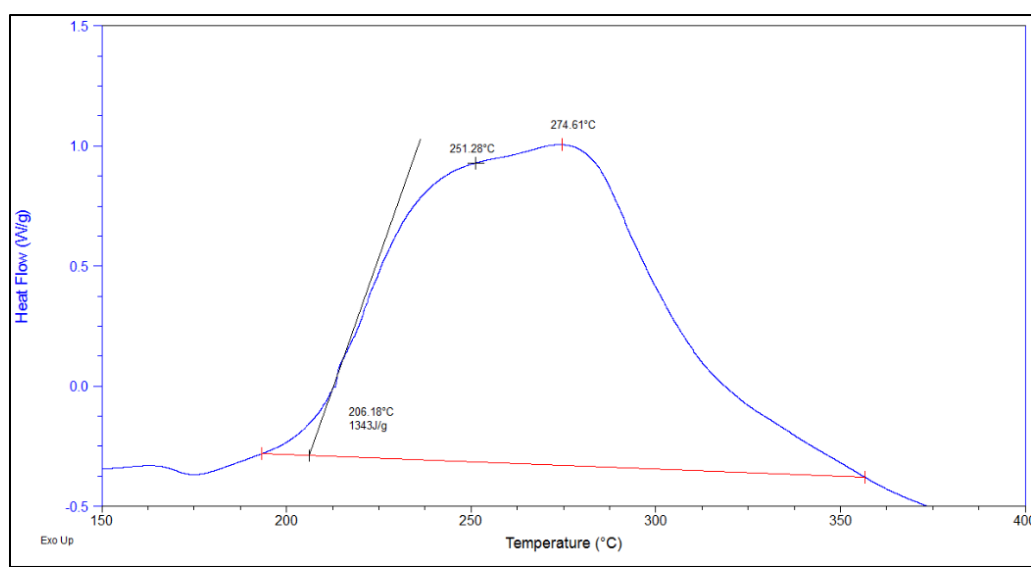


Figure 4.11 DSC decomposition curve for PVT

For the case of PVT-PAN (Figure 4.12), the peak around 274 °C remains the same, and the difference in the shape for the exothermic peak which might be due to the less energetic nature of the PVT-PAN polymer.

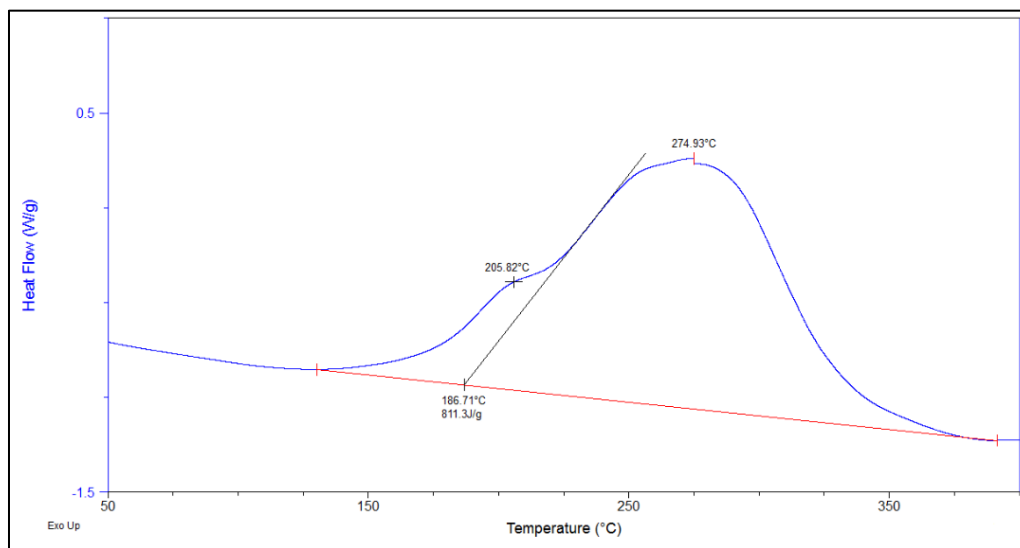


Figure 4.12 DSC decomposition curve for PVT-PAN

The DSC curve for the decomposition of PVT-PMA can be seen in Figure 4.13, and it shows the signal for the tetrazole groups around 277 °C, as expected. There is also an exothermic signal at 246 °C which might be assumed to correspond to the decomposition of the ester group, probably by decarboxylation.

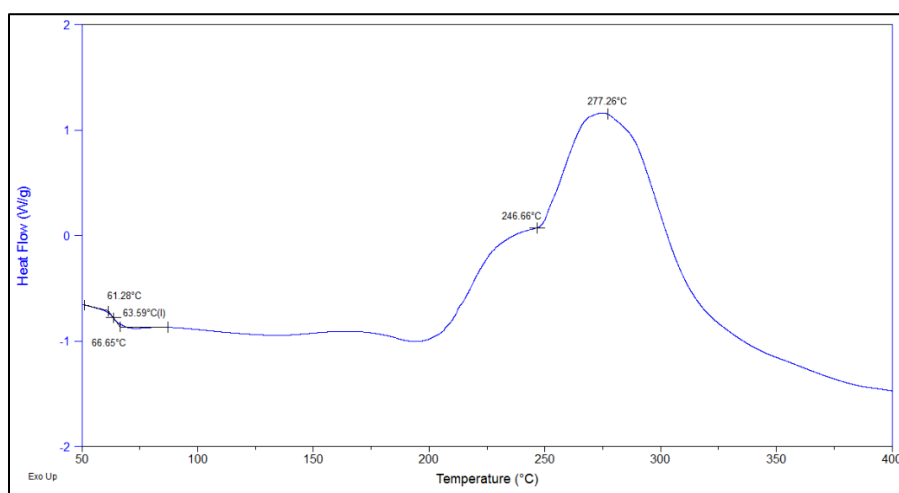


Figure 4.13 DSC decomposition curve for PVT-PMA

In Figure 4.14 are shown the DSC curves for the glycidyl azide polymer used in this project, the plasticizer “GAP-700”, which would be referred to hereon as GAP. This resin-like compound shows a clear glass transition temperature at around $-66\text{ }^{\circ}\text{C}$, and then an exothermic decomposition of the azide groups around $240\text{ }^{\circ}\text{C}$ due to the release of N_2 . These two signals will be referred to later in the discussion of the DSC curves of the crosslinked polymers GAP-BPM and GAP-DCHD.

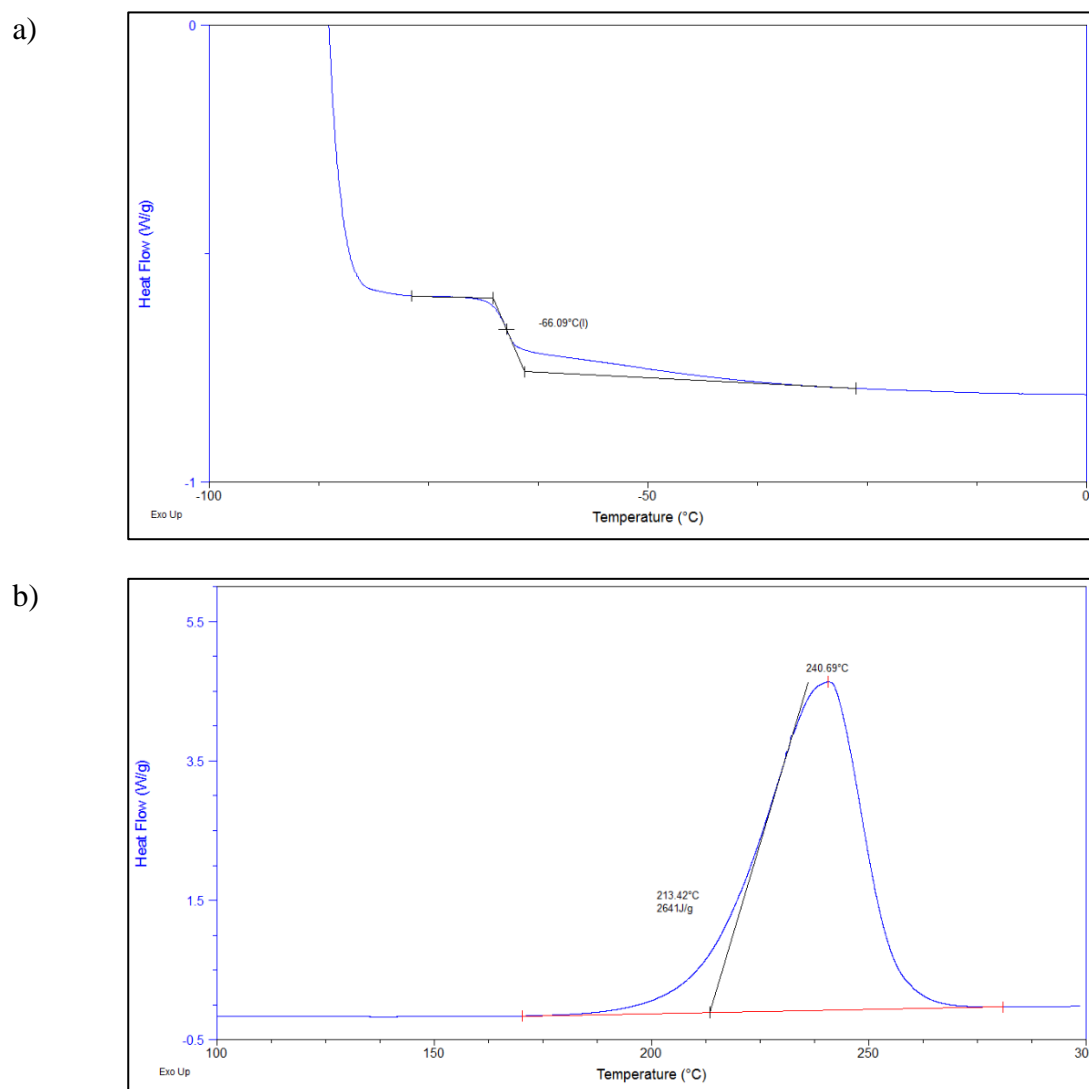


Figure 4.14 DSC curves for GAP-700 a) T_g b) Decomposition

4.2.2 DMA

The mechanical properties of the biodegraded polymers were only studied for the case of GAP-BPM and GAP-DCHD. In the case of PVT and PVT-PAN, the samples deformed very much during the composting experiments, making it impossible to obtain a sample with a uniform shape for the tests of traction and dynamic analysis (single or double cantilever). Also, as has been discussed before, some soil particles got embedded into the samples during the composting, which would also affect the mechanical properties of the polymers, and their measurement.

For the case of GAP-BPM and GAP-DCHD, the softness of the samples would hinder the analysis by traction, as there are few available testing methods for extremely soft gels and this particular result is not of great interest. The analysis of the DMA results is shown in section 4.3.5 together with the composted samples.

4.3 Composting Results

4.3.1 Soluble Fraction

In Figure 4.15 are shown the polymeric samples after the composting experiment. For clarity purposes, the samples were cut in half, and only one half was photographed.

It can be seen from Figure 4.15 that the PVT sample decomposed faster than the other samples, to the point that one of the samples of the triplicate could not be recovered from the soil after $t = 15$ days. It was noted that both PVT and PVT-PAN samples swelled, as a result of the hygroscopicity of the PVT chains, which is expected from the tetrazole groups [3]. Because the tetrazole ring is a functional group with high polarity and a low pKa, it can attract small molecules like water, and would easily form hydrogen bonds with them. Also, as the tetrazole can form tetrazolate salts with metal ions in the soil. Because of all these factors, it was not possible to completely remove all the soil particles at the end of the experiment.

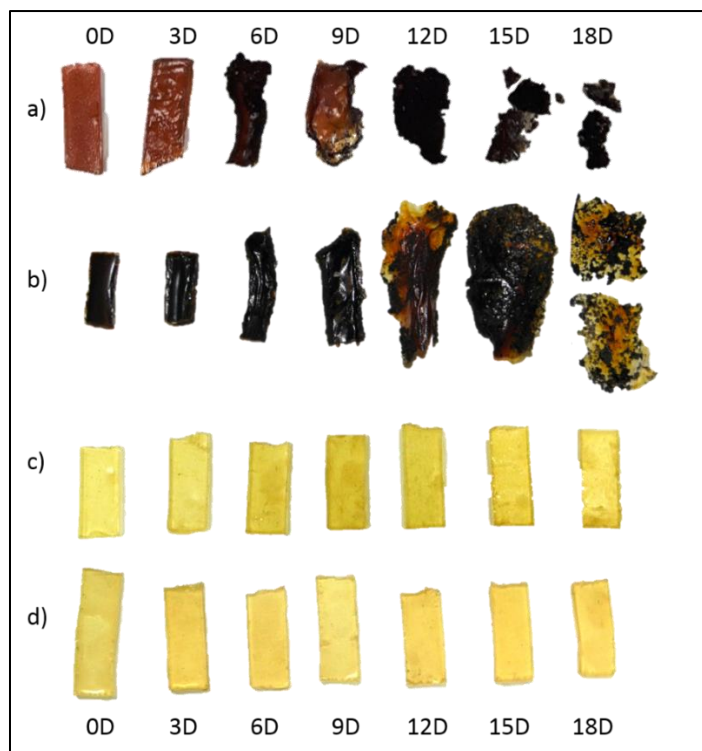


Figure 4.15 Polymeric samples after the composting experiment: a) PVT b) PVT-PAN c) GAP-BPM d) GAP-DCHD

For the samples of GAP-BPM and GAP-DCHD, after the composting experiments the appearance did not change considerably, and only a slight cloudiness was perceived on the samples composted for 15 and 18 days.

The behavior of the mass loss for the samples is shown in Figure 4.16, where the error bars correspond to the standard deviation obtained for each sample triplicate at each day of analysis. In this case, it can be seen that for both GAP-BPM and GAP-DCHD, the results are very similar, and the mass loss of some samples of GAP-BPM overlaps the values for GAP-DCHD.

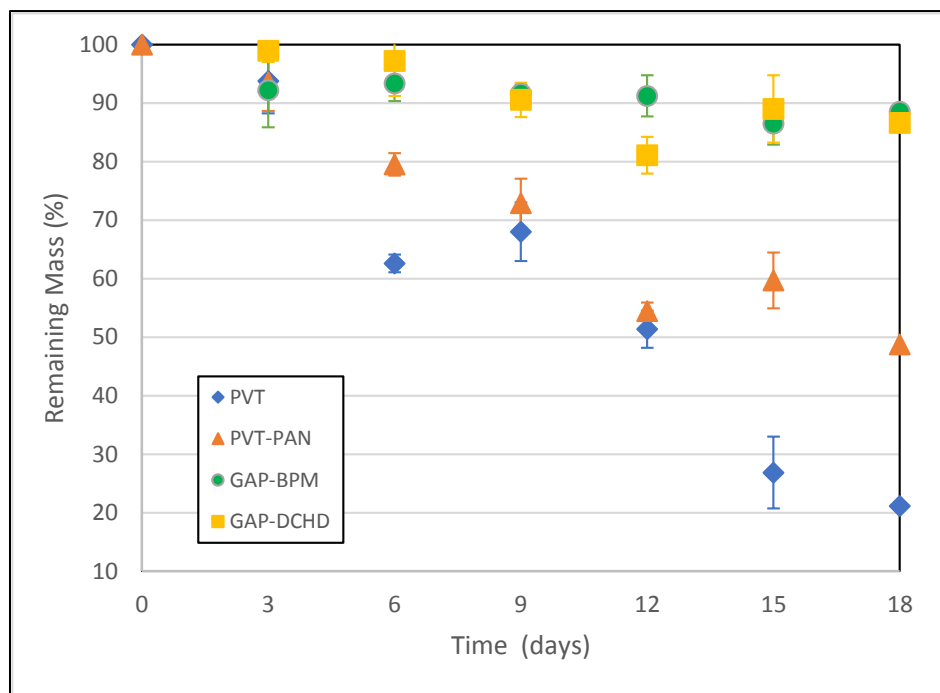


Figure 4.16 Mass change for the composted samples

As it has been discussed by Spain, J. [100], the breakdown or disappearance of an energetic compound is not a guarantee of the harmlessness of said chemical, as it could bind to the soil, react with biomass elements or even form substances that might be more toxic or hazardous than the initial compound, as is the case for some biodegradation products of TNT. For both GAP crosslinked products, the low degree of biodegradation might actually be an advantage for recovery processes in contaminated areas. The contrary could be said about PVT and PVT-PAN, which showed to decompose easily, which might prevent the treatment of contaminated soils by recovery but might require other treatments, like percolation, subcritical or supercritical extraction, among others. In Table 4.6 is shown a comparison between several composting experiments on various energetic materials, mainly TNT, as the environmental impact of this compound has been exhaustively studied. In this study, no microbiologic nor organic amendments or additives were used; and it would be expected that the contaminant removal would increase in the presence of a higher microbiological charge on the compost.

Table 4.6 Comparison of the behavior of different energetic materials in composting experiments

| | Energetic Material | Composting type | Conditions | Time (days) | Contaminant removal (Approx. %) |
|--------------------|---------------------------|------------------------|---------------------------|--------------------|--|
| This study | PVT | Static | 55 °C | 18 | 79 (PVT) |
| | PVT-PAN | Aerobic | No bacteria inoc. | | 51 (PVT-PAN) |
| | GAP-BPM | No Amendments | 60% humidity | | 12 (GAP-BPM) ^a |
| | GAP-DCHD | | | | 14 (GAP-DCHD) ^a |
| Gumuscu [102] | TNT | Static | 35-45 °C | 15 | ~20 |
| | | Aerobic | No bacteria inoc. | | |
| | | With Amendments | 60% humidity | | |
| Park [155] | TNT | Static | 30 °C | 45 | 88-89 (20 days) |
| | | Aerobic | Sewage sludge as inoculum | | 92-96 (45 days) |
| | | With Amendments | | | |
| Rezaei [156] | TNT | Static | 55 °C | 27 | 30 (anaerobic) |
| | | Aerobic/Anaerobic | 60% humidity | | 74 (aerobic) |
| | | With Amendments | | | |
| In [103] | TNT | Static | 30 °C | 45 | 20 |
| | Aerobic | No bacteria inoc. | | | |
| | No Amendments | 100% humidity | | | |
| Elgh Dalgren [104] | TNT | Static | 20 °C | 182 | 67 (TNT) |
| | RDX | Aerobic | 80% humidity | | 0 (RDX and HMX) |
| | HMX | With Amendments | | | |

^a evaluated on a gel (R=0.20).

The results for the soluble fraction determination through extraction with CH₂Cl₂ can be seen in the Figure 4.17, and the error bars correspond to the standard deviation obtained for each sample triplicate at each day of analysis. The behaviour of the cross-linked GAP polymers differs from that of the PVT-related polymers: in both cases of the GAP polymers, the starting soluble fraction was high (around 0.7), which can be interpreted as 70% of the sample being extractable. This could be related to several factors, for example, the 1:5 alkyne/azide ratio used for the crosslinking, implying that the extractable fraction of the samples consists of GAP that did not form triazole rings with the bisalkynes. Another factor is the difference in the molecular weights between the GAP-crosslinked samples and the PVT and PVT-PAN, as the starting GAP-700 is a rather light oligomer usually considered more of a plasticizer than a binder (~700 g/mol, so roughly 7 units long), so there is a high possibility that at R=0.20, the polymer chains are not bridged by triazoles to form an immobile network. In this case, the shortest chains would diffuse away very quickly under composting conditions, causing the quick weight loss observed.

The biggest change on the soluble fraction occurs between the day 0 and the day 3, but the soluble fraction does not decrease significantly, suggesting a gradual release of GAP over the 18 days of the study, with some degradation of the polymeric matrix that might form end groups that could interact with the leaving GAP molecules, or a swelling of the sample because of the entering of water; both situations would explain why the soluble fraction is not the same in all the degradation times. The gradual release of GAP from the polymer into the soil could be an environmental problem because of the biocide activity and toxicity of some organic azides [157, 158] and the known toxicity of the azide ion [14]. The leakage of GAP could also prevent or delay the further degradation of the polymer as it might have been the case for GAP-BPM, where the ester linkage was expected to be easily hydrolyzed in mild conditions. Given that the GAP used had a low molecular weight (~ 700 g/mole), it is expected that the use of a higher molecular weight pre-polymer would result in a decrease of the soluble fraction.

The short chains of GAP are not soluble in water, which might prevent the action of soil microorganisms from the soil, which allows GAP to filtrate and disperse into the soil, similar to the case of non-polar solvents or dense non-aqueous phase liquids (DNAPL) leakage [159, 160]. This possibility of leakage has not been reported before and would be an important characteristic of GAP to be considered in cases of remediation of sites polluted with GAP.

On the other hand, both PVT and PVT-PAN show a soluble fraction that increases over time, which is expected for decomposing samples. The swelling of the samples due to the presence of water also contributes to this degradation process, as the entering water will carry microorganisms into the polymeric matrix, and also dissolve the small fragments of the polymer during its breakdown.

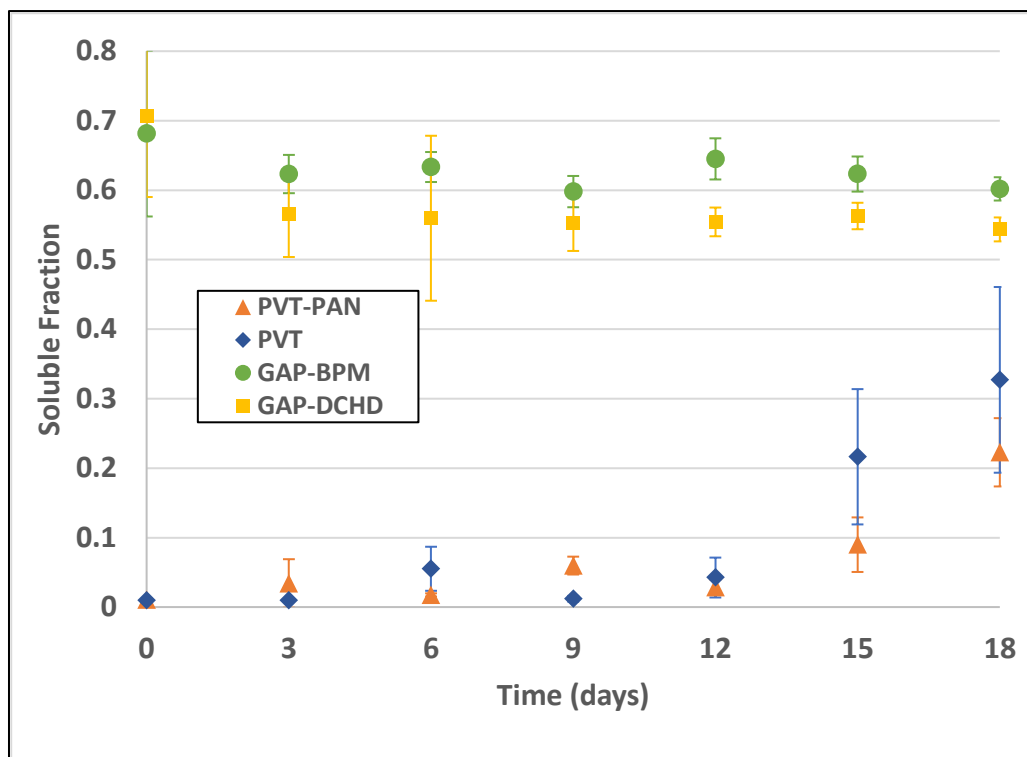


Figure 4.17 Soluble fraction results for the composted samples

4.3.2 Infrared Spectroscopy

The infrared spectra were taken first directly from the surface of the samples, but to understand better the degradation process of the samples, it was necessary to study the changes below the surface. One of the most common techniques for in-depth infrared analysis is the Photo Acoustic Spectroscopy (PAS-FTIR), but this study was not done by PAS because the samples were too opaque and had a several compost particles embedded.

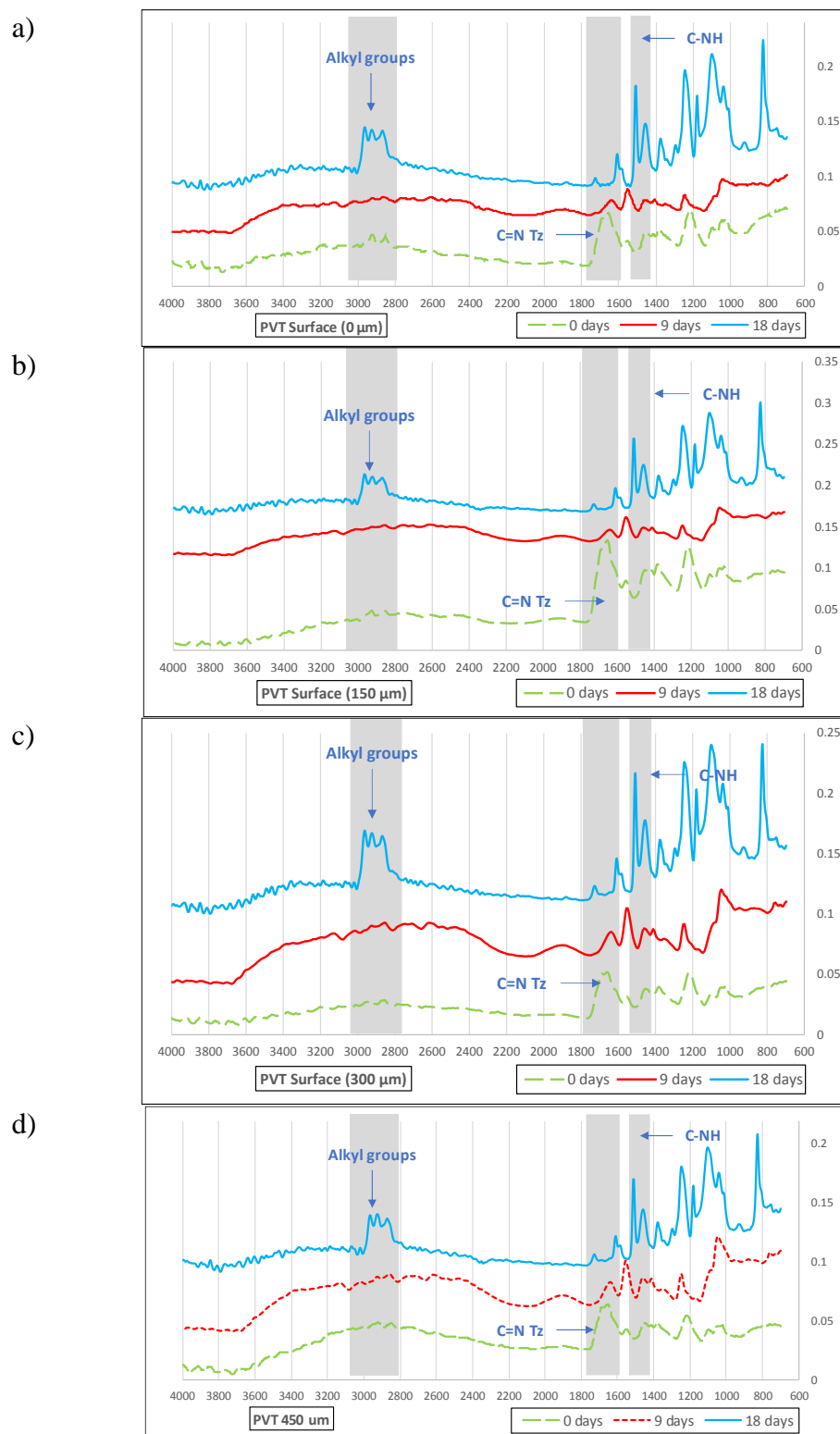


Figure 4.18 FTIR Spectra of PVT at depths: a) Surface b) 150 μm c) 300 μm d) 450 μm

The signals around 2800-3000 cm^{-1} in the 18 days samples suggest that the proportion of alkyl groups become significantly more important in the polymer, compared to the amount of tetrazole groups, probably by elimination of the tetrazole groups from the backbone.

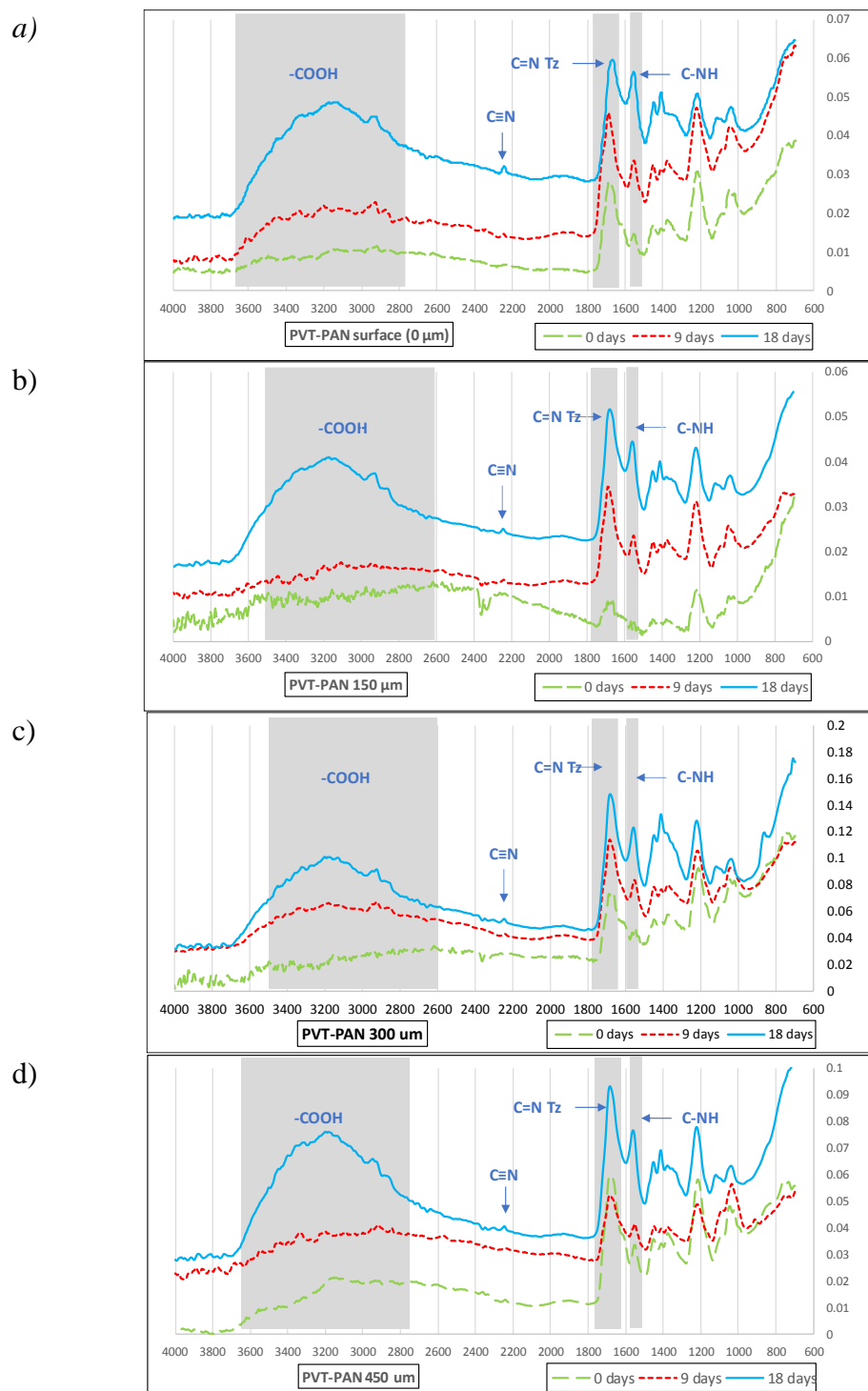


Figure 4.19 FTIR Spectra of PVT-PAN at depths: a) Surface b) 150 μm c) 300 μm d) 450 μm

As can be seen in Figure 4.19, in the spectra for the sample after 18 days of degradation, the signals between 3500 and 2600 cm^{-1} paired with the signal at 2900 cm^{-1} suggest the hydrolysis of the nitrile groups into carboxylates for the acrylonitrile parts of the copolymer. Also, the presence of the signal at $\sim 1550 \text{ cm}^{-1}$ which increases with the degradation time and becomes significant after 18 days of composting, implies the deprotonation of the carboxylic group, and the formation of carboxylate salts, as shown in Figure 4.20

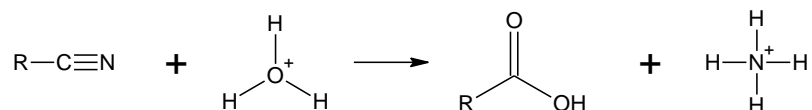


Figure 4.20 General equation of the hydrolysis of nitriles to carboxylates

For the cases of GAP-BPM and GAP-DCHD, the FTIR spectra did not show any significant degradation, except for the azide signal around 2100 cm^{-1} in some samples at surface depth, which might be due to oxidation during the biodegradation or during the storage. The spectra for the GAP-BPM samples at various depths can be seen in Figure 4.21, while the spectra for GAP-DCHD are shown in Figure 4.22.

To find evidence of biodegradation in the GAP-BPM and GAP-DCHD samples, some extracts were taken from the soluble fraction determination procedure with dichloromethane, and those extracts were analyzed by FTIR, and their spectra are shown in Figure 4.23 for GAP-BPM and in Figure 4.24 for GAP-DCHD.

While the main tendency from the FTIR spectra of the GAP-BPM extracts is the presence of GAP, it can be seen that for the 18-days sample, the spectrum shows a signal around 1700 cm^{-1} , which could maybe be some carbonyl fragment being released from the polymeric matrix, possibly a small fragment from the malonic group. In the case of the GAP-DCHD extracts, there was no significant difference seen in the spectra. The emergence of a slight carbonyl signal around 9 days, might be due to some hydrolysis of the nitrile groups of the DCHD, but it cannot be confirmed.

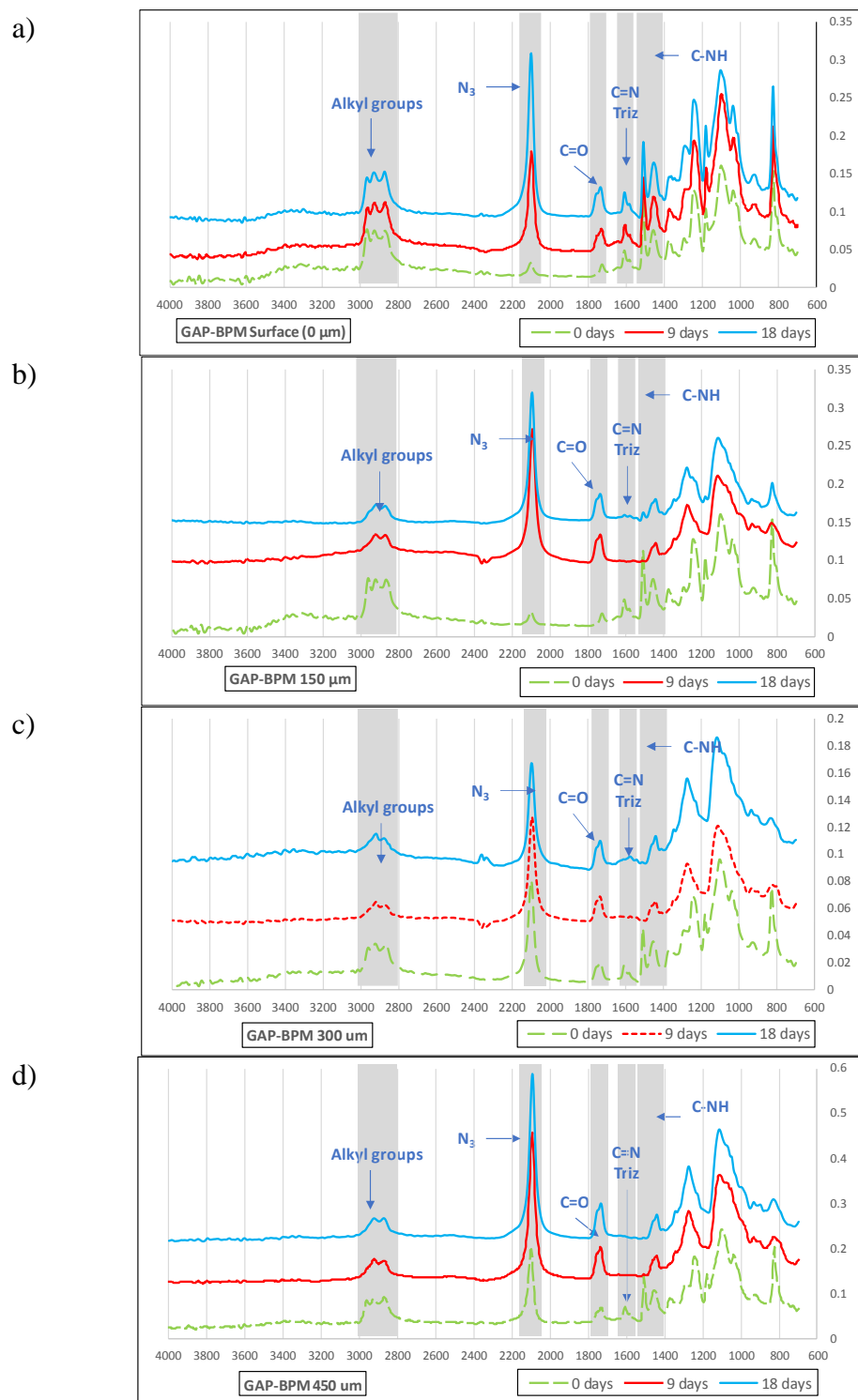


Figure 4.21 FTIR Spectra of GAP-BPM at depths: a) Surface b) 150 μm c) 300 μm d) 450 μm

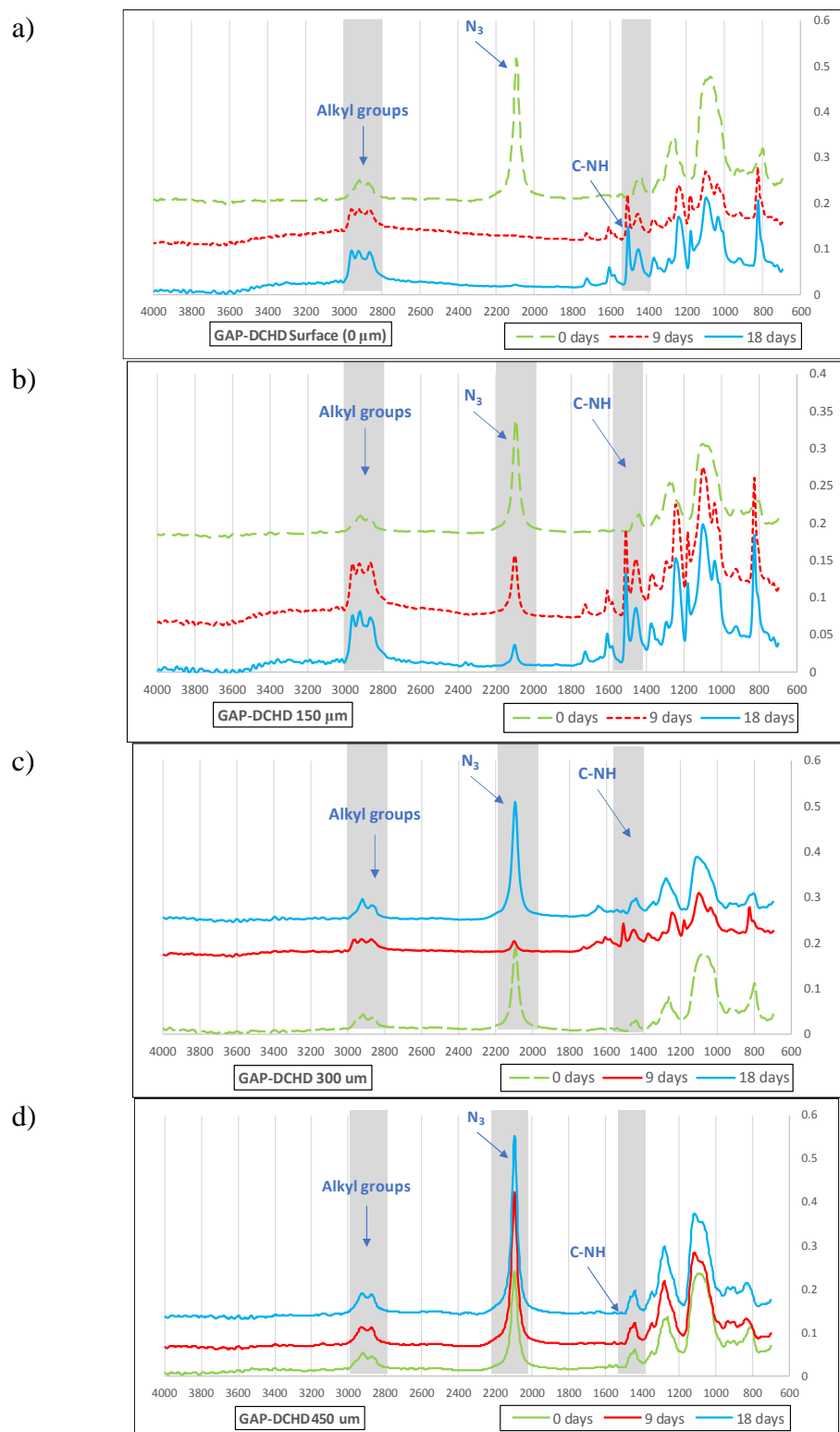


Figure 4.22 FTIR Spectra of GAP-DCHD at depths: a) Surface b) 150 μm c) 300 μm d) 450 μm

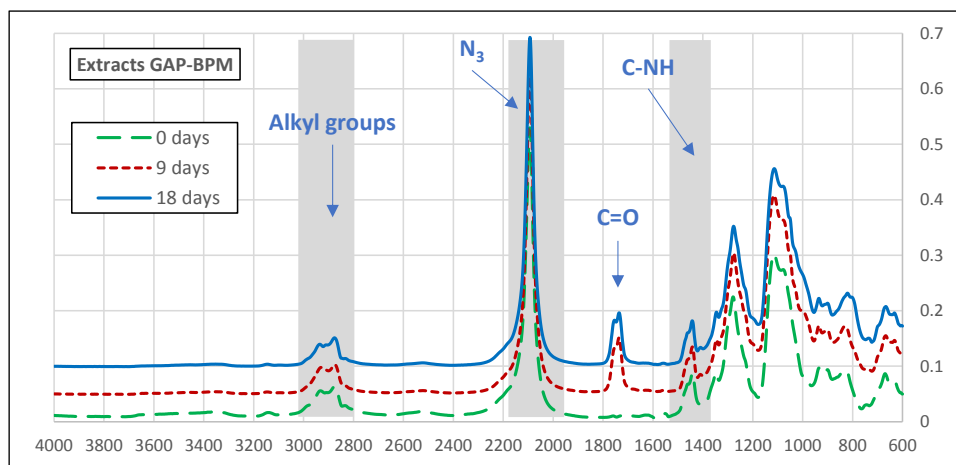


Figure 4.23 FTIR Spectra of GAP-BPM extracts

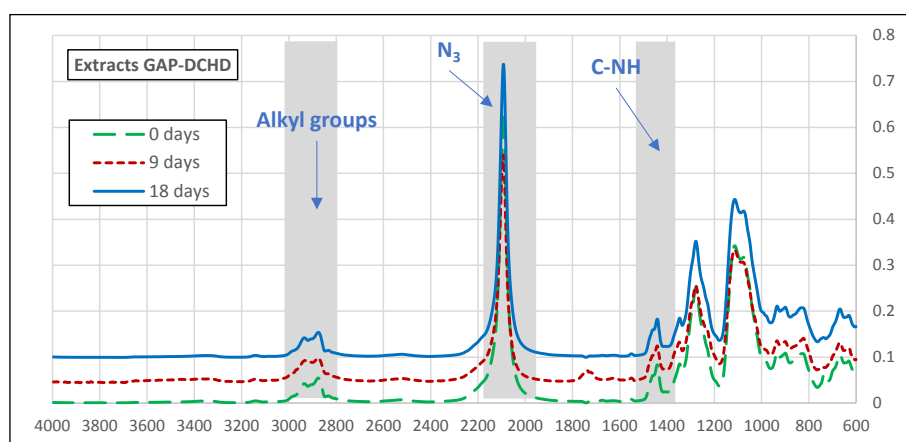


Figure 4.24 FTIR Spectra of GAP-DCHD extracts

4.3.3 NMR Spectroscopy

When analyzing the extracts obtained from the Soluble Fraction determination in both GAP-BPM and GAP-DCHD, the presence of GAP was confirmed, especially by the azide band at 2100 cm^{-1} . This is expected as the crosslinking of the polymer is around 20%, meaning that the rest of the GAP polymer could escape the matrix. In the case of GAP-BPM, it was also found evidence of the presence of malonic acid or malonic esters, produced by the hydrolysis of the ester group of BPM.

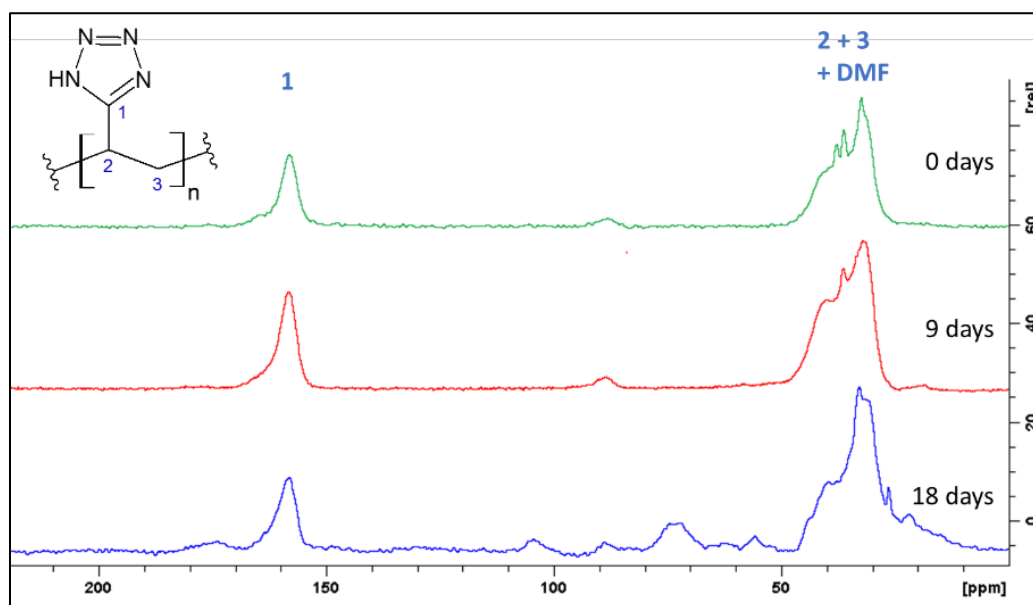
^{13}C Solid State PVT

Figure 4.25 Solid State ^{13}C NMR spectra for PVT composted samples at 0, 9 and 18 days

In the ^{13}C - NMR spectra for PVT, the “shoulder” around 40 ppm is due to the presence of solvent DMF, which apparently remains trapped in the polymer matrix during the composting. It can also be seen that at 18 days, a signal at ~175 ppm starts appearing, where alkene groups are found, suggesting either the release of some of the tetrazole rings via elimination reactions, forming double bonds on the backbone: or the opening of the tetrazole ring with the formation of some C=N or C=C bonds, being the elimination, shown in Figure 4.26, more probable, in contrast with the stability of the tetrazole group. The presence of several signals around 80 ppm, can be attributed to the decomposition of the backbone or to reactions on the tetrazole ring to form allenes or alkynes, being the latter a less plausible option, due to the stability of the tetrazole group that would make the inverse Huisgen reaction improbable. Still, the presence of these signals would mean that the molecular weight is decreasing, which would speed up the degradation of the sample even further.

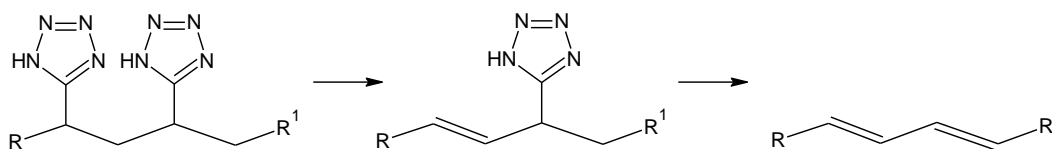


Figure 4.26 General equation of the elimination of tetrazole groups in PVT

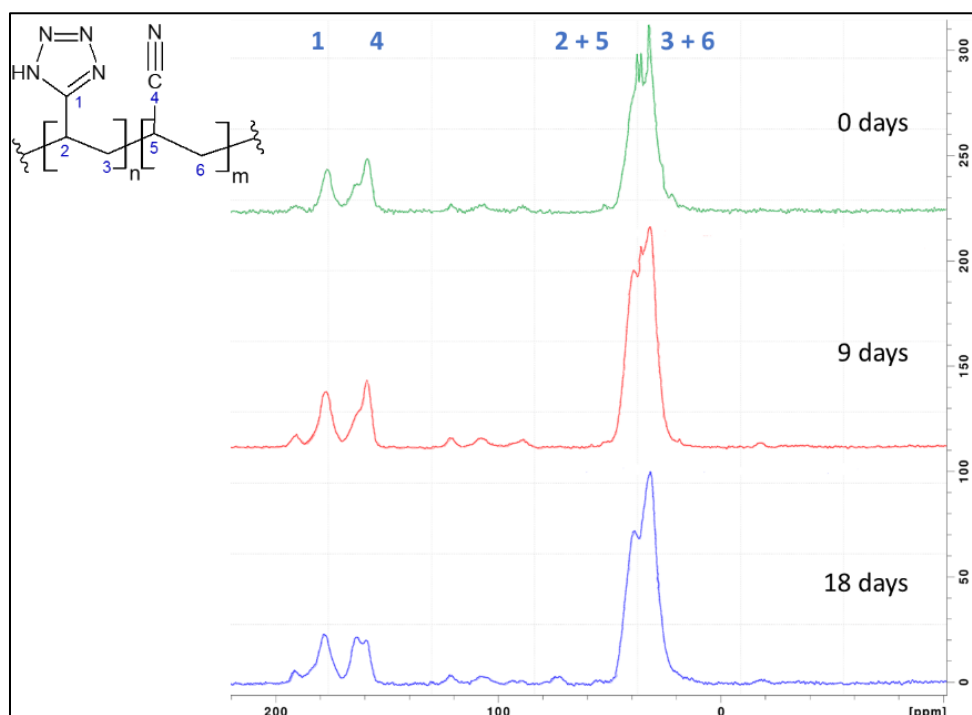
^{13}C Solid State PVT-PAN

Figure 4.27 Solid State ^{13}C NMR spectra for PVT-PAN composted samples at 0, 9 and 18 days

The solid state ^{13}C NMR spectra for PVT-PAN is shown in Figure 4.27. Changes in the signal around 160 ppm, which can be assigned to the triazole carbons, might be due to changes in the triazole ring, either by direct reactions on the two carbons of the ring, or by changes in the nitrogen atoms nearby. The apparition of a signal around 190 ppm would suggest the formation of a new functional group with a highly oxidized carbon, most probably a carboxylate result of the oxidation of the nitrile group.

The signal around 40 ppm becomes more complicated due possibly to the presence of solvent DMF from the solvent-casting, which apparently remains trapped in the polymer matrix during the composting.

^{13}C Solid State GAP-BPM

In Figure 4.28 are shown the spectra for GAP-BPM, and as can be seen, there is little change on the signals. The signal around 110 ppm is an impurity, as it did not appear in other samples. It is worth to clarify that because of the reaction mechanism for the formation of the triazole group, the carbon 6 can be attached either to carbon 4 or to carbon 5. This does not change greatly the vicinity for the carbon 6, but it does change the connectivity for carbons 4 and 5, which might explain why the signals for these two carbons is more complex and “diluted”.

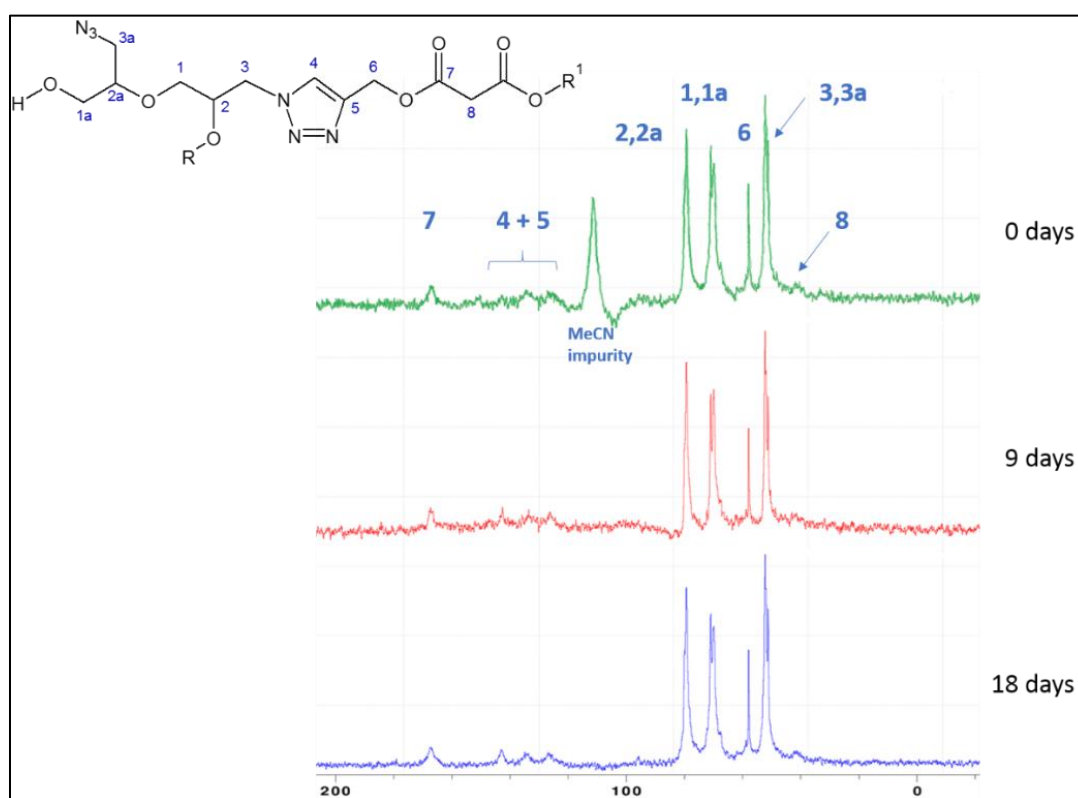


Figure 4.28 Solid State ^{13}C NMR spectra for GAP-BPM composted samples at 0, 9 and 18 days

By comparing the ^{13}C NMR spectra of BPM and GAP with the spectrum of the extract of the composted material, it can be seen that the extract is mostly GAP, as seen in Figure 4.29. That implies that all the BPM is forming triazoles. No strong evidence can be seen for the hydrolysis of the ester groups on the BPM which would have released malonic acid or its salts into the soil or into the polymeric matrix. The spectra suggest very slight change of the GAP-BPM network.

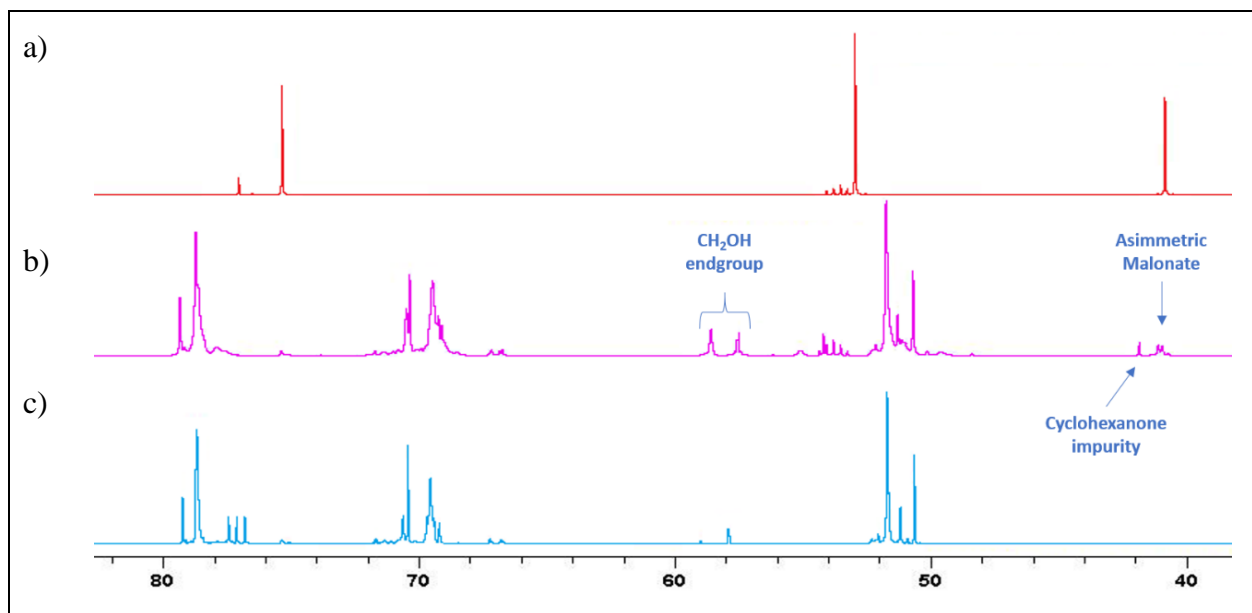


Figure 4.29 Comparison of the ^{13}C -NMR spectra of a) BPM b) extract from sample GAP-BPM 18 days c) GAP

^{13}C Solid State GAP-DCHD

In the ^{13}C -NMR spectra taken for the GAP-DCHD samples (Figure 4.30), no change can be seen in the signals, and no new signals appear as the composting experiment progresses, suggesting a lack of biodegradation on this material under the studied conditions.

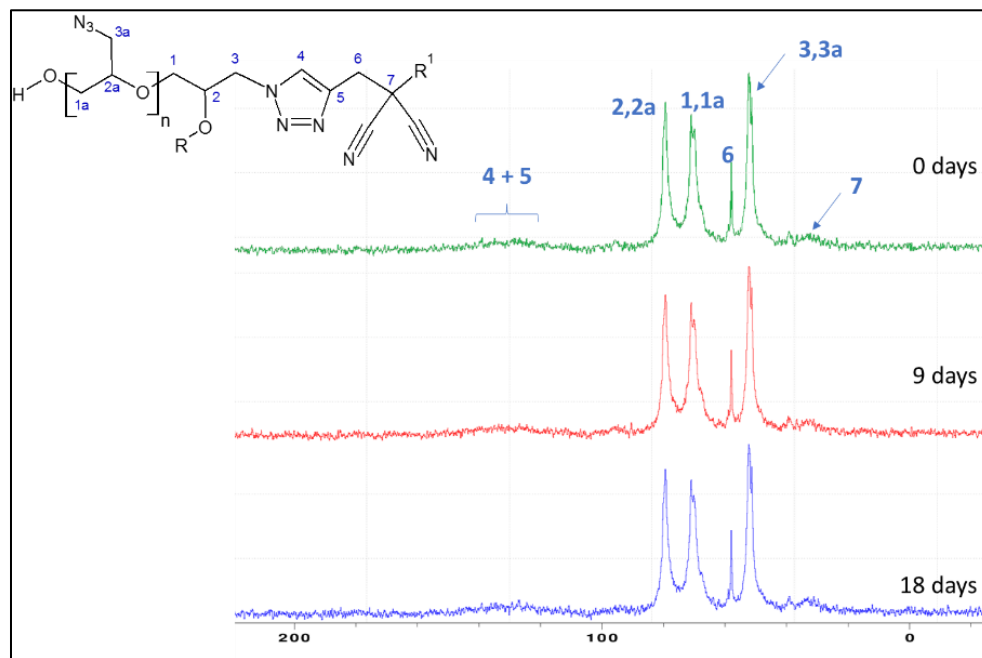


Figure 4.30 Solid State ^{13}C NMR spectra for GAP-DCHD composted samples at 0, 9 and 18 days

4.3.4 DSC

PVT

As it can be seen in Figure 4.31, the DSC curve for PVT demonstrates how this compound has a broad decomposition peak around 260 °C, which belongs to the tetrazole group, that can be seen still in the scans of the samples at 9 days of composting, but as the composting experiment progresses, the thermal decomposition of PVT changes, and at the final stage (18 days of composting), the expected signal for the decomposition of either the azide group or the tetrazole has decreased considerably from ~1000 J/g to ~400 J/g. This suggests the disappearance of the explosophoric groups, though it is not clear from the results if the tetrazole leaves the polymeric backbone, or if a ring opening reaction is occurring.

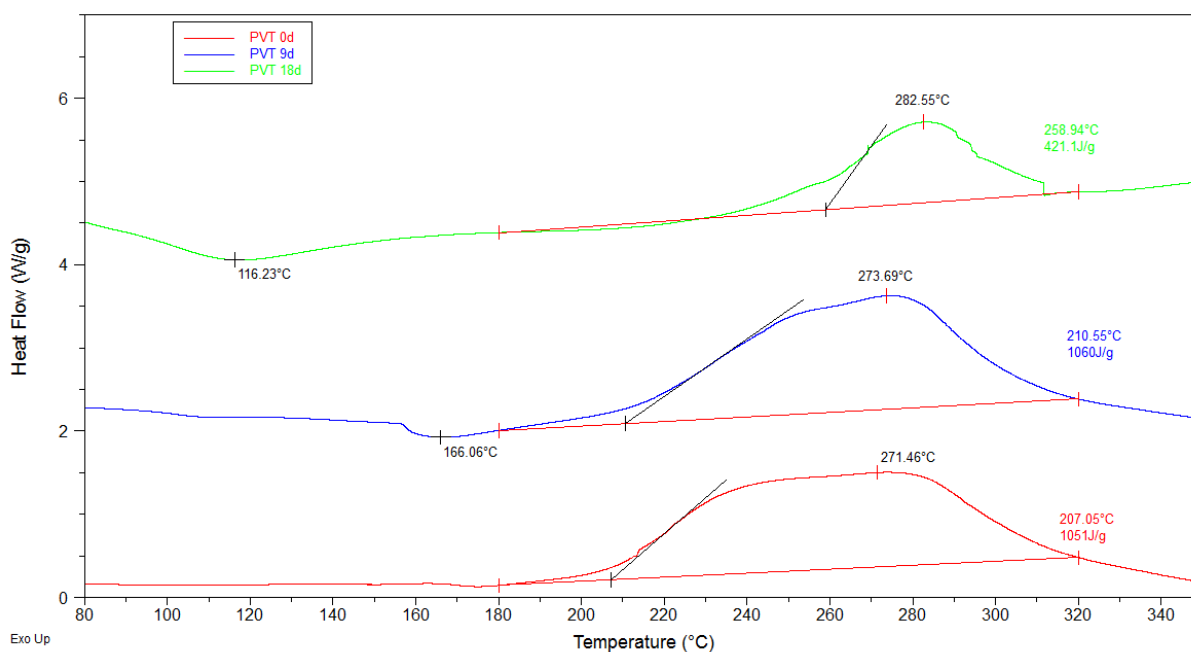


Figure 4.31 DSC curve for PVT

PVT-PAN

The DSC for the 0 days sample shows what would appear as a 2-step decomposition, being the first one, at around 240 °C, while the second one over 267 °C. As can be seen in Figure 4.32, by the day 9 of the composting, the decomposition signal becomes broader and simpler.

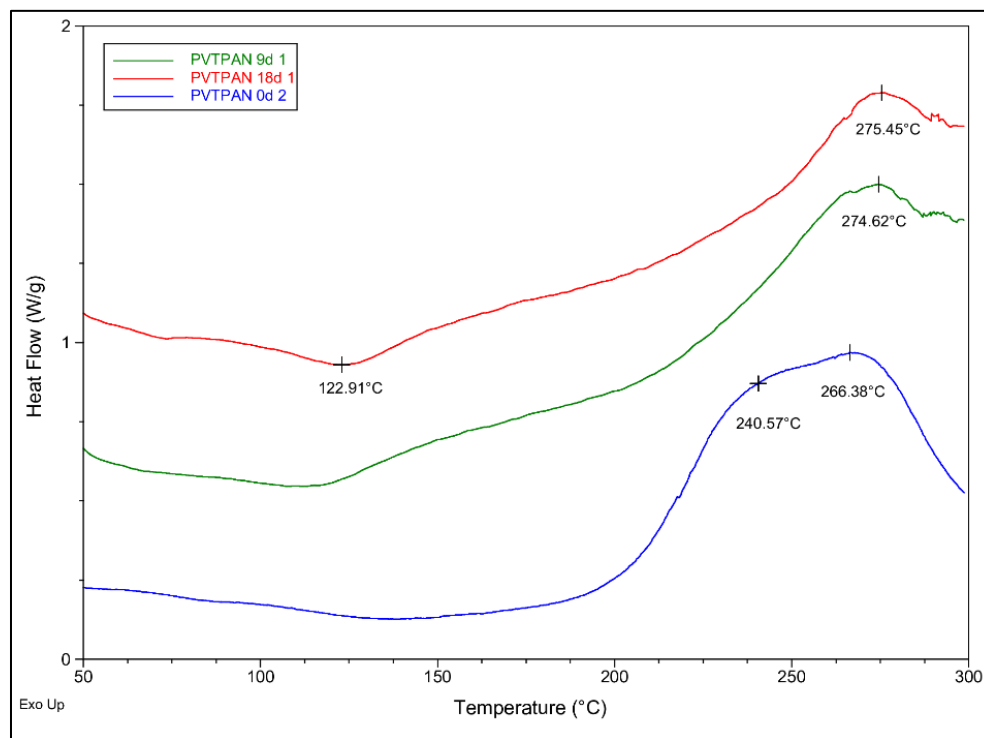


Figure 4.32 DSC curves for PVT-PAN

GAP-BPM

Eroglu described in his review that the thermal decomposition of GAP has two stages, being the first one the exothermic decomposition of the azide groups with the release of N_2 , and the second stage would include the decomposition of the polyether main chain [20]. It has to be noted that after the elimination of N_2 , the remaining nitrenes can have various reactions with the surrounding groups, making it impossible to determine the specific reaction occurring. This first decomposition peak can be seen in Figure 4.33 at around 238 °C. The curves show that this peak does not change position nor broadens as the composting experiment progresses, and no new peaks appear implying a very low decomposition of the polymeric matrix.

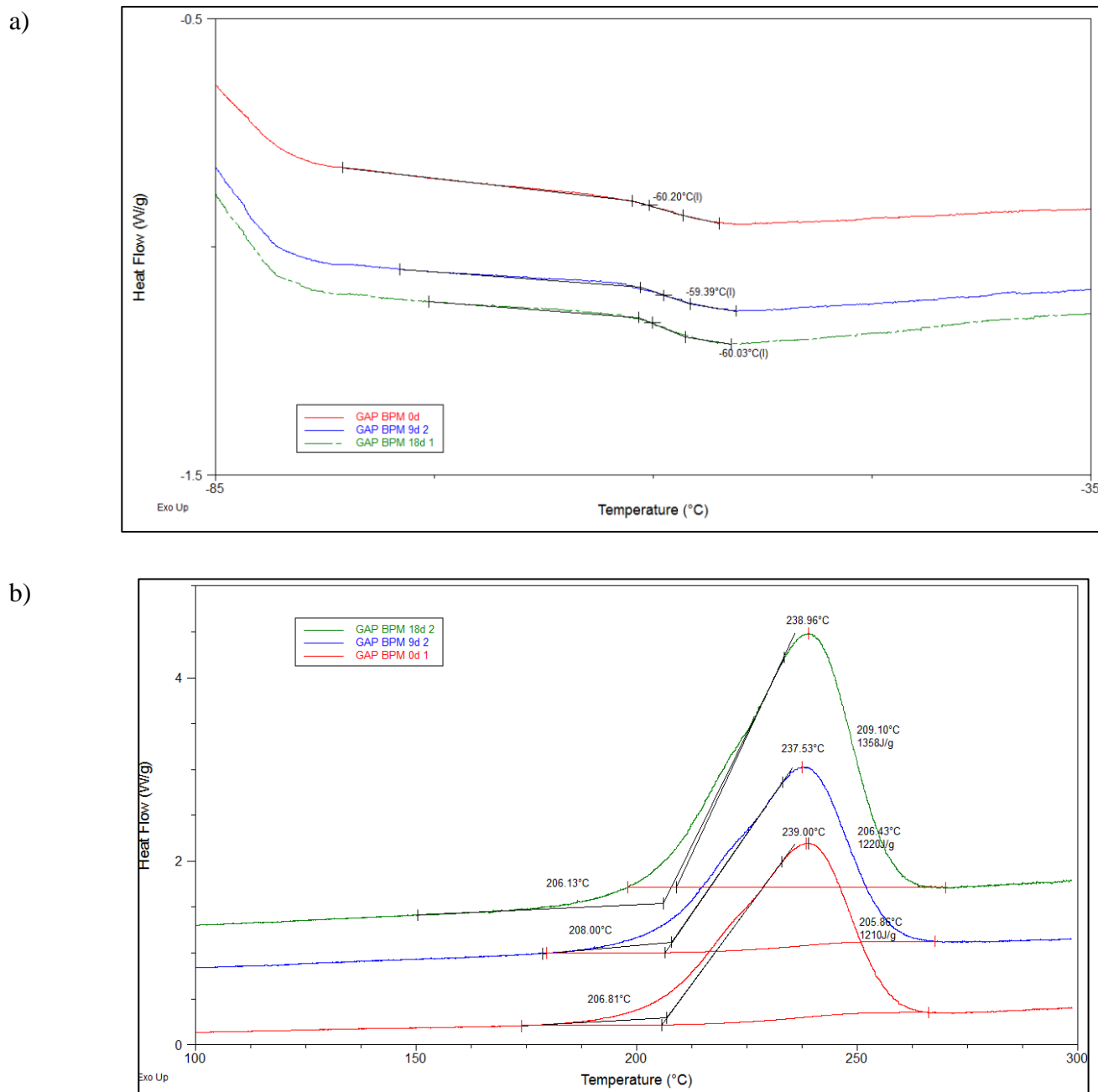


Figure 4.33 DSC curves for GAP-BPM showing a) T_g b) Decomposition

GAP-DCHD

The DSC curves for the decomposition of GAP-DCHD are shown in Figure 4.34. As is the case with GAP-BPM, the curves show the same signal for the azide groups decomposition around 237 °C, which in this case was also a very stable signal. The T_g for the GAP-DCHD samples agrees

with the one found for the GAP-BPM samples. The T_g of GAP in Figure 4.14 is at $-66\text{ }^\circ\text{C}$, and the difference can be credited to the crosslinking of the chains, that would hold in place the oligomers during the phase transition, resulting in a higher T_g for GAP-BPM and for GAP-DCHD, compared with GAP being a resin formed by short chains with more freedom of movement.

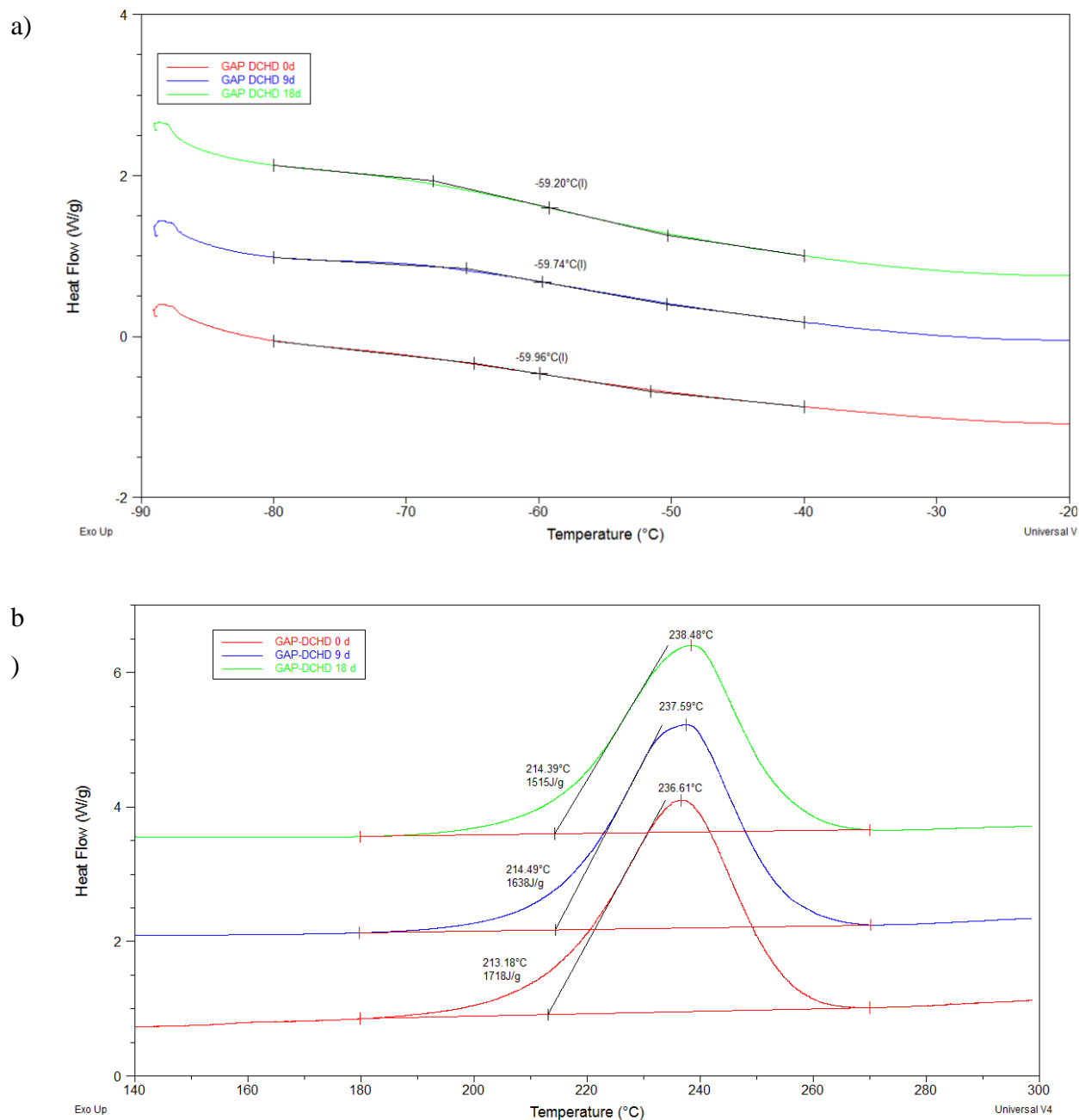


Figure 4.34 DSC Decomposition curves for GAP-DCHD showing a) T_g b) Decomposition.

Table 4.7 DSC and DMA thermal analysis results for the composted samples

| Sample | | T _g DSC ^a (°C) | T _g DMA (°C) | T _{dec} (°C) (onset) | T _{dec} (°C) (max) | E _{dec} ^a (±30 J/g) |
|----------------------------------|---------|---|----------------------------|----------------------------------|--------------------------------|--|
| PVT | 0 days | 100.18 | --- | 205.35 | 266.90 | 1210 |
| | 9 days | 99.31 | --- | 214.71 | 274.15 | 1149 |
| | 18 days | 98.46 | --- | 255.23 | 282.50 | 332 |
| PVT- PAN | 0 days | N./A. ^b | --- | 209.54 | 259.82 | 1380 |
| | 9 days | N./A. ^b | --- | 239.54 | 265.86 | 153 |
| | 18 days | N./A. ^b | --- | 266.27 | 279.72 | 134 |
| GAP- BPM | 0 days | -60.20 | -38.14 | 206.81 | 239.00 | 1220 |
| | 9 days | -59.39 | -37.16 | 208.00 | 237.53 | 1231 |
| | 18 days | -60.03 | -37.04 | 206.13 | 238.96 | 1250 |
| GAP- DCHD | 0 days | -58.86 | -37.45 | 212.62 | 236.59 | 1690 |
| | 9 days | -59.50 | -37.40 | 214.48 | 237.59 | 1608 |
| | 18 days | -59.41 | -36.33 | 214.40 | 238.48 | 1550 |
| GAP-700 | | -66.16 | --- | 213.49 | 240.69 | 2633 |
| ¹⁵N PVT powder | | 110 | --- | 199.96 | 272.69 | 1090 |

^a: DSC results presented as an average of two measurements.

^b: The T_g of PVT-PAN could not be observed on DSC due to the shape of the curve.

4.3.5 Dynamic Mechanical Analysis, DMA

As was commented in section 4.2.2, the PVT and PVT-PAN samples were not analyzed by DMA, as they got very deformed during the composting. Not only the samples became too fragile to withstand the different analyses that were tried, but also their dimensions and shapes were too irregular to comply with the standard tests like traction or Dynamic Mechanical Analysis (DMA) by single or dual cantilever. As the samples become fragile and soft on the late stages of the composting experiments, it was also impossible to obtain a proper sample for DMA by compression or “shear sandwich”.

In the case of GAP-BPM and GAP-DCHD, the DMA was used to find evidence of biodegradation, given that the appearance for the composted samples was very similar to the appearance of the

sample at 0 days. Different techniques were used on these samples to analyse their mechanical properties, but it was not possible to get good results with either traction tests or with various types of DMA (compression, “shear sandwich” and double cantilever). The traction tests were not successful because the samples were too soft, and they broke down when put inside the Instron clamps. The softness of the samples also prevented the analysis by DMA with dual cantilever and compression setups, as they would not withstand the repetitive deformation without breaking, thus the results shown here are the ones performed with single cantilever. For example, the dimensions required for tensile properties of plastics, as defined in ASTM D638-14 [161] for the type V kind of sample, are: Width = 3.18 ± 0.03 mm, Length = 9.53 ± 0.08 mm, and Thickness = 3.2 ± 0.4 mm. These dimensions make it difficult to obtain a good sample for testing, as usually the samples for qualifiable tests like this one have to be shaped into “dog-bone” geometries.

The glass transition temperatures (T_g) were measured by DMA at a heating rate of $3\text{ }^\circ\text{C}/\text{min}$, and the T_g is reported as the temperature for which the loss modulus (E'') is maximal. The results are shown in Table 4.7 together with the DSC results, and as can be seen in both Figure 4.35 and Figure 4.36, the shape of the curves remain constant, and the variations on the maximum for the loss modulus are not significant, indicating that no change in the mechanical properties can be appreciated during the composting of the GAP crosslinked samples. This suggests that the molecular weight of the chains, and the average length between crosslinks was not significantly impacted during the composting.

The differences between the T_g values between both techniques may be due to several factors, like the cooling rate of the DSC experiments compared to the rate of the DMA experiments ($3\text{ }^\circ\text{C}/\text{min}$ for DMA and $5\text{ }^\circ\text{C}/\text{min}$ for DSC), but in essence, the main difference is that as stated by Gracia-Fernandez [162]: both techniques measure different manifestations of the glass transition in the samples. The DSC technique is sensitive to the changes in the heat capacity during the glass transition, for which the T_g is defined as the midpoint in the heat capacity shift; the DMA technique is sensitive to the mechanical relaxation of the sample during the glass transition, defined by changes in its dynamic mechanical properties (E' , E''). Regardless of the technique, both experiments are consistent in the tendency they show and there is no significant change in the T_g of the samples after the composting experiments.

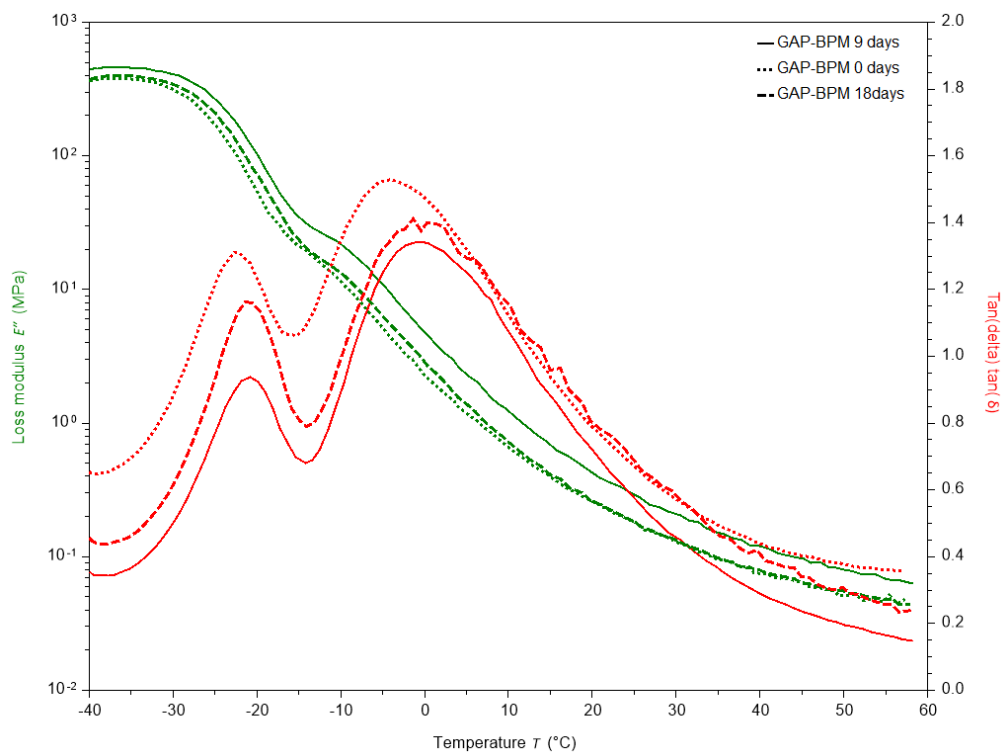


Figure 4.35 DMA curves for GAP-BPM: a) 0 days b) 9 days c) 18 days E'' (green) and $\text{Tan } \delta$ (red)

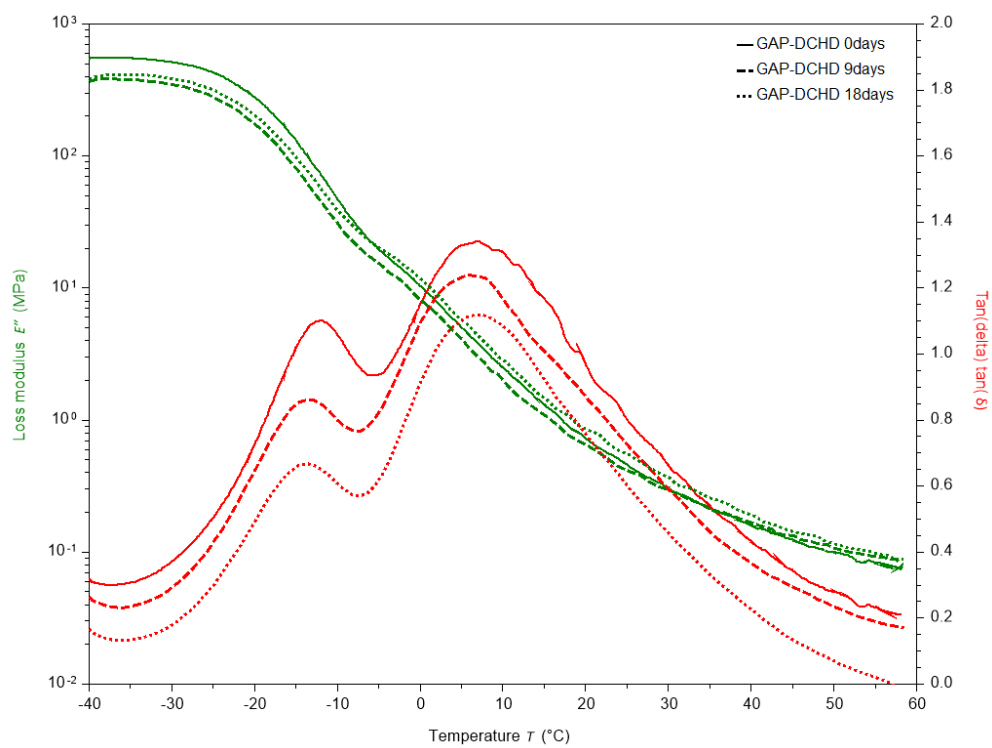


Figure 4.36 DMA curves for GAP-DCHD: a) 0 days b) 9 days c) 18 days E'' (green) and $\text{Tan } \delta$ (red)

4.3.6 Scanning Electronic Microscopy and Energy-Dispersive X-Ray Spectroscopy (SEM-EDS)

In this section are only shown the images for days 0, 9 and 18 of the composting experiments. The complete set of images can be found in the Appendix A.

The analysis of the samples by SEM was performed without the use of metal deposition, as the samples were later analyzed by EDS to identify their elemental composition. Nevertheless, the obtained images clearly show the changes in the samples during the composting experiments.

PVT

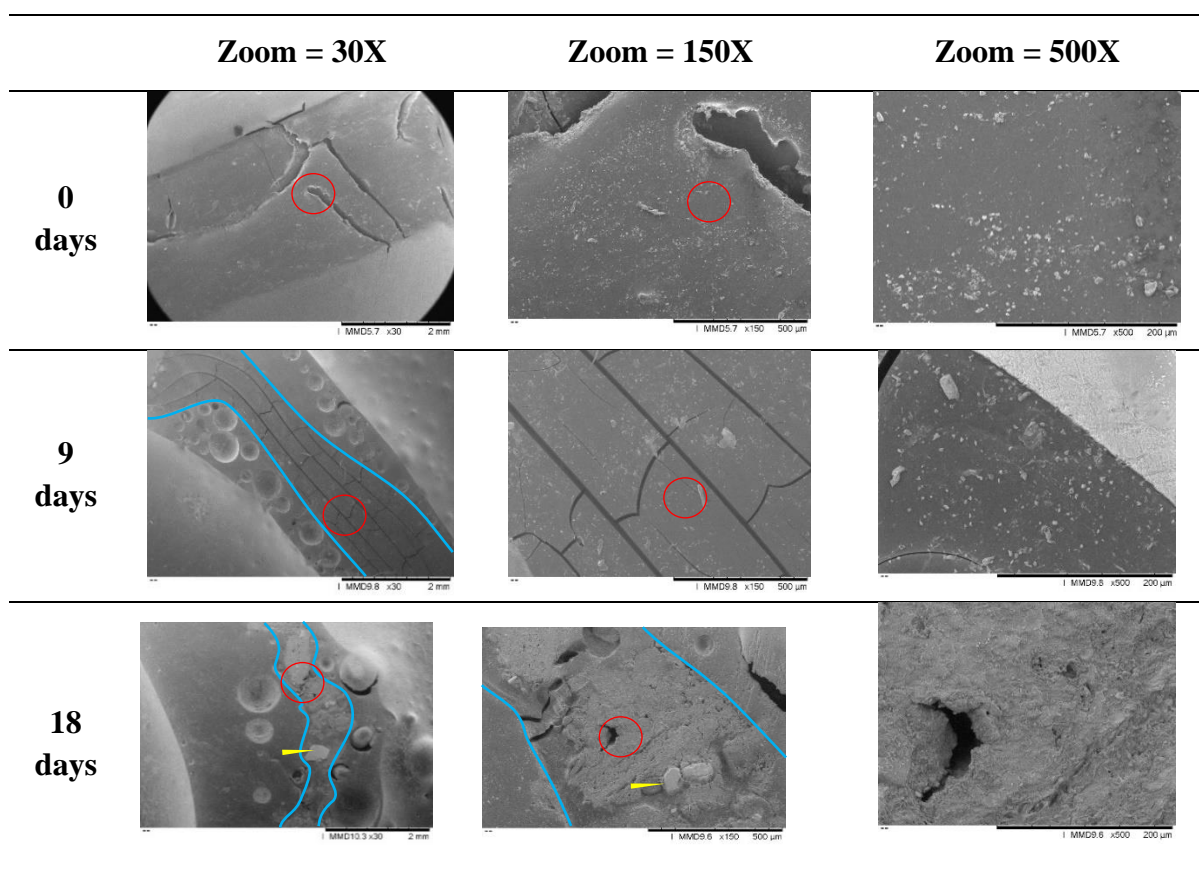


Figure 4.37 SEM images of PVT during composting, at different magnifications

In the case of the images in Figure 4.37 at the lowest magnification (zoom = 30X), the circles are due to bubbles present in the epoxy used for encasing the sample. Shown in blue is the outer limit of the samples encased in the epoxy resin, and as a red circle, the areas that were magnified. As the composting progressed, the samples of PVT became smaller, and as can be seen on the SEM images, their texture became less homogenous and their surface becomes rougher, as the polymer degraded. At $t=18$ days, it can be seen the presence of soil particles encased on the polymer (marked with yellow arrows in the images), which could not be removed, and give the images their rough texture. As the samples were sanded and polished, the polymer part would become somewhat smoother, but the encased particles would not.

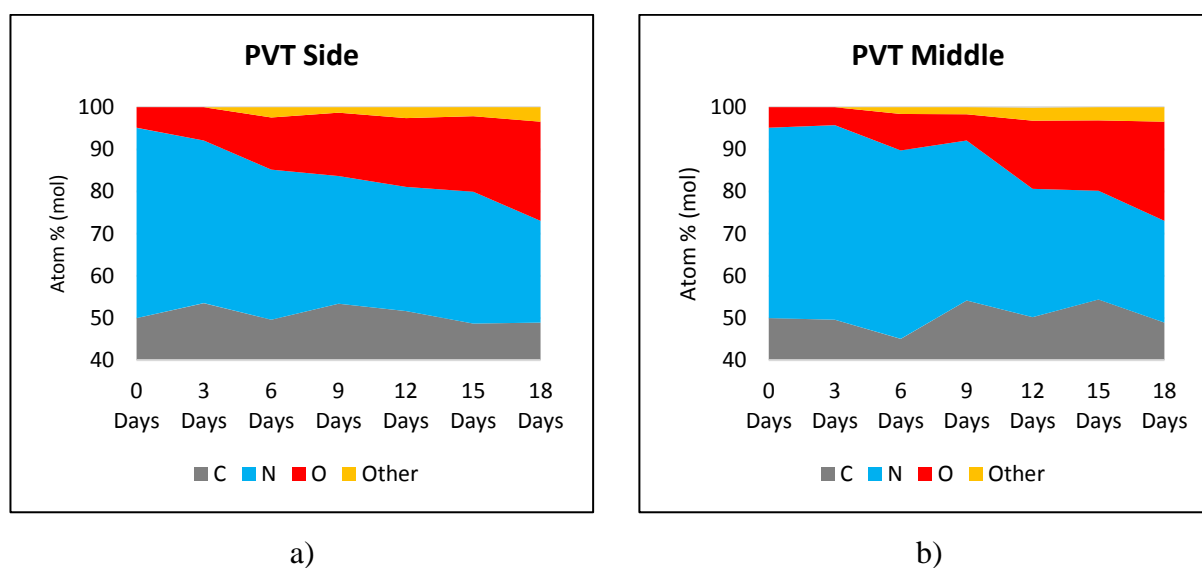


Figure 4.38 Progression of the elemental composition of PVT during composting a) middle of the sample b) surface of the sample

The increase on the percentage of “foreign” elements like Ca, K, Na, Si and Al, shown in Figure 4.38, is all attributable to salts present in the soil, indicates that the compost entered the matrix of the sample, due to the swelling of the samples, but also possibly to the degradation of the polymer. The presence of these elements can also imply the activity of microorganisms, which would help the biodegradation. While the carbon content remains relatively stable, the nitrogen percentage decreases over time, implying that the tetrazole groups of the polymer are reacting or being cleaved from the polymer’s backbone. In the case of the sample of 18 days, the results from the external part and the internal part (“side” and “middle”) are the same, because of the very small size of the

sample and its high deformation. The oxygen percentage increases over time, due to oxidation of the samples, but also due to the entry of salts (i.e., phosphates, silicates, etc.) present in the compost, or related to the action of microorganisms.

PVT-PAN

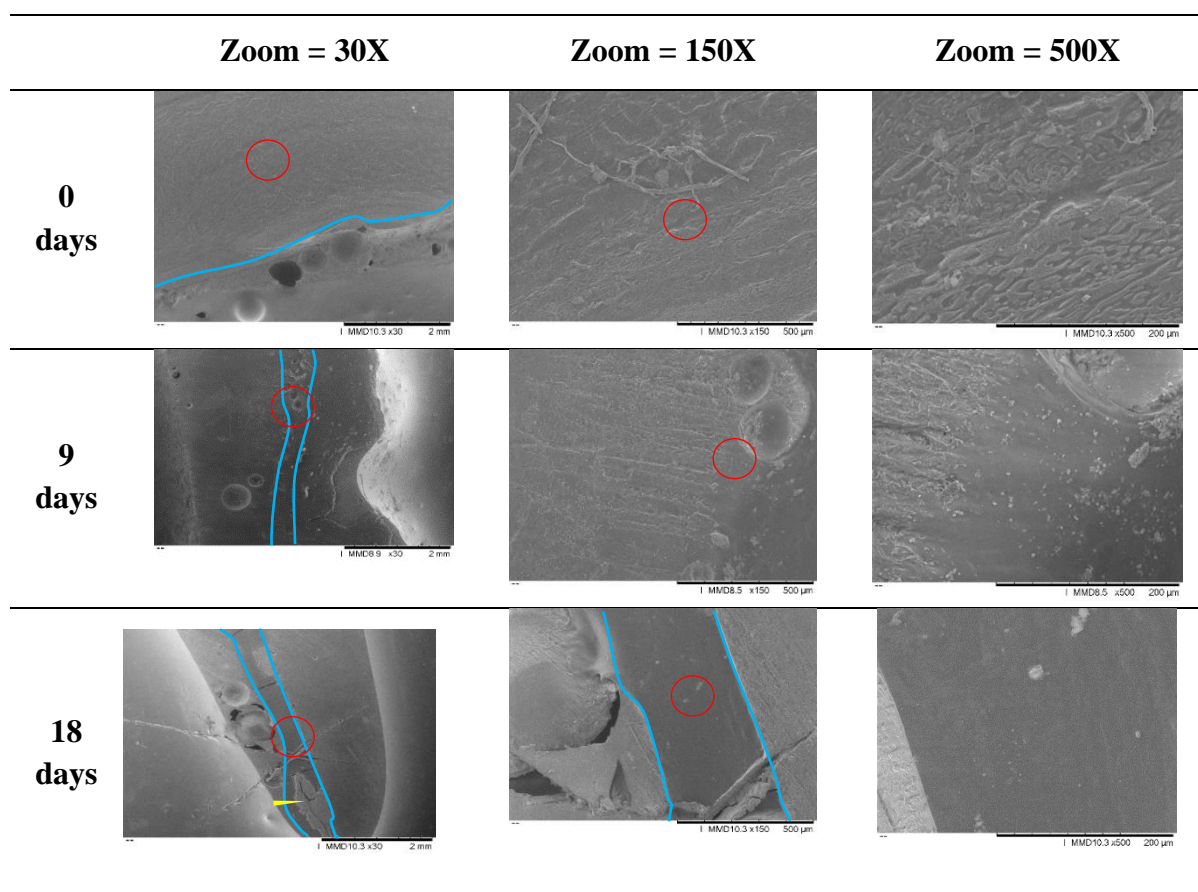


Figure 4.39 SEM images of PVT-PAN during composting, at different magnifications

The SEM images show that the PVT-PAN samples (Figure 4.39) present also the bubbles found at the epoxy resin as was the case in the PVT samples. They also presented some inclusion of soil material (marked with yellow arrows in the images), and very fine soil dust embedded in the polymer, seen as small white dots in the highest magnification.

The carbon content shown in Figure 4.40 remains more or less stable, while the reduction of the amount of nitrogen and the increase of the oxygen content suggest oxidation of groups, specifically the hydrolysis of the nitrile group to carboxylates, as was shown in Figure 4.20. As with PVT, the

increase of foreign elements is expected as the soil particles and the salts start to move into the polymer matrix.

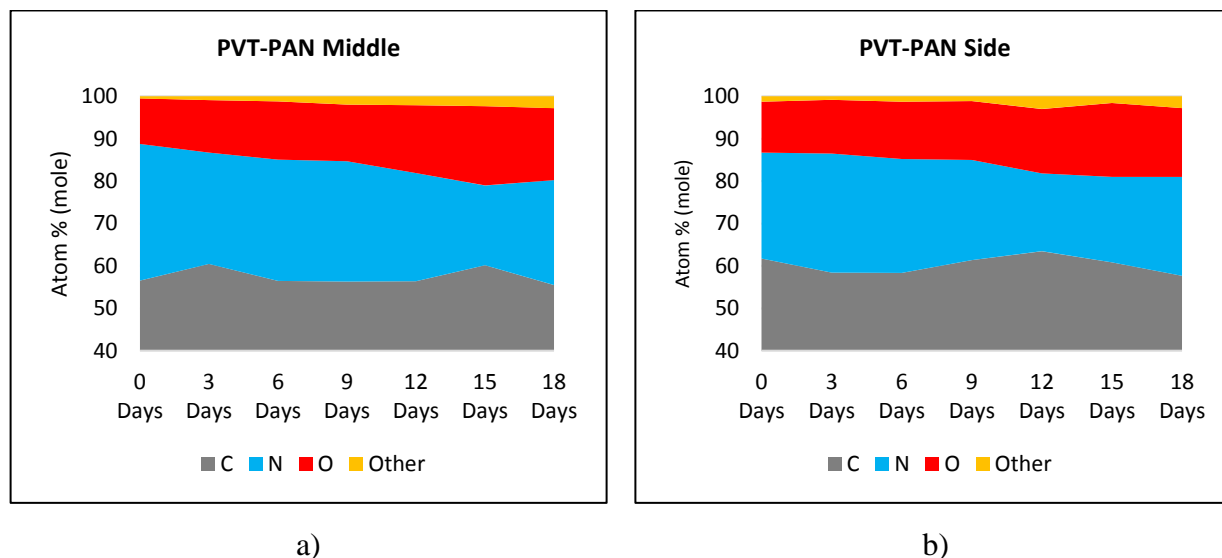


Figure 4.40 Progression of the elemental composition of PVT-PAN during composting a) middle of the sample b) surface of the sample

GAP-BPM

The images in Figure 4.41 show that the texture of the GAP-BPM is different to the texture of the PVT and PVT-PAN samples, as the GAP-BPM samples were softer and more gel-like. These samples were slightly sanded to remove any possible residue of epoxy resin attached to the center of the samples. This caused some disruption in the surface (especially in the GAP-DCHD samples), but it did not affect the elemental analysis. The most notable difference in these samples is the fact that there are no soil particles incorporated into the polymer matrix, which suggests a lesser biodegradation, meaning that the GAP-BPM sample is, in general terms, stable.

For the GAP-BPM samples, the initial content of oxygen, as shown in Figure 4.42, is expected to be the highest of all the analyzed polymers, as the malonate group presents two carboxylate groups. This contrasts with the low original oxygen content found for PVT and PVT-PAN.

The analysis of these samples shows a very consistent composition for the polymeric samples, in which the nitrogen content remains very stable, and there are practically no foreign elements. This would imply a very low degradation of the polymeric matrix, due maybe to the release of GAP into

the soil. The release of this compound might kill the microorganisms that would have biodegraded the sample, given that some organic azides have been shown to be toxic for the environment [158].

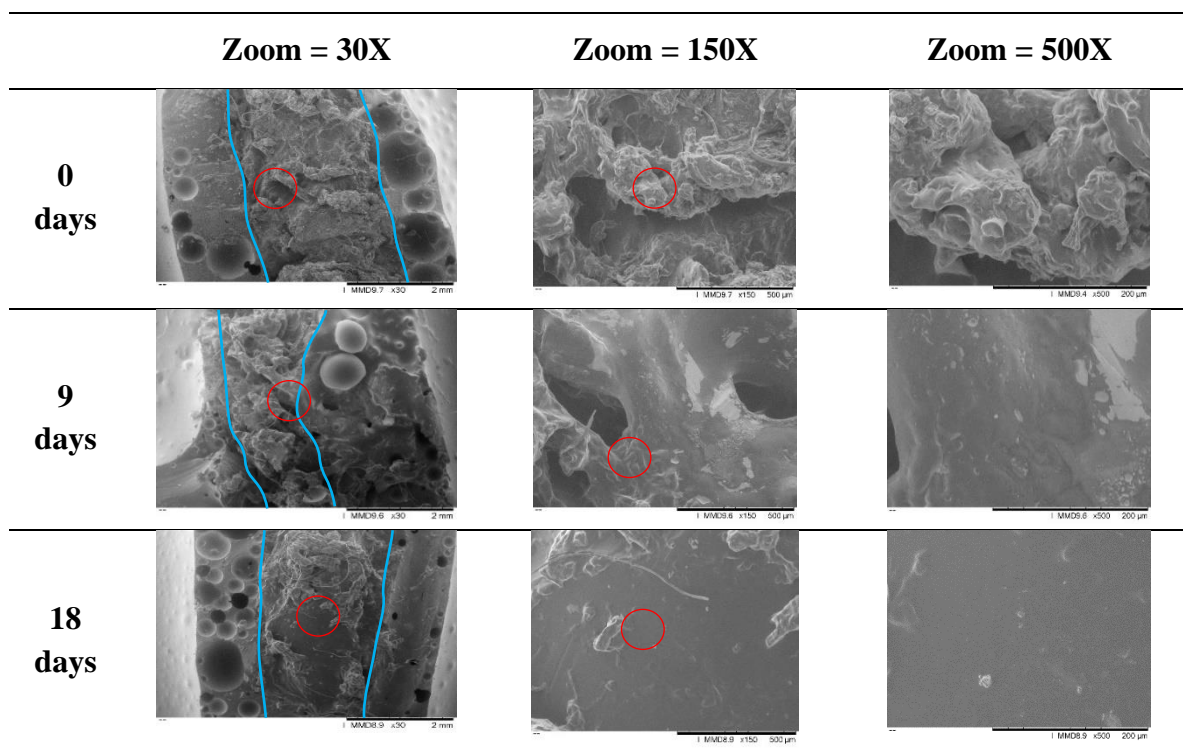


Figure 4.41 SEM images of GAP-BPM during composting, at different magnifications

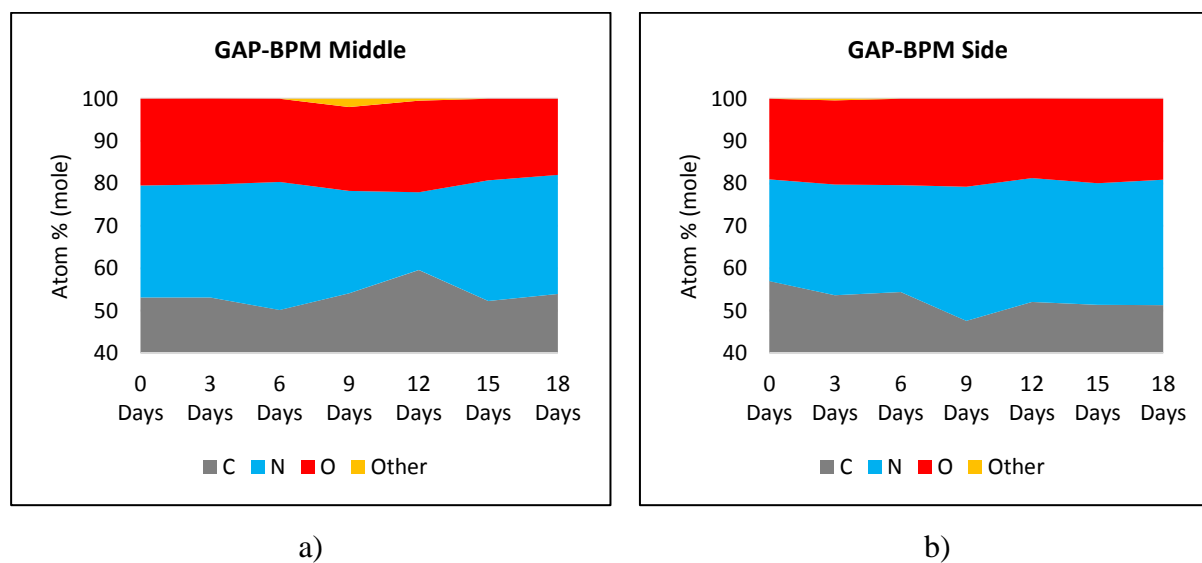


Figure 4.42 Progression of the elemental composition of GAP-BPM during composting a) middle of the sample b) surface of the sample

GAP-DCHD

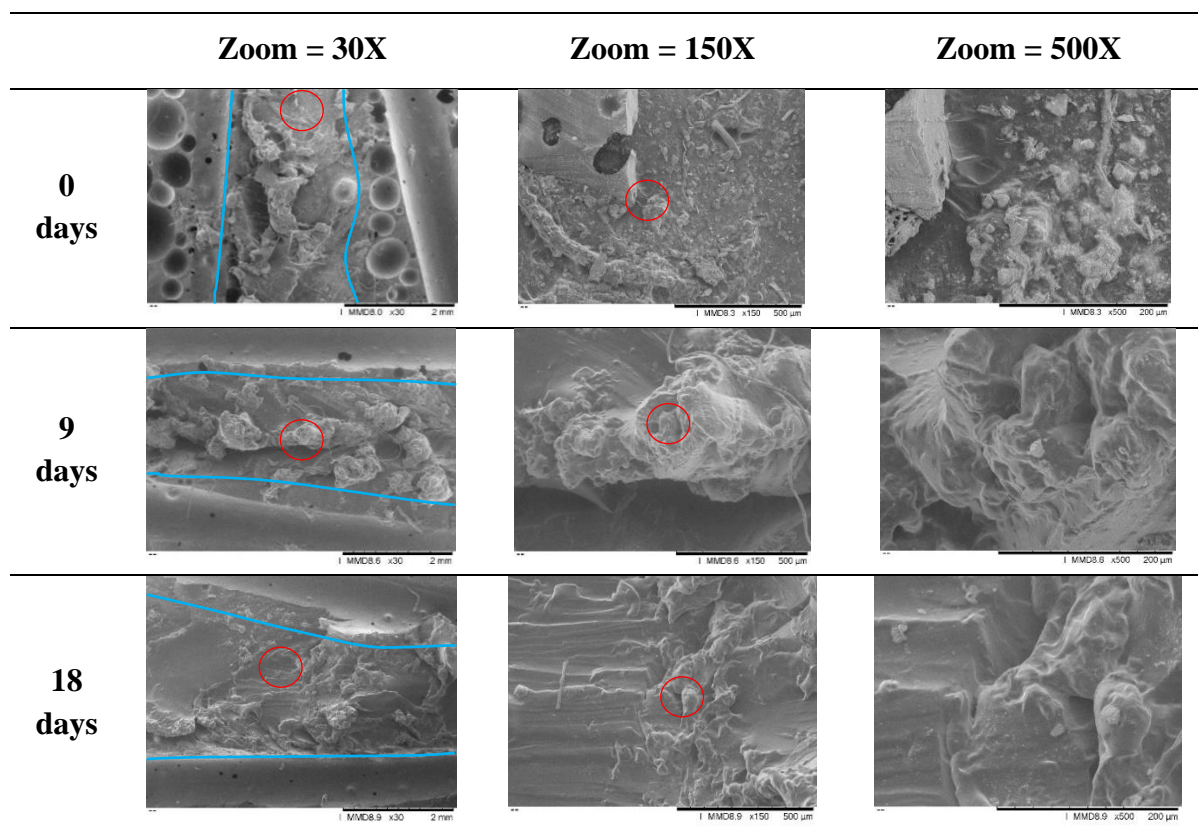


Figure 4.43 SEM images of GAP-DCHD during composting, at different amplifications

The images in Figure 4.43 show that as it was the case for GAP-BPM, the texture of GAP-DCHD is also very different to the texture of PVT and PVT-PAN during the composting. GAP-DCHD also presented a rubbery texture, and there are also some surface disruptions caused by the sanding of the samples. This sanding process did not have an effect on the elemental analysis results, and it can be seen, as it was in the case of GAP-BPM, that no foreign elements were incorporated into the polymer matrix, which implies a low degree of degradation.

In the case of GAP-DCHD, the elemental composition presents a behavior similar to the one seen for GAP-BPM, where the nitrogen content and the oxygen content do not change after the third day, suggesting a very low degree of biodegradation on the polymers, as shown in Figure 4.44. This can be also confirmed by the practically-absent foreign elements, whose presence would be linked to the presence of microorganisms penetrating the polymeric matrix.

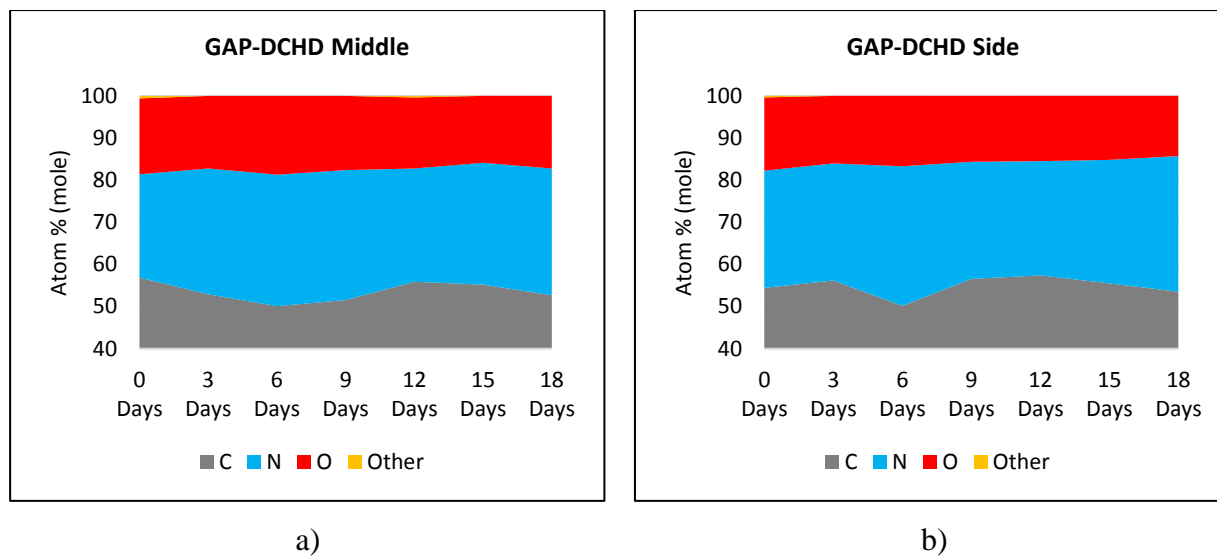


Figure 4.44 Progression of the elemental composition of GAP-DCHD during composting a) middle of the sample b) surface of the sample

4.4 Characterization of an Isotope-marked Polymer

4.4.1 DSC

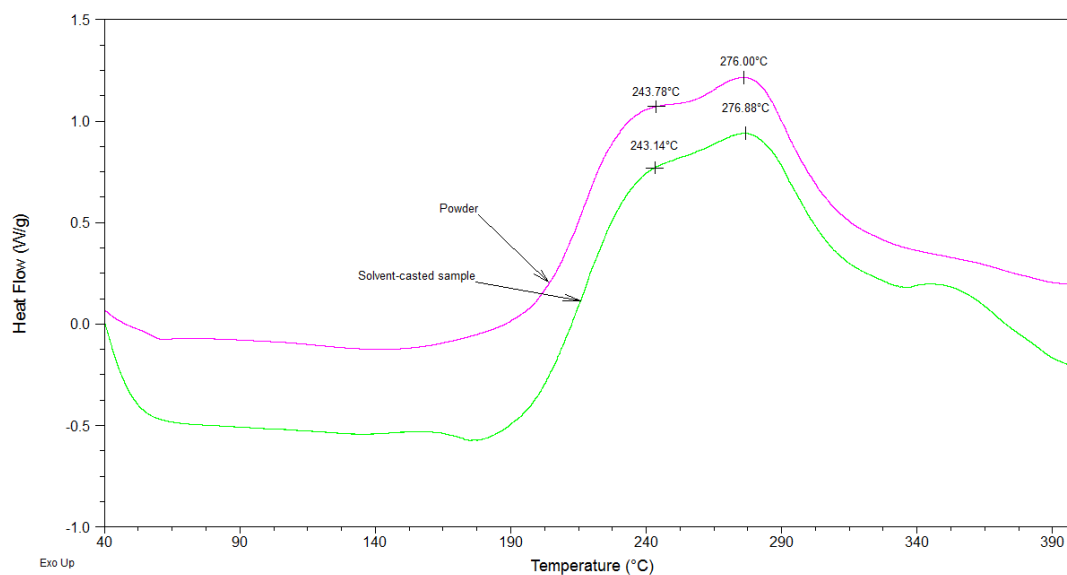


Figure 4.45 DSC of ^{15}N PVT in powder and after solvent casting preparation

In Figure 4.45 it is shown the DSC of the PVT marked with ^{15}N isotopes. In this case, it was of interest to know if there would be any difference before and after the solvent-casting preparation of the samples prior their composting. It is possible that some cross-linking reactions happened during the solvent-casting, increasing the molecular weight changes during the long periods of heating, which could explain why the solvent-casted samples of PVT and PVT-PAN were less soluble than their powder counterparts. In any case, the lower solubility of the samples forced for the NMR analysis to be performed by solid state instead of by liquid phase. It is also possible that as the heating rate is not slow, some solvent (DMF, BP around $153\text{ }^{\circ}\text{C}$) might be trapped inside the polymer matrix during the heating and it could only evaporate at a temperature higher than its normal boiling point.

4.5 Composting of Isotope-marked Polymers

For the isotope-marked samples, the composting experiment was carried only for 6 days, to better understand the initial stages of the decomposition. Also, as was indicated in Section 3.1, the salt required for the azidation ($1\text{-}^{15}\text{N NaN}_3$) was very expensive, so it was decided to restrict the experiment to a few samples, and to only run the compost experiment for a short period, as to require less amount of sample, and to reduce the loss of marked polymer into the soil.

4.5.1 ^{15}N -NMR

The ^{15}N -NMR analysis was performed using the Solid-State technique, due to the low solubility of the samples. It has to be noted that, due to the very low abundance of ^{15}N , it was necessary to add active isotopes to the PVT polymer, by means of using NaN_3 in which one of the nitrogen ions was a ^{15}N . The labelling of the PVT through click-chemistry was performed in the totality of the sample of interest, meaning that for that specific synthesis, the $^{15}\text{N NaN}_3$ was not mixed with regular sodium azide. This was done to counteract the low sensitivity to NMR that characterises this isotope, as shown in Table 4.8, which causes that the NMR analyses of the samples have to be performed over longer time periods.

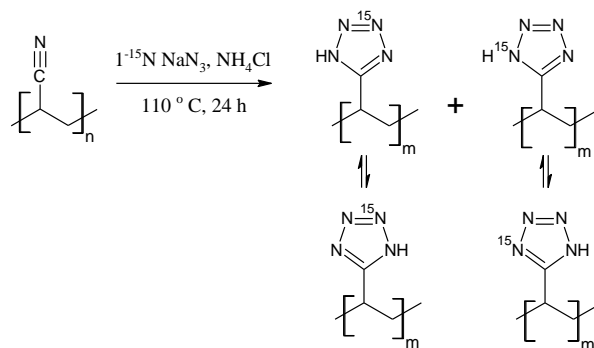
Table 4.8 Abundance and relative sensitivity of isotopes of H, C and N

| Isotope | Abundance % ^a [128, 129] | Detectable in NMR | Sensitivity ^b [153] |
|------------------------------------|-------------------------------------|-------------------|--------------------------------|
| ¹ H | 99.98 | Yes | 1 |
| ² H (or ² D) | 0.015 | No | – |
| ³ H | traces | Yes | 1.21 |
| ¹² C | 98.9 | No | – |
| ¹³ C | 1.11 | Yes | 0.016 |
| ¹⁴ C | < 1 ppb | No | – |
| ¹⁴ N | 99.63 | No | – |
| ¹⁵ N | 0.366 | Yes | 0.001 |

a: Expressed as the ratio of the natural abundance of the heavier isotope to the natural abundance of the lighter isotope.

b: Relative to ¹H, at constant field and for equal number of nuclei

It must be noted that the labeled salt used for the preparation of the samples had only one ¹⁵N isotope in one of the three nitrogens of the azide group, and it was located “at the end” of the group. Still, as the azide ion is symmetric, when it reacts with the nitrile group of PAN it could form two different species. Lastly, as the tetrazole ring presents tautomerism, the position of the proton could change, giving rise to four different species. This means that by adding only one ¹⁵N isotope in the azide group, it is possible to have spectroscopic information of all four nitrogens in the tetrazole group (see Figure 4.46).

Figure 4.46 Possible positions of the ¹⁵N isotope in the azidation products of PAN

In Table 4.9 are shown the general chemical shifts for different functional groups and nitrogen configurations, using liquid ammonia as the tabulated zero even though in the experiments

performed the inner standard for the zero was glycine: the obtained chemical shifts were corrected for comparison with the reference values.

Table 4.9 General ^{15}N -NMR chemical shifts in liquid state (using $\text{NH}_3(l) = 0$ ppm)

| Signal (ppm) | Interpretation [153] |
|--------------|---|
| 0 - 100 | Aliphatic amines |
| 40 - 110 | Enamines |
| 95 - 160 | Amides |
| 160 - 260 | Pyrrole-like nitrogens |
| 225 - 240 | Nitriles |
| 245 - 520 | Pyridine-like nitrogens |
| 305 - 375 | Imines |
| 445 - 465 | Triazenes $-\text{RN}=\text{N}=\text{N}-$ |

In Figure 4.47 are shown the spectra for the PVT samples labeled with $1\text{-}^{15}\text{N}\text{-NaN}_3$, that were composted only 6 days in order to assess any change that might happen in the early stages of the decomposition of the samples. The signals marked with asterisks are spinning “sidebands” that result from the modulation of the magnetic field at the spinning frequency, so are not considered for the analysis. The chemical shifts in the spectra match those described by Naumenko [163], being the only deviance the signal at 278 ppm in the 0 days spectrum, which might be due to a hydrogen bond with DMF used for the solvent casting [164]. This signal appeared again when the analysis was repeated. Nevertheless, the important conclusion to take out of these spectra is that by comparing the signals at 3 and 6 days, it can be noted that no changes occurred on the tetrazole rings during these early stages of the composting, meaning that the degradation of PVT shown in the 18-days composting experiments might be either by scission of the backbone, or by elimination of the tetrazole groups.

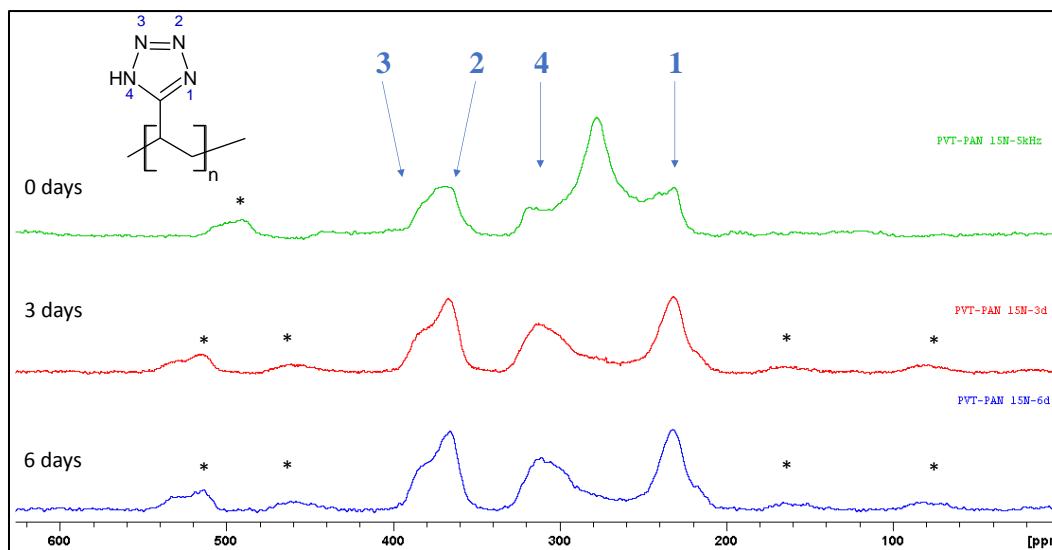


Figure 4.47 Solid State ^{15}N -NMR spectra for PVT composted samples at 0, 3 and 6 days

CHAPTER 5 GENERAL DISCUSSION

The survey of the literature for this work showed that up to this point, the research on the biodegradability of poly vinyl tetrazoles and glycidyl azide polymers is almost nonexistent. These are important research subjects as these substances have attracted interest and might become more prominent in the future: in the case of GAP polymers, as plasticizer or binder in energetic formulations; and in the case of poly vinyl tetrazoles, either in energetic applications, or in water treatment processes.

The criteria used for the selection of the polymers to be used in the composting experiments, centered on the synthesis feasibility: a simple preparation of the polymers with the minimum risks, high yields that were easily reproduced in the laboratory, and products with high purity that would minimize the need for separation or purification. For these reasons, of the several options of polymers with tetrazole groups that were surveyed in this work, only PVT and PVT-PAN were chosen for the composting stage, even though it was the original goal of this research to study in detail the changes in biodegradability due to different polymer backbones (i.e., poly vinyl tetrazole versus poly allyl tetrazole), different substituents in the tetrazole ring (tert-butyl or allyl groups), or different vinyl tetrazole co-polymers (poly vinyl-co-acrylo nitrile versus poly vinyl-co-methyl acrylate or poly vinyl-co-allyl azide). A similar reasoning led to the exclusion of poly vinyl azide, that was expected to be crosslinked and compared to GAP in terms of different polymer backbones.

The synthetic reactions were kept at such conditions that would be easily controlled in the laboratory, being that all the prepared substances were nitrogen-rich energetic substances. For this reason, the syntheses were performed in small batches in solution, with constant agitation to avoid the formation of hotspots in the polymer that could cause a detonation. Because of the preparation in small batches, it was essential that the obtained products would have a high yield that could be easily reproduced, with high purity. In the case of PVT-PAN and PVT (both with and without isotope labelling), the final polymers contained DMF as an impurity, but as that was the solvent used also for the solvent casting process, no further purification was done.

The choice of characterization techniques in this research was influenced by the low solubility of the polymers. For example, the molecular weight could not be determined, as the gel permeation chromatography (GPC) essays performed in PVT and PVT-PAN could not separate properly the molecules. This limits the reach of this research in terms of the discussion of the changes of molecular weight, which is a parameter widely use on biodegradability studies. The nuclear magnetic resonance (NMR) analysis was also affected by the low solubility of the samples, which prevented the essays on solution, hence the experiments had to be performed under the solid-state mode. The spectra obtained in solid-state possess broader signals, which hindered the identification of more specific changes occurring in the polymer chains.

For the crosslinked-GAP polymers, the lack of solubility was expected as the polymer would become a complex matrix; meanwhile, for both PVT and PVT-PAN, the solubility decreased after the solvent casting process, due possibly to ageing, though this was not characterized in this work.

To obtain the samples for the composting experiments, various forming techniques were considered, like injection molding, but the high temperatures required were incompatible with the energetic nature of the samples. The chosen technique was solvent casting, as the use of vacuum during the heating would imply that the samples were not exposed to very high temperatures. Nevertheless, the better solvent for PVT and for PVT-PAN was DMF, which has a high boiling point (153 °C); this turned the solvent casting process into a time-consuming one.

Another challenge was the forming of the samples, as the metal molds usually used to this end (for example with PLA samples) were not suitable for solvent casting. This was solved by making flexible silicon molds that would be temperature-resistant, which allowed for an easier solvent casting process, and a very constant and uniform shape of the samples.

The molecular labelling could have been done in a different way, for example by using the ^{15}N sodium azide in the azidation of poly epichlorohydrin PECH to form GAP, but because of safety concerns, this strategy was rejected. Another possibility for the isotope labelling would be to use a species with ^{13}C , for example, ^{13}C -propargyl alcohol to produce the BPM that would react with the azide groups of GAP to form triazoles. Nevertheless, this option proved to be more expensive than

the use of $^{13}\text{N-NaN}_3$ (\$2970 per gram of ^{13}C -propargyl alcohol versus \$1000 per gram of $^{15}\text{N-NaN}_3$).

In terms of the composting, the temperature chosen in this research corresponds to the mesophilic stage, which is associated to the initial steps of the biodegradation, and it is in this stage where the highest proportion of microorganisms break down the more available molecules. If the composting would occur at a higher temperature (“thermophilic stage”, 60-70 °C), most of the microorganisms would perish, and the high temperature would accelerate the breakdown of more complex molecules like fats, proteins, and complex carbohydrates. Thus, it is possible that at a higher temperature, the biodegradation of the studied polymers would have accelerated, but with several risks: the absence of the mesophilic stage would prevent the decomposition of smaller molecules, and as the bacterial community would be exclusively formed by thermophilic bacteria, or even absent, the breakdown of the polymers would be caused by abiotic factors.

Regarding the results from the composting experiments, in Figure 5.1 are shown the reactions observed for PVT. The elimination of tetrazole groups from the polymer chain would leave alkene groups that might react in a variety of ways (addition reactions, crosslinking, oxidation, etc.), which would produce a complex mixture of pollutants. The other observed reaction was the breakdown of the polymer, that would entail a reduction in the molecular weight caused by the scission of the chain. This chain scission results in the release of vinyl tetrazole oligomers; and due to the low biological reactivity of the tetrazole group, and its capacity to form metallic salts when deprotonated, this might cause either a higher solubility in water, or the fixation of these moieties in the soil minerals.

In the case of the biodegradation of PVT-PAN, the observed reactions are shown in Figure 5.2, and as it was the case for PVT, there is also elimination of tetrazole groups and chain scission. Also, the nitrile groups of the acrylonitrile monomers can undergo hydrolysis to carboxylates. The capacity of these carboxylate groups to interact with cations present in the soil, might increase the possibility of formation of organometallic complexes and might have repercussions in the fixation of the metabolites of PVT-PAN, as it was already discussed for the PVT oligomers.

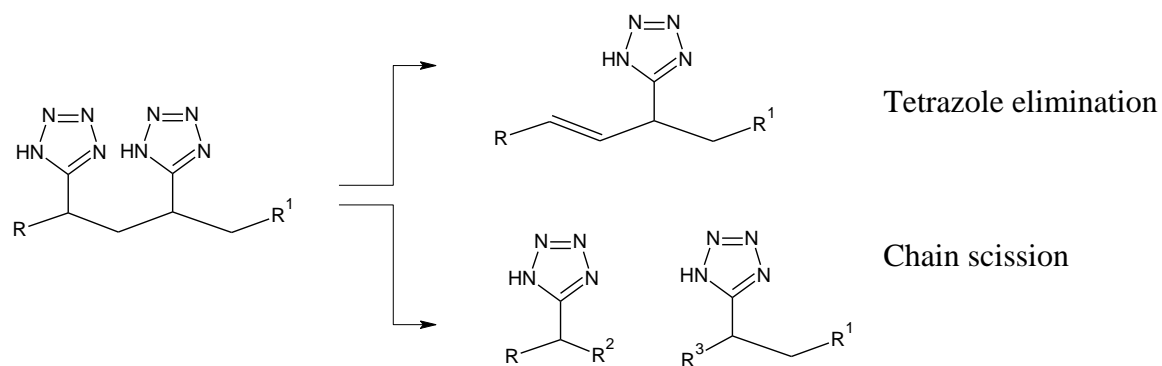


Figure 5.1 Observed biodegradation reactions for PVT.

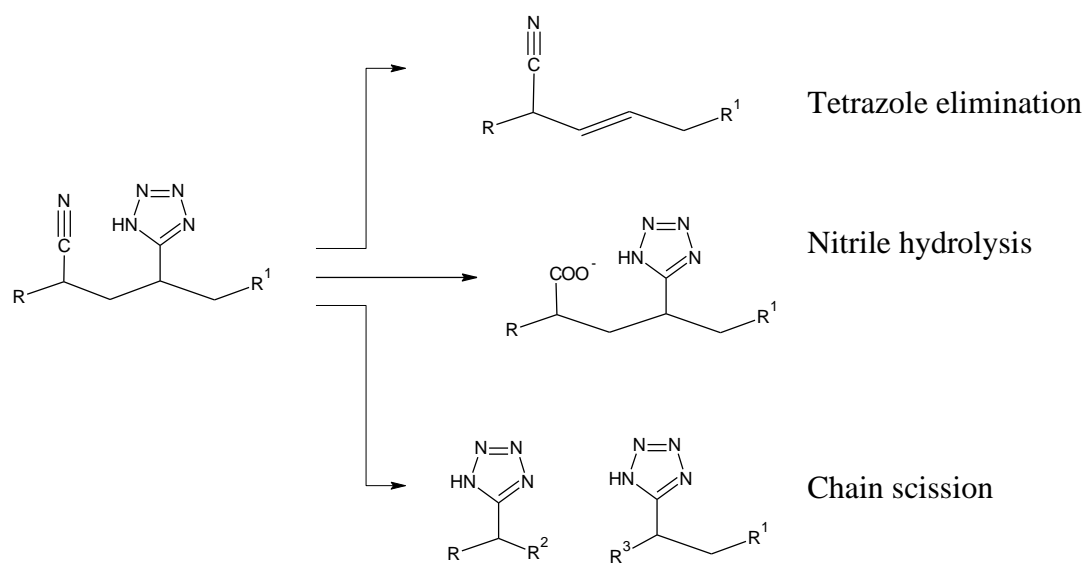


Figure 5.2 Observed biodegradation reactions for PVT-PAN.

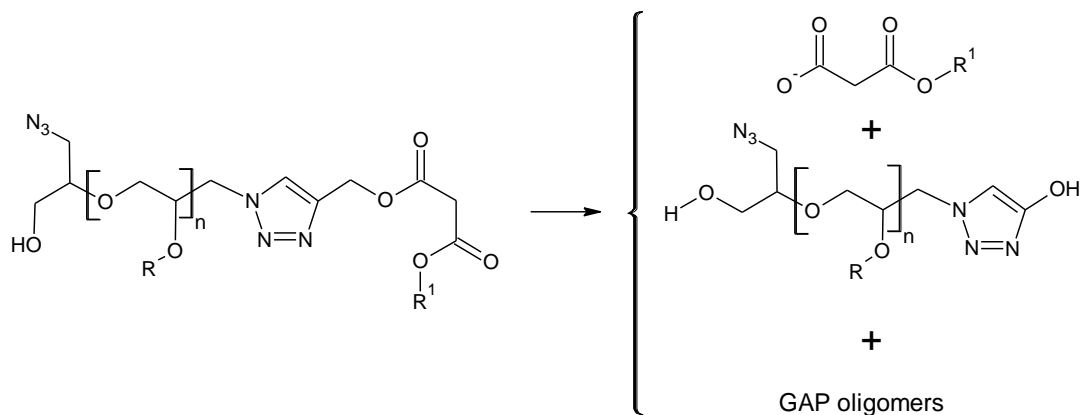


Figure 5.3 Observed biodegradation reactions for GAP-BPM.

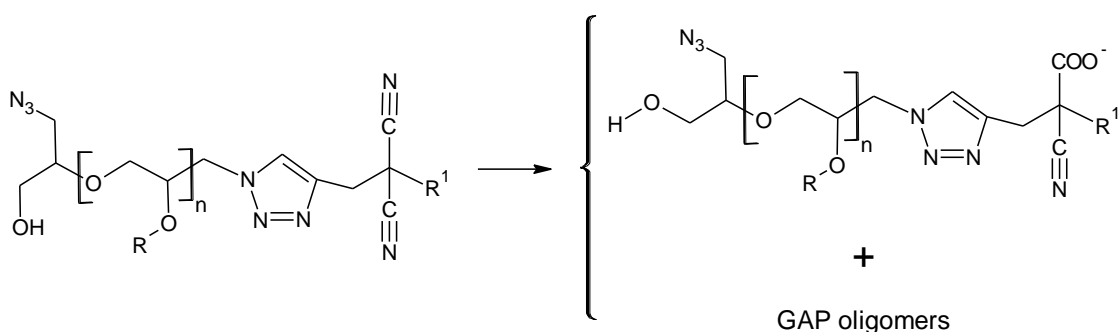


Figure 5.4 Observed biodegradation reactions for GAP-DCHD.

The results of this work show a very low biodegradability of both GAP-BPM and GAP-DCHD, and for both polymers the most notable change was the release of GAP oligomers into the soil, which is reasonable due to the low molecular weight of the GAP plasticizer used (around 700 Da). For GAP-BPM, there is evidence of partial hydrolysis of the ester bond of the bispropargyl malonate (Figure 5.3), which would decrease the crosslinking of the polymer, and release either the malonate anion or GAP-malonates. On the other hand, for GAP-DCHD it is presumed that some of the nitrile groups might suffer hydrolysis into carboxylates (Figure 5.4.), but the evidence was not conclusive. The observed biodegradation reactions previously discussed are summarized in Table 5.1, and in Figure 5.5

Table 5.1 Summary of the observed biodegradation reactions

| | Heterocycles | Hydrolysis | Polymer Backbone |
|-----------------|---------------------------|--|--|
| PVT | • Tetrazole groups intact | • N.A. | • Elimination of tetrazole groups (presumed) • Chain scission |
| PVT-PAN | • Tetrazole groups intact | • Hydrolysis of nitrile group | • Elimination of tetrazole groups (presumed) • Chain scission |
| GAP-BPM | • Triazole groups intact | • Partial hydrolysis of ester bonds | • Release of GAP oligomers |
| GAP-DCHD | • Triazole groups intact | • Hydrolysis of nitrile group (presumed) | • Release of GAP oligomers |

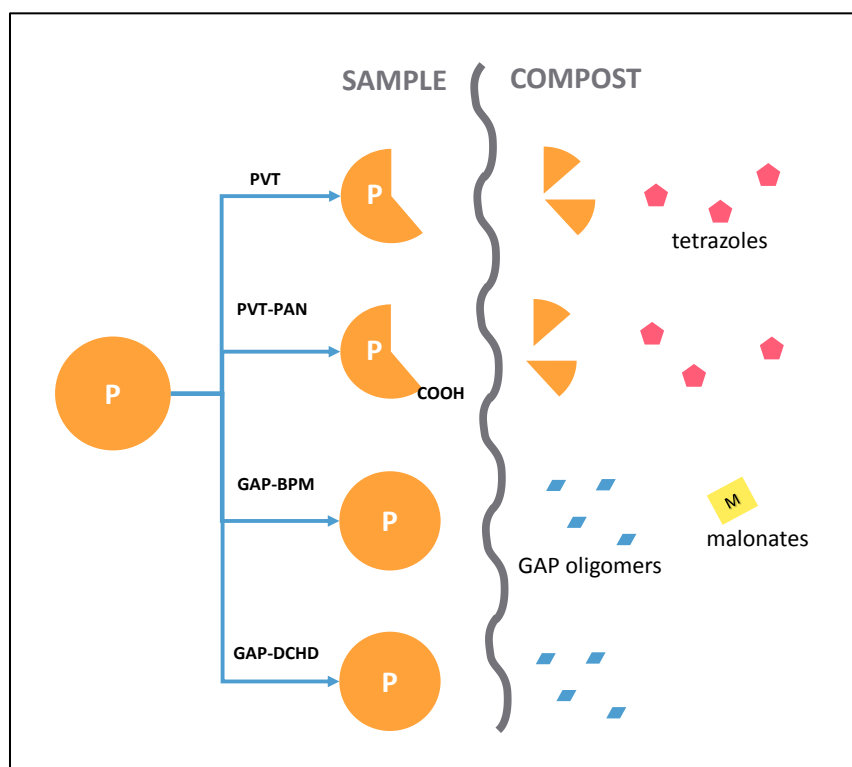


Figure 5.5 Graphic summary of the observed biodegradation reactions

It is difficult to define an ideal biodegradation scenario: in the case of substances that do not decompose, this might facilitate the collection of particles of the contaminant, and their treatment, either for elimination, or for recycling. This case of a substance remaining in the environment for a long time might pose a risk depending on its inertness, and its tendency to spread over large areas. In the specific case of this work, both crosslinked-GAP substances showed evidence that suggest the release of GAP into the environment. This might be explained by the low molecular weight of the GAP used, which in this product format would be used as a plasticizer; nevertheless, this release into the environment of a polymer with azide groups might bring negative toxicologic effects.

On the other hand, if a substance is easily biodegraded, this might suggest a more “environmentally friendly” substance, but only if the products formed are less toxic than the original compound. The survey of the literature revealed that TNT is an example of a compound that degrades easily in different ecological systems, but its metabolites pose a big threat due to their toxicity. In this work, both PVT and PVT-PAN showed a high degree of decomposition into the compost, but it would be necessary to evaluate the toxicity of their metabolites (alkene groups, vinyl tetrazole oligomers, etc.) to properly assess the ecological impact of the presence of these polymers in the environment.

The findings of this work provide clues about the environmental fate of the studied polymers in the soil. From these two opposite behaviors in biodegradation (two polymers easily decomposed and two polymers with low biodegradability), the hypothetical remediation of soil contaminated with these compounds would have to follow two different approaches: for PVT and PVT-PAN, that degraded easily, the remediation could be done by phytoremediation to fixate the vinyl tetrazole oligomers. Meanwhile, for GAP-BPM and GAP-DCHD, that did not decompose notably, a strategy like collection of the particles might be the better solution, followed by some extraction method to retrieve the GAP oligomers released into the soil.

CHAPTER 6 CONCLUSION AND RECOMMENDATIONS

6.1 Scientific Contribution

The present research contributes to the field of energetic polymers, by providing information about the biodegradation of samples of prototypical energetic polymers prepared in our research group. This kind of information is usually not studied until after the industrial application of energetic materials. The study of how the biodegradation can be affected by different chemical conditions like functional groups, polymeric backbone, and crosslinking agents, provides information for the design of more environmentally friendly energetic materials. The results herein shown are of interest as an early approach for the understanding of environmental fate and biodegradation pathways of energetic polymers containing tetrazole or triazole groups.

By having a first approximation of the biodegradation of these samples on composting conditions, the pertinent actors of the industrial and military applications can design products that use these polymers, considering beforehand strategies that minimize the ecological effect of waste materials produced from unused elements, training sessions, or demilitarization procedures.

The results of this research are ready to be sent for publication in a scientific journal to be defined.

6.2 Conclusions

The polymers based on tetrazoles, PVT and PVT-PAN, shown high biodegradability, and in some cases even total disappearance of the sample in the 18-days timeframe of this study. The biodegradability of both polymers was helped in part by factors like the swelling of the polymeric matrix in the presence of water. The nitrile moiety of the PVT-PAN showed hydrolysis into carboxylic salts, which might help the water solubility of the polymer, and its interaction with microorganisms from the soil.

In the case of GAP-BPM and GAP-DCHD, the samples did not show high biodegradability in any of the characterisation tests performed, and it can be seen that the main degradation process is the release of glycidyl azide polymer into the soil. It is possible that the release into the soil of GAP, a polymer with a high number of azide groups, complicates or even prevents the biodegradation process, as it has been shown that the azide groups have biocide activity.

6.3 Recommendations

1. Use of PAN with lower molecular weight, to ensure a higher solubility of the obtained PVT, as it would facilitate the solvent casting and the characterization analyses (GPC, NMR).
2. Study of the biodegradability of GAP with other crosslinkers like bis propargyl ether BPE, bis propargyl oxalate BPO and bis propargyl succinate BPS, among others.
3. Study of the by-products of biodegradation of the composted polymers (PVT, PVT-PAN, GAP-BPM and GAP-DCHD) by means of the analysis of soil extracts by chromatography (either GC or HPLC) paired with mass spectrometry for the identification of metabolites in the different fractions, to determine the impact on microorganisms.
4. Study of the transportation processes and mobility of energetic materials with triazole or tetrazole groups in soil and/or water through the determination of partition coefficients like the octanol-water partition constant K_{ow} , or the organic carbon-water partition coefficient K_{oc} .
5. Comparison of different setups for the biodegradation of energetic materials with triazole or tetrazole groups: aerobic composting versus anaerobic composting, bacterial inoculated composting, phytoremediation, etc.

REFERENCES

- [1] I. Sutton, "Formal safety assessments," pp. 214-260, 2012.
- [2] S. Chatterjee, U. Deb, S. Datta, C. Walther, and D. K. Gupta, "Common explosives (TNT, RDX, HMX) and their fate in the environment: Emphasizing bioremediation," *Chemosphere*, vol. 184, pp. 438-451, Oct 2017.
- [3] R. Matyáš and J. Pachman, *Primary Explosives*: Springer-Verlag Berlin Heidelberg, 2013.
- [4] S. Thiboutot, G. Ampleman, and A. Hewitt, "Guide for characterization of sites contaminated with energetic materials.," vol. Tech. Rep. ERDC/CRREL TR-02-1, ed. Hanover, NH, USA: US Army Engineer Research and Development Center, 2002.
- [5] A. International, "ASTM E2552-16 Standard Guide for Assessing the Environmental and Human Health Impacts of New Compounds for Military Use," ed. West Conshohocken, PA: ASTM International, 2016.
- [6] S. P. How Ghee Ang, *Energetic Polymers: Binders and plasticizers for enhancing performance*: Wiley-VCH, 2012.
- [7] B. A. Stenuit and S. N. Agathos, "Microbial 2,4,6-trinitrotoluene degradation: could we learn from (bio)chemistry for bioremediation and vice versa?," *Appl Microbiol Biotechnol*, vol. 88, pp. 1043-64, Nov 2010.
- [8] P. W. Cooper, *Explosives engineering*. New York, N.Y.: VCH, 1996.
- [9] O. Bolton, L. R. Simke, P. F. Pagoria, and A. J. Matzger, "High Power Explosive with Good Sensitivity: A 2:1 Cocrystal of CL-20:HMX," *Crystal Growth & Design*, vol. 12, pp. 4311-4314, 2012.
- [10] F. Monteil-Rivera, A. Halasz, D. Manno, R. G. Kuperman, S. Thiboutot, G. Ampleman, *et al.*, "Fate of CL-20 in sandy soils: degradation products as potential markers of natural attenuation," *Environ Pollut*, vol. 157, pp. 77-85, Jan 2009.
- [11] A. Provasas, "Energetic Polymers and Plasticisers for explosive formulations - A review of recent advances," vol. Technical Report DSTO-TR-0966, D. o. Defence, Ed., ed. Australia, 2000.
- [12] S. Salvi, A. Druka, S. G. Milner, and D. Gruszka, "Induced Genetic Variation, TILLING and NGS-Based Cloning," vol. 69, pp. 287-310, 2014.
- [13] L. Hernández, D. Gómez, B. Valle, C. C. Tebbe, R. Trethowan, R. Acosta, *et al.*, "Carotenoids in roots indicated the level of stress induced by mannitol and sodium azide treatment during the early stages of maize germination," *Acta Physiologiae Plantarum*, vol. 40, 2018.
- [14] S. Chang and S. H. Lamm, "Human health effects of sodium azide exposure: a literature review and analysis," *Int J Toxicol*, vol. 22, pp. 175-86, May-Jun 2003.
- [15] Z. Xiao, W. He, and S. Ying, "Current trends in energetic thermoplastic elastomers as binders in high energy insensitive propellants in China," *Science and technology of energetic materials : Journal of the Japan Explosives Society*, vol. 75, pp. 37-43, 2014 2014.
- [16] T. Cheng, "Review of novel energetic polymers and binders - high energy propellant ingredients for the new space race," *Des Monomers Polym*, vol. 22, pp. 54-65, 2019.
- [17] C. Dubois, S. Désilets, G. Nadeau, and N. Gagnon, "Chemical Kinetics and Heat Transfer Issues for a Safe Bench Scale Production of Partially Triazole Substituted Glycidyl Azide Polymer (GAP)," *Propellants, Explosives, Pyrotechnics*, vol. 28, pp. 107-113, 2003.
- [18] S. K. Manu, T. L. Varghese, S. Mathew, and K. N. Ninan, "Studies on structure property correlation of cross-linked glycidyl azide polymer," *Journal of Applied Polymer Science*, vol. 114, pp. 3360-3368, 2009.
- [19] M. B. Talawar, R. Sivabalan, T. Mukundan, H. Muthurajan, A. K. Sikder, B. R. Gandhe, *et al.*, "Environmentally compatible next generation green energetic materials (GEMs)," *J Hazard Mater*, vol. 161, pp. 589-607, Jan 30 2009.

- [20] M. S. Eroglu and M. S. Bostan, "GAP pre-polymer, as an energetic binder and high performance additive for propellants and explosives: A review," *Organic Communications*, vol. 10, pp. 135-143, 2017.
- [21] S. Mathew, S. K. Manu, and T. L. Varghese, "Thermomechanical and Morphological Characteristics of Cross-Linked GAP and GAP-HTPB Networks with Different Diisocyanates," *Propellants, Explosives, Pyrotechnics*, vol. 33, pp. 146-152, 2008.
- [22] M. B. Frankel, L. R. Grant, and J. E. Flanagan, "Historical development of glycidyl azide polymer," *Journal of Propulsion and Power*, vol. 8, pp. 560-563, 1992.
- [23] B. Sun Min, "Characterization of the Plasticized GAP/PEG and GAP/PCL Block Copolyurethane Binder Matrices and its Propellants," *Propellants, Explosives, Pyrotechnics*, vol. 33, pp. 131-138, 2008.
- [24] E. Landsem, T. L. Jensen, T. E. Kristensen, F. K. Hansen, T. Benneche, and E. Unneberg, "Isocyanate-Free and Dual Curing of Smokeless Composite Rocket Propellants," *Propellants, Explosives, Pyrotechnics*, vol. 38, pp. 75-86, 2013.
- [25] J. Athar, R. Soman, N. Agawane, R. Wagh, and M. Talwar, "Optimization of Curing Agents for Linear Difunctional Glycidyl Azide Polymer (GAP), with and without Isocyanate, for Binder Applications," *Central European Journal of Energetic Materials*, vol. 15, pp. 206-222, 2018.
- [26] E. Pasquinet, "Nitrogen-Rich Polymers as Candidates for Energetic Applications," 2012.
- [27] V. N. Kizhnyayev, F. A. Pokatilov, and L. I. Vereshchagin, "Branched tetrazole-containing polymers," *Polymer Science Series A*, vol. 49, pp. 28-34, 2007.
- [28] M.-R. Huang, X.-G. Li, S.-X. Li, and W. Zhang, "Resultful synthesis of polyvinyltetrazole from polyacrylonitrile," *Reactive and Functional Polymers*, vol. 59, pp. 53-61, 2004.
- [29] P. N. Gaponik, O. A. Ivashkevich, V. P. Karavai, A. I. Lesnikovich, N. I. Chernavina, G. T. Sukhanov, *et al.*, "Polymers and copolymers based on vinyl tetrazoles, 1. Synthesis of poly(5-vinyl tetrazole) by polymer-analogous conversion of polyacrylonitrile" *Angewandte Makromolekulare Chemie*, vol. 219, pp. 77-88, 1994.
- [30] P. N. Gaponik, O. A. Ivashkevich, N. I. Chernavina, A. I. Lesnikovich, G. T. Sukhanov, and G. A. Gareev, "Polymers and copolymers based on vinyl tetrazoles, 2. Alkylation of poly(5-vinyl tetrazole)," *Angewandte Makromolekulare Chemie*, vol. 219, pp. 89-99, 1994.
- [31] W. Liang, Y. Chenyang, Z. Bin, W. Xiaona, Y. Zijun, Z. Lixiang, *et al.*, "Hydrophobic polyacrylonitrile membrane preparation and its use in membrane contactor for CO₂ absorption," *Journal of Membrane Science*, vol. 569, pp. 157-165, 2019.
- [32] Y. Hu, X. Chen, H.-L. Cong, B. Yu, X.-Y. Meng, H. Yuan, *et al.*, "Preparation of chelating hollow-fiber ultrafiltration membrane," *Integrated Ferroelectrics*, vol. 179, pp. 38-44, 2017.
- [33] W. Zhao, L. Liu, L. Wang, and N. Li, "Functionalization of polyacrylonitrile with tetrazole groups for ultrafiltration membranes," *RSC Advances*, vol. 6, pp. 72133-72140, 2016.
- [34] Y. Chen, M. He, C. Wang, and Y. Wei, "A novel polyvinyltetrazole-grafted resin with high capacity for adsorption of Pb(ii), Cu(ii) and Cr(iii) ions from aqueous solutions," *Journal of Materials Chemistry A*, vol. 2, p. 10444, 2014.
- [35] S. Yan, M. Zhao, G. Lei, and Y. Wei, "Novel tetrazole-functionalized absorbent from polyacrylonitrile fiber for heavy-metal ion adsorption," *Journal of Applied Polymer Science*, vol. 125, pp. 382-389, 2012.
- [36] J. Boileau, "Overview on Energetic Polymers," *MRS Online Proceedings Library Archive*, vol. 418, p. 91, 1995.
- [37] E. E. Gilbert, "A comparative study of the reactivity of poly(vinyl chloride) and of poly(vinyl nitrate) with sodium azide," *Journal of Polymer Science: Polymer Chemistry Edition*, vol. 22, pp. 3603-3606, 1984.
- [38] A. Ouerghui, H. Elamari, M. Dardouri, S. Ncib, F. Meganem, and C. Girard, "Chemical modifications of poly(vinyl chloride) to poly(vinyl azide) and "clicked" triazole bearing groups for application in metal cation extraction," *Reactive and Functional Polymers*, vol. 100, pp. 191-197, 2016.

- [39] B. Gaur, B. Lochab, V. Choudhary, and I. K. Varma, "Thermal behaviour of poly(allyl azide)," *Journal of Thermal Analysis and Calorimetry*, vol. 71, pp. 467-479, 2003.
- [40] J. P. Agrawal, "Status of Explosives," in *High Energy Materials*, ed: Wiley-VCH Verlag GmbH & Co. KGaA, 2010, pp. 69-161.
- [41] F. Monteil-Rivera, S. Deschamps, G. Ampleman, S. Thiboutot, and J. Hawari, "Dissolution of a new explosive formulation containing TNT and HMX: comparison with octol," *J Hazard Mater*, vol. 174, pp. 281-8, Feb 15 2010.
- [42] G. Amplemant, P. Brousseau, S. Thiboutot, S. Trudel, P. Beland, and A. Marois, "Synthesis and characterization of a greener insensitive melt cast explosive," *Science and Technology of Energetic Materials*, vol. 75, pp. 69-76, 2014.
- [43] A. Halasz, J. Hawari, and N. N. Perreault, "New Insights into the Photochemical Degradation of the Insensitive Munition Formulation IMX-101 in Water," *Environ Sci Technol*, vol. 52, pp. 589-596, Jan 16 2018.
- [44] T. M. Klapötke, C. Miró Sabaté, and M. Rasp, "Synthesis and properties of 5-nitrotetrazole derivatives as new energetic materials," *Journal of Materials Chemistry*, vol. 19, p. 2240, 2009.
- [45] H. Gao and J. M. Shreeve, "The Many Faces of FOX-7: A Precursor to High-Performance Energetic Materials," *Angew Chem Int Ed Engl*, vol. 54, pp. 6335-8, May 18 2015.
- [46] H. R. Blomquist and A. Gilbert, "Gas generating composition comprising guanyleurea dinitramide," USA Patent, 2000.
- [47] T. Klapötke, N. Fischer, D. Fischer, D. G. Piercey, J. Stierstorfer, and M. Reymann, "Energetic active composition comprising a dihydroxylammonium salt or diammonium salt of a bistetrazeodiol," 2016.
- [48] P. C. Painter and M. M. Coleman, *Fundamentals of polymer science : an introductory text*: Lancaster, 1997.
- [49] J. Taylor, "1 Polymers as Binders and Plasticizers@ Historical Perspective," 2011.
- [50] H. Ang and S. Pisharath, *Energetic Polymers: Binders and plasticizers for enhancing performance*: Wiley-VCH, 2012.
- [51] S. Domenek, P. Feuilleley, J. Gratraud, M.-H. Morel, and S. Guilbert, "Biodegradability of wheat gluten based bioplastics," *Chemosphere*, vol. 54, pp. 551-559, 2004.
- [52] A. Harat, "Influence of Selected Environmental Management Systems on the Properties and Functional Parameters of Explosive Materials," *Journal of Ecological Engineering*, vol. 20, pp. 7-14, 2019.
- [53] R. G. Kuperman, M. L. Minyard, R. T. Checkai, G. I. Sunahara, S. Rocheleau, S. G. Dodard, *et al.*, "Inhibition of soil microbial activity by nitrogen-based energetic materials," *Environ Toxicol Chem*, vol. 36, pp. 2981-2990, Nov 2017.
- [54] B. Gaur, B. Lochab, V. Choudhary, and I. K. Varma, "Azido Polymers—Energetic Binders for Solid Rocket Propellants," *Journal of Macromolecular Science, Part C: Polymer Reviews*, vol. 43, pp. 505-545, 2003.
- [55] T. Keicher, W. Kuglstatler, S. Eisele, T. Wetzler, and H. Krause, "Isocyanate-Free Curing of Glycidyl Azide Polymer (GAP) with Bis-Propargyl-Succinate (II)," *Propellants, Explosives, Pyrotechnics*, vol. 34, pp. 210-217, 2009.
- [56] S. Sonawane, M. Anniyappan, J. Athar, A. Singh, M. B. Talawar, R. K. Sinha, *et al.*, "Isocyanate-Free Curing of Glycidyl Azide Polymer with Bis-propargylhydroquinone," *Propellants, Explosives, Pyrotechnics*, vol. 42, pp. 386-393, 2017.
- [57] H. C. Kolb, M. G. Finn, and K. B. Sharpless, "Click Chemistry: Diverse Chemical Function from a Few Good Reactions," *Angewandte Chemie International Edition*, vol. 40, pp. 2004-2021, 2001.
- [58] S. Q. Liu, P. L. Ee, C. Y. Ke, J. L. Hedrick, and Y. Y. Yang, "Biodegradable poly(ethylene glycol)-peptide hydrogels with well-defined structure and properties for cell delivery," *Biomaterials*, vol. 30, pp. 1453-61, Mar 2009.

- [59] M. Malkoch, R. Vestberg, N. Gupta, L. Mespouille, P. Dubois, A. F. Mason, *et al.*, "Synthesis of well-defined hydrogel networks using Click chemistry," *Chemical Communications*, pp. 2774-2776, 2006.
- [60] D. A. Ossipov and J. Hilborn, "Poly(vinyl alcohol)-Based Hydrogels Formed by "Click Chemistry"," *Macromolecules*, vol. 39, pp. 1709-1718, 2006.
- [61] H. Awada and C. Daneault, "Chemical Modification of Poly(Vinyl Alcohol) in Water," *Applied Sciences*, vol. 5, pp. 840-850, 2015.
- [62] K. Hakkou, M. Bueno-Martínez, I. Molina-Pinilla, and J. A. Galbis, "Degradable poly(ester triazole)s based on renewable resources," *Journal of Polymer Science Part A: Polymer Chemistry*, vol. 53, pp. 2481-2493, 2015.
- [63] H. DeFrancesco, J. Dudley, and A. Coca, "Undergraduate Organic Experiment: Tetrazole Formation by Microwave Heated (3 + 2) Cycloaddition in Aqueous Solution," *Journal of Chemical Education*, vol. 95, pp. 433-437, 2018.
- [64] "GAO-04-147 MILITARY MUNITIONS: DOD Needs to develop a comprehensive approach for cleaning up contaminated sites," U. S. G. A. Office, Ed., ed. Washington, D.C., 2003.
- [65] G. I. Sunahara, G. Lotufo, R. G. Kuperman, and J. Hawari, *Ecotoxicology of Explosives*: CRC Press, 2009.
- [66] P. Anastas and N. Eghbali, "Green chemistry: principles and practice," *Chem Soc Rev*, vol. 39, pp. 301-12, Jan 2010.
- [67] T. Brinck, *Green Energetic Materials*: John Wiley & Sons Ltd, 2014.
- [68] S. Anand and S. M. Celin, "Green Technologies for the Safe Disposal of Energetic Materials in the Environment," pp. 835-860, 2017.
- [69] P. Y. Robidoux, J. Hawari, S. Thiboutot, G. Ampleman, and G. I. Sunahara, "Chronic toxicity of octahydro-1,3,5,7-tetranitro-1,3,5,7-tetrazocine (HMX) in soil determined using the earthworm (*Eisenia andrei*) reproduction test," *Environmental Pollution*, vol. 111, pp. 283-292, 2001.
- [70] J. L. Clausen and N. Korte, "Fate and Transport of Energetics from Surface Soils to Groundwater," *Environmental Chemistry of Explosives and Propellant Compounds in Soils and Marine Systems: Distributed Source Characterization and Remedial Technologies*, vol. 1069, pp. 273-316, 2011.
- [71] G. I. Sunahara, P. Y. Robidoux, B. Lachance, A. Y. Renoux, P. Gong, S. Rocheleau, *et al.*, "Laboratory and Field Approaches to Characterize the Soil Ecotoxicology of Polynitro Explosives," pp. 293-293-20, 2000.
- [72] N. Petrea, R. Ginghina, A. Pretorian, R. Petre, G. Barsan, P. Otrisal, *et al.*, "Experimental survey regarding the dangerous chemical compounds from military polygons that affect the military health and the environment," *Rev. Chim*, vol. 69, pp. 1640-1644, 2018.
- [73] J. Clausen, J. Robb, D. Curry, and N. Korte, "A case study of contaminants on military ranges: Camp Edwards, Massachusetts, USA," *Environmental Pollution*, vol. 129, pp. 13-21, 2004.
- [74] M. C. Lapointe, R. Martel, and E. Diaz, "A Conceptual Model of Fate and Transport Processes for RDX Deposited to Surface Soils of North American Active Demolition Sites," *J Environ Qual*, vol. 46, pp. 1444-1454, Nov 2017.
- [75] R. Martel, M. Mailloux, U. Gabriel, R. Lefebvre, S. Thiboutot, and G. Ampleman, "Behavior of energetic materials in ground water at an anti-tank range," *J Environ Qual*, vol. 38, pp. 75-92, Jan-Feb 2009.
- [76] C. A. Groom, A. Halasz, L. Paquet, N. Morris, L. Olivier, C. Dubois, *et al.*, "Accumulation of HMX (octahydro-1,3,5,7-tetranitro-1,3,5,7-tetrazocine) in indigenous and agricultural plants grown in HMX-contaminated anti-tank firing-range soil," *Environ Sci Technol*, vol. 36, pp. 112-8, Jan 1 2002.
- [77] USEPA, "Integrated Risk Information System (IRIS): 2,4,6-Trinitrotoluene (TNT);," N. C. f. E. Assessment, Ed., ed. U.S.A., 2002.
- [78] C. Bolognesi, X. Baur, B. Marczyński, H. Norppa, O. Sepai, and G. Sabbioni, "Carcinogenic risk of toluene diisocyanate and 4,4'-methylenediphenyl diisocyanate: epidemiological and experimental evidence," *Crit Rev Toxicol*, vol. 31, pp. 737-72, Nov 2001.

- [79] M. B. Colovic, D. Z. Krstic, T. D. Lazarevic-Pasti, A. M. Bondzic, and V. M. Vasic, "Acetylcholinesterase inhibitors: pharmacology and toxicology," *Curr Neuropharmacol*, vol. 11, pp. 315-35, May 2013.
- [80] O. Y. Shyyka, N. T. Pokhodylo, Y. I. Slyvka, E. A. Goreshnik, and M. D. Obushak, "Understanding the tetrazole ring cleavage reaction with hydrazines: Structural determination and mechanistic insight," *Tetrahedron Letters*, vol. 59, pp. 1112-1115, 2018.
- [81] M. A. Malik, M. Y. Wani, S. A. Al-Thabaiti, and R. A. Shiekh, "Tetrazoles as carboxylic acid isosteres: chemistry and biology," *Journal of Inclusion Phenomena and Macrocyclic Chemistry*, vol. 78, pp. 15-37, 2013.
- [82] I. E. Valverde and T. L. Mindt, "1,2,3-Triazoles as amide-bond surrogates in peptidomimetics," *Chimia (Aarau)*, vol. 67, pp. 262-6, 2013.
- [83] A. Qian, Y. Zheng, R. Wang, J. Wei, Y. Cui, X. Cao, *et al.*, "Design, synthesis, and structure-activity relationship studies of novel tetrazole antifungal agents with potent activity, broad antifungal spectrum and high selectivity," *Bioorg Med Chem Lett*, vol. 28, pp. 344-350, Feb 1 2018.
- [84] D. N. Obanda and T. F. Shupe, "Biotransformation of Tebuconazole by Microorganisms: Evidence of a Common Mechanism," 2009.
- [85] N. M. Dummer, "4(5)-Methylbenzotriazole: a review of the life-cycle of an emerging contaminant," *Reviews in Environmental Science and Bio/Technology*, vol. 13, pp. 53-61, 2013.
- [86] Z. Q. Shi, Y. S. Liu, Q. Xiong, W. W. Cai, and G. G. Ying, "Occurrence, toxicity and transformation of six typical benzotriazoles in the environment: A review," *Sci Total Environ*, vol. 661, pp. 407-421, Apr 15 2019.
- [87] M. A. Abu-Dalo, I. O'Brien, and M. T. Hernandez, "Effects of Substitutions on the Biodegradation Potential of Benzotriazole Derivatives," *IOP Conference Series: Materials Science and Engineering*, vol. 305, p. 012020, 2018.
- [88] M. K. Durjava, B. Kolar, L. Arnus, E. Papa, S. Kovarich, U. Sahlin, *et al.*, "Experimental assessment of the environmental fate and effects of triazoles and benzotriazole," *Altern Lab Anim*, vol. 41, pp. 65-75, Mar 2013.
- [89] A. Halasz, C. Groom, E. Zhou, L. Paquet, C. Beaulieu, S. Deschamps, *et al.*, "Detection of explosives and their degradation products in soil environments," *Journal of Chromatography A*, vol. 963, pp. 411-418, 2002.
- [90] K. G. Furton, J. R. Almirall, M. Bi, J. Wang, and L. Wu, "Application of solid-phase microextraction to the recovery of explosives and ignitable liquid residues from forensic specimens," *Journal of Chromatography A*, vol. 885, pp. 419-432, 2000.
- [91] F. Monteil-Rivera, C. Beaulieu, S. Deschamps, L. Paquet, and J. Hawari, "Determination of explosives in environmental water samples by solid-phase microextraction-liquid chromatography," *Journal of Chromatography A*, vol. 1048, pp. 213-221, 2004.
- [92] A. Halasz and J. Hawari, "Degradation Routes of RDX in Various Redox Systems," vol. 1071, pp. 441-462, 2011.
- [93] G. Bordeleau, R. Martel, G. Ampleman, and S. Thiboutot, "Environmental impacts of training activities at an air weapons range," *J Environ Qual*, vol. 37, pp. 308-17, Mar-Apr 2008.
- [94] J. E. Landmeyer, *Introduction to phytoremediation of contaminated groundwater: historical foundation, hydrologic control, and contaminant remediation*: Springer Science & Business Media, 2011.
- [95] B. W. Schoenmuth and W. Pestemer, "Dendroremediation of trinitrotoluene (TNT). Part 2: fate of radio-labelled TNT in trees," *Environ Sci Pollut Res Int*, vol. 11, pp. 331-9, 2004.
- [96] C. F. Hoehamer, N. L. Wolfe, and K. E. Eriksson, "Differences in the biotransformation of 2,4,6-trinitrotoluene (TNT) between wild and axenically grown isolates of *Myriophyllum aquaticum*," *Int J Phytoremediation*, vol. 8, pp. 107-15, 2006.
- [97] B. Van Aken, "Transgenic plants for enhanced phytoremediation of toxic explosives," *Curr Opin Biotechnol*, vol. 20, pp. 231-6, Apr 2009.

- [98] K. Panz and K. Miksch, "Phytoremediation of explosives (TNT, RDX, HMX) by wild-type and transgenic plants," *J Environ Manage*, vol. 113, pp. 85-92, Dec 30 2012.
- [99] Y. Luo, Z. Lin, and G. Guo, "Biodegradation Assessment of Poly (Lactic Acid) Filled with Functionalized Titania Nanoparticles (PLA/TiO₂) under Compost Conditions," *Nanoscale Res Lett*, vol. 14, p. 56, Feb 14 2019.
- [100] J. Spain, *BIODEGRADATION OF NITROAROMATIC COMPOUNDS*, 1 ed.: Springer US, 1995.
- [101] K. A. Thorn, J. C. Pennington, and C. A. Hayes, "15N NMR investigation of the reduction and binding of TNT in an aerobic bench scale reactor simulating windrow composting," *Environ Sci Technol*, vol. 36, pp. 3797-805, Sep 1 2002.
- [102] B. Gumuscu, D. Cekmecelioglu, and T. Tekinay, "Complete dissipation of 2,4,6-trinitrotoluene by in-vessel composting," *RSC Advances*, vol. 5, pp. 51812-51819, 2015.
- [103] B. H. In, J. S. Park, W. Namkoong, J. D. Kim, and B. I. Ko, "Effect of sewage sludge mixing ratio on composting of TNT-contaminated soil.," *Journal of Industrial and Engineering Chemistry*, vol. 13(2), pp. 190-197, 2007.
- [104] K. Elgh Dalgren, S. Waara, A. Düker, T. von Kronhelm, and P. A. W. van Hees, "Anaerobic Bioremediation of a Soil With Mixed Contaminants: Explosives Degradation and Influence on Heavy Metal Distribution, Monitored as Changes in Concentration and Toxicity," *Water, Air, and Soil Pollution*, vol. 202, pp. 301-313, 2009.
- [105] T. Richard and J. Weidhaas, "Biodegradation of IMX-101 explosive formulation constituents: 2,4-dinitroanisole (DNAN), 3-nitro-1,2,4-triazol-5-one (NTO), and nitroguanidine," *J Hazard Mater*, vol. 280, pp. 372-9, Sep 15 2014.
- [106] S. G. Dodard, M. Sarrazin, J. Hawari, L. Paquet, G. Ampleman, S. Thiboutot, *et al.*, "Ecotoxicological assessment of a high energetic and insensitive munitions compound: 2,4-dinitroanisole (DNAN)," *J Hazard Mater*, vol. 262, pp. 143-50, Nov 15 2013.
- [107] C. Cossu, M.-C. Heuzey, L.-S. Lussier, and C. Dubois, "Early development of a biodegradable energetic elastomer," *Journal of Applied Polymer Science*, vol. 119, pp. 3645-3657, 2011.
- [108] G. Ampleman, P. Brousseau, S. Thiboutot, S. Rocheleau, F. Monteil-Rivera, Z. Radovic-Hrapovic, *et al.*, "Evaluation of Gim as a Greener Insensitive Melt-Cast Explosive," *International Journal of Energetic Materials and Chemical Propulsion*, vol. 11, pp. 59-87, 2012.
- [109] A. L. Andrady, "Assessment of Environmental Biodegradation of Synthetic Polymers," *Journal of Macromolecular Science, Part C: Polymer Reviews*, vol. 34, pp. 25-76, 1994.
- [110] M. Vert, Y. Doi, K.-H. Hellwich, M. Hess, P. Hodge, P. Kubisa, *et al.*, "Terminology for biorelated polymers and applications (IUPAC Recommendations 2012)," *Pure and Applied Chemistry*, vol. 84, pp. 377-410, 2012.
- [111] A. D. McNaught and A. Wilkinson, "IUPAC. Compendium of Chemical Terminology," in *IUPAC. Compendium of Chemical Terminology ("The Gold book")*, 2nd. ed, 2009.
- [112] N. Lucas, C. Bienaime, C. Belloy, M. Queneudec, F. Silvestre, and J. E. Nava-Saucedo, "Polymer biodegradation: mechanisms and estimation techniques," *Chemosphere*, vol. 73, pp. 429-42, Sep 2008.
- [113] T. P. Haider, C. Volker, J. Kramm, K. Landfester, and F. R. Wurm, "Plastics of the Future? The Impact of Biodegradable Polymers on the Environment and on Society," *Angew Chem Int Ed Engl*, vol. 58, pp. 50-62, Jan 2 2019.
- [114] H. S. Toogood, J. M. Gardiner, and N. S. Scrutton, "Biocatalytic Reductions and Chemical Versatility of the Old Yellow Enzyme Family of Flavoprotein Oxidoreductases," *ChemCatChem*, vol. 2, pp. 892-914, 2010.
- [115] S. Brochu, S. Thiboutot, G. Ampleman, E. Diaz, I. Poulin, and R. Martel, "Canadian Approach to the Environmental Characterization and Risk Assessment of Military Training," vol. 1069, pp. 49-76, 2011.
- [116] J. C. Pennington and J. M. Brannon, "Environmental fate of explosives," *Thermochimica Acta*, vol. 384, pp. 163-172, 2002.

- [117] D. L. Kaplan and A. M. Kaplan, "Thermophilic biotransformations of 2,4,6-trinitrotoluene under simulated composting conditions," *Applied and environmental microbiology*, vol. 44, pp. 757-760, 1982.
- [118] F. H. Crocker, K. J. Indest, and H. L. Fredrickson, "Biodegradation of the cyclic nitramine explosives RDX, HMX, and CL-20," *Applied Microbiology and Biotechnology*, vol. 73, pp. 274-290, 2006.
- [119] F. Monteil-Rivera, C. Groom, and J. Hawari, "Sorption and Degradation of Octahydro-1,3,5,7-tetranitro-1,3,5,7-tetrazocine in Soil," *Environmental Science & Technology*, vol. 37, pp. 3878-3884, 2003.
- [120] E. L. Rylott, A. Lorenz, and N. C. Bruce, "Biodegradation and biotransformation of explosives," *Curr Opin Biotechnol*, vol. 22, pp. 434-40, Jun 2011.
- [121] P. Gong, G. I. Sunahara, S. Rocheleau, S. G. Dodard, P. Y. Robidoux, and J. Hawari, "Preliminary ecotoxicological characterization of a new energetic substance, CL-20," *Chemosphere*, vol. 56, pp. 653-8, Aug 2004.
- [122] T. Temple, M. Ladyman, N. Mai, E. Galante, M. Ricamora, R. Shirazi, *et al.*, "Investigation into the environmental fate of the combined Insensitive High Explosive constituents 2,4-dinitroanisole (DNAN), 1-nitroguanidine (NQ) and nitrotriazolone (NTO) in soil," *Sci Total Environ*, vol. 625, pp. 1264-1271, Jun 1 2018.
- [123] K. J. Indest, D. E. Hancock, F. H. Crocker, J. O. Eberly, C. M. Jung, G. A. Blakeney, *et al.*, "Biodegradation of insensitive munition formulations IMX101 and IMX104 in surface soils," *J Ind Microbiol Biotechnol*, vol. 44, pp. 987-995, Jul 2017.
- [124] C. L. Madeira, S. A. Speet, C. A. Nieto, L. Abrell, J. Chorover, R. Sierra-Alvarez, *et al.*, "Sequential anaerobic-aerobic biodegradation of emerging insensitive munitions compound 3-nitro-1,2,4-triazol-5-one (NTO)," *Chemosphere*, vol. 167, pp. 478-484, Jan 2017.
- [125] A. J. Kennedy, A. R. Poda, N. L. Melby, L. C. Moores, S. M. Jordan, K. A. Gust, *et al.*, "Aquatic toxicity of photo-degraded insensitive munition 101 (IMX-101) constituents," *Environ Toxicol Chem*, vol. 36, pp. 2050-2057, Aug 2017.
- [126] J. B. Becher, S. A. Beal, S. Taylor, K. Dontsova, and D. E. Wilcox, "Photo-transformation of aqueous nitroguanidine and 3-nitro-1,2,4-triazol-5-one: Emerging munitions compounds," *Chemosphere*, vol. 228, pp. 418-426, Aug 2019.
- [127] B. R. Linker, R. Khatiwada, N. Perdrial, L. Abrell, R. Sierra-Alvarez, J. A. Field, *et al.*, "Adsorption of novel insensitive munitions compounds at clay mineral and metal oxide surfaces," *Environmental Chemistry*, vol. 12, p. 74, 2015.
- [128] T. C. Schmidt, L. Zwank, M. Elsner, M. Berg, R. U. Meckenstock, and S. B. Haderlein, "Compound-specific stable isotope analysis of organic contaminants in natural environments: a critical review of the state of the art, prospects, and future challenges," *Anal Bioanal Chem*, vol. 378, pp. 283-300, Jan 2004.
- [129] W. Meier-Augenstein and H. F. Kemp, "Stable Isotope Analysis: General Principles and Limitations," in *Wiley Encyclopedia of Forensic Science*, ed: Wiley Online Library, 2012.
- [130] I. Limam, M. Mezni, A. Guenne, C. Madigou, M. R. Driss, T. Bouchez, *et al.*, "Evaluation of biodegradability of phenol and bisphenol A during mesophilic and thermophilic municipal solid waste anaerobic digestion using ¹³C-labeled contaminants," *Chemosphere*, vol. 90, pp. 512-20, Jan 2013.
- [131] C. F. Shen, S. R. Guiot, S. Thiboutot, G. Ampleman, and J. Hawari, "Fate of explosives and their metabolites in bioslurry treatment processes," *Biodegradation*, vol. 8, pp. 339-347, 1997.
- [132] G. E. Speitel, T. L. Engels, and D. C. McKinney, "Biodegradation of RDX in Unsaturated Soil," *Bioremediation Journal*, vol. 5, pp. 1-11, 2001.
- [133] E. M. Gallagher, L. Y. Young, L. M. McGuinness, and L. J. Kerkhof, "Detection of 2,4,6-trinitrotoluene-utilizing anaerobic bacteria by ¹⁵N and ¹³C incorporation," *Appl Environ Microbiol*, vol. 76, pp. 1695-8, Mar 2010.

- [134] U. Jaekel, C. Vogt, A. Fischer, H. H. Richnow, and F. Musat, "Carbon and hydrogen stable isotope fractionation associated with the anaerobic degradation of propane and butane by marine sulfate-reducing bacteria," *Environ Microbiol*, vol. 16, pp. 130-40, Jan 2014.
- [135] H. I. F. Amaral, J. Fernandes, M. Berg, R. P. Schwarzenbach, and R. Kipfer, "Assessing TNT and DNT groundwater contamination by compound-specific isotope analysis and ^3H - ^3He groundwater dating: A case study in Portugal," *Chemosphere*, vol. 77, pp. 805-812, 2009.
- [136] T. Ariyaratna, M. Ballentine, P. Vlahos, R. W. Smith, C. Cooper, J. K. Bohlke, *et al.*, "Tracing the cycling and fate of the munition, Hexahydro-1,3,5-trinitro-1,3,5-triazine in a simulated sandy coastal marine habitat with a stable isotopic tracer, $(^{15}\text{N})\text{-[RDX]}$," *Sci Total Environ*, vol. 647, pp. 369-378, Jan 10 2019.
- [137] S. Sagi-Ben Moshe, Z. Ronen, O. Dahan, A. Bernstein, N. Weisbrod, F. Gelman, *et al.*, "Isotopic evidence and quantification assessment of in situ RDX biodegradation in the deep unsaturated zone," *Soil Biology and Biochemistry*, vol. 42, pp. 1253-1262, 2010.
- [138] A. Bernstein, E. Adar, Z. Ronen, H. Lowag, W. Stichler, and R. U. Meckenstock, "Quantifying RDX biodegradation in groundwater using $\delta^{15}\text{N}$ isotope analysis," *J Contam Hydrol*, vol. 111, pp. 25-35, Jan 15 2010.
- [139] S. Ringuette, R. Stowe, C. Dubois, G. Charlet, Q. Kwok, and D. E. G. Jones, "Deuterium Effect on Thermal Decomposition of Deuterated GAP: 1. Slow Thermal Analysis with a TGA-DTA-FTIR-MS," *Journal of Energetic Materials*, vol. 24, pp. 307-320, 2006.
- [140] S. Ringuette, C. Dubois, R. A. Stowe, and G. Charlet, "Synthesis and Characterization of Deuterated Glycidyl Azide Polymer (GAP)," *Propellants, Explosives, Pyrotechnics*, vol. 31, pp. 131-138, 2006.
- [141] G. Bordeleau, M. M. Savard, R. Martel, G. Ampleman, and S. Thiboutot, "Determination of the origin of groundwater nitrate at an air weapons range using the dual isotope approach," *J Contam Hydrol*, vol. 98, pp. 97-105, Jun 6 2008.
- [142] G. Bordeleau, M. M. Savard, R. Martel, A. Smirnoff, G. Ampleman, and S. Thiboutot, "Stable isotopes of nitrate reflect natural attenuation of propellant residues on military training ranges," *Environ Sci Technol*, vol. 47, pp. 8265-72, Aug 6 2013.
- [143] C. Cossu, "Early development of an energetic biodegradable thermoset elastomer," Master in Applied Sciences, Génie Chimique, Université de Montréal, Montréal, Québec, Canada, 2009.
- [144] J. R. Caldwell, "Copolymers of Acrylonitrile and allyl and 2-methylallyl chlorides," USA Patent, 1953.
- [145] R. J. Schmitt, J. C. Bottaro, P. M., and P. P., "Synthesis of New High Energy Density Matter (HEDM): Extra High Energy Oxidizers and Fuels," ed. Edwards Air Force Base CA, USA: Air Force Research Laboratory, 1998.
- [146] J. Lavoie, "Biodégradabilité et propriétés énergétiques d'élastomères azoturés," Maîtrise en Sciences Appliquées (Génie Chimique), Département de Génie Chimique, École Polytechnique de Montréal, Montréal, 2012.
- [147] C. I. e. a. e. g. d. sites, "Protocole Standard d'Operation PSOA23: Capacité de rétention d'eau au champ d'un échantillon de sol ", ed. CIRAIG, Polytechnique de Montréal, QC: Centre international de référence sur le cycle de vie des produits, procédés et services, CIRAIG, 2002, p. 4.
- [148] A. International, "ASTM D2976-15 Standard Test Method for pH of Peat Materials," ed, 2015.
- [149] C. I. C. e. a. e. g. d. sites, "Protocole Standard d'Opération PSOA8: Détermination du pH d'un échantillon de tourbe à l'aide d'un pH-metre," ed, 2000, p. 4.
- [150] M. Araya-Marchena, J. C. St-Charles, and C. Dubois, "Investigations on Non-isocyanate Based Reticulation of Glycidyl Azide Pre-polymers," *Propellants, Explosives, Pyrotechnics*, vol. 44, pp. 769-775, 2019.
- [151] G. R. Fulmer, A. J. M. Miller, N. H. Sherden, H. E. Gottlieb, A. Nudelman, B. M. Stoltz, *et al.*, "NMR Chemical Shifts of Trace Impurities: Common Laboratory Solvents, Organics, and Gases in Deuterated Solvents Relevant to the Organometallic Chemist," *Organometallics*, vol. 29, pp. 2176-2179, 2010.
- [152] J. A. Joule and K. Mills, *Heterocyclic chemistry*, 5th ed. ed.: John Wiley & Sons, Ltd., 2010.

- [153] R. M. Silverstein, F. X. Webster, and D. Kiemle, *Spectrometric Identification of Organic Compounds, 7th Edition*: Wiley, 2005.
- [154] N. Fischer, K. Karaghiosoff, Thomas M. Klapötke, and J. Stierstorfer, "New Energetic Materials featuring Tetrazoles and Nitramines - Synthesis, Characterization and Properties," *Zeitschrift für anorganische und allgemeine Chemie*, vol. 636, pp. 735-749, 2010.
- [155] J.-S. Park, B.-H. In, and W. Namkoong, "Toxicological evaluation for bioremediation processes of TNT-contaminated soil by Salmonella mutagenicity assay," *Korean Journal of Chemical Engineering*, vol. 29, pp. 1074-1080, 2012.
- [156] M. R. Rezaei, M. A. Abdoli, A. Karbassi, A. Baghvand, and R. Khalilzadeh, "Bioremediation of TNT Contaminated Soil by Composting with Municipal Solid Wastes," *Soil and Sediment Contamination: An International Journal*, vol. 19, pp. 504-514, 2010.
- [157] S. Miljourns and C. M. Braun, "A neuropsychotoxicological assessment of workers in a sodium azide production plant," *Int Arch Occup Environ Health*, vol. 76, pp. 225-32, Apr 2003.
- [158] S. Bråse and K. Banert, *Organic Azides: Syntheses and Applications*: John Wiley & Sons Ltd, 2010.
- [159] H. S. G.; and W. J. W., "Ground Water Issue: Dense Nonaqueous Phase Liquids," vol. EPA/540/4-91-002, 1991.
- [160] C. W. Fetter, T. B. Boving, and D. K. Kreamer, *Contaminant hydrogeology* vol. 500: Prentice hall Upper Saddle River, NJ, 1999.
- [161] ASTM, "ASTM D638-14 Standard Test Method for Tensile Properties of Plastics," ed, 2014.
- [162] C. A. Gracia-Fernández, S. Gómez-Barreiro, J. López-Beceiro, J. Tarrío Saavedra, S. Naya, and R. Artiaga, "Comparative study of the dynamic glass transition temperature by DMA and TMDSC," *Polymer Testing*, vol. 29, pp. 1002-1006, 2010.
- [163] V. N. Naumenko, A. O. Koren, and P. N. Gaponik, "¹⁵N NMR study of tetrazoles," *Magnetic Resonance in Chemistry*, vol. 30, pp. 558-560, 1992.
- [164] W. Koźmiński, F. Aguilar-Parrilla, I. Wawer, H.-H. Limbach, and L. Stefaniak, "¹⁵N and ¹³C solid-state nuclear magnetic resonance study of 5-thiomethyltetrazole," *Solid State Nuclear Magnetic Resonance*, vol. 4, pp. 121-124, 1995.

APPENDIX A SEM IMAGES OF COMPOSTED SAMPLES

